ACCSCIENCE PUBLISHING

OR

REVIEW ARTICLE

Synergistic engineering of organoids and organ-on-a-chip systems through microengineering and sensor integration for advanced biomedical research

Diantong Xie[1,2†], Yixu Zhao[1,2†], Yubing Leng[2,3†], Xiaorui Li[2,4†*], Hongxin Li[2,3], Hui Liu[2,3], Xudong Wang[2,3], Jingkai Liu[2,3], Yulong Liao[2], Tianyu Yang[2], Jie Liu[2], Yinuo Zhang[2,3], Fengde Peng[2], Ji Song[2], Zizheng Deng[2], Shiyao Chen[2], Kairui Sun[5], Yingran Liu[5], Keyi Chen[6], Jiashu Li[2], Yu Wang[7*], Zhongze Gu[8*], and Fuyin Zheng[2,3*]

[1]School of Biomedical Engineering, Tsinghua Medicine, Tsinghua University, Beijing, China

[2]Key Laboratory for Biomechanics and Mechanobiology of Ministry of Education, Beijing Advanced Innovation Center for Biomedical Engineering, School of Biological Science and Medical Engineering, School of Engineering Medicine, Beihang University, Beijing, China

[3]Vita Tech Innovation Center, Beijing Key Laboratory of Clinical Innovation and Translation for Active Implantable and Interventional Medical Devices, Beijing Tsinghua Changgung Hospital, School of Clinical Medicine, Tsinghua Medicine, Tsinghua University, Beijing, China

[4]Independent Cardiovascular Research Lab, Chinese Institutes for Medical Research, Capital Medical University, Beijing, China

[5]School of Beijing, Beihang University, Beijing, China

[6]School of Astronautics, Beihang University, Beijing, China

[7]Department of Orthopedic Surgery, Institute of Orthopedics, The Fourth Medical Center of Chinese PLA General Hospital, Beijing, China

[8]State Key Laboratory of Digital Medical Engineering, School of Biological Science & Medical Engineering, Southeast University, Nanjing, Jiangsu, China

***Corresponding authors:** Xiaorui Li (lixiaorui@cimrbj.ac.cn); Yu Wang (wangyu@301hospital.com.cn); Zhongze Gu (gu@seu.edu.cn); Fuyin Zheng (zhengfy@tsinghua.edu.cn)

†*These authors contributed equally to this work*

Citation: Xie D, Zhao Y, Leng Y, *et al*. Synergistic engineering of organoids and organ-on-a-chip systems through microengineering and sensor integration for advanced biomedical research. *Organoid Res*. doi: 10.36922/OR026020001

Received: January 7, 2026

Revised: September 9, 2026

Accepted: September 10, 2026

Published online: September 30, 2026

Copyright: © 2026 Author(s). This is an Open-Access article distributed under the terms of the Creative Commons Attribution License, permitting distribution, and reproduction in any medium, which provided that the original work is properly cited.

Publisher's Note: AccScience Publishing remains neutral with regard to jurisdictional claims in published maps and institutional affiliations.

Abstract

Microphysiological systems, including organoids, organ-on-a-chip (OoC) platforms, and their integrated forms, are increasingly used to model human physiology *in vitro*. Organoids contribute self-organized cellular diversity and tissue architecture, whereas OoC platforms provide controlled geometry, perfusion, mechanical cues, and access to real-time measurements. Their integration into organoid-on-a-chip and multi-tissue systems can improve physiological relevance for efficacy evaluation, quality control, mechanistic studies, and personalized medicine. This review examines organoid generation, organ-specific OoC models, hybrid systems, 3D bioprinting, acoustic bioassembly, and sensor integration. It also discusses the principal barriers to translation, including scalability, reproducibility, standardization, and the responsible use of artificial intelligence and multi-omics data. Together, these advances position synergistically engineered microphysiological systems as promising translational tools, provided that performance is validated against standardized, reproducible, and clinically relevant benchmarks.

Keywords: Synergistic engineering; Organoids; Organ-on-a-chip; 3D bioprinting; Biosensors

1. Introduction

Recently, the integration of advanced biotechnology and sensors has improved biomedical research, opening unprecedented avenues for disease modeling, drug discovery, and personalized medicine. In parallel, microphysiological systems (MPS), encompassing organoids, organ-on-a-chip (OoC), and integrated organoid-on-a-chip technologies, provide tools for disease modeling, drug discovery, and personalized medicine.[1,2] By reproducing selected biological features of human tissues and organs, MPS can complement conventional two-dimensional (2D) cultures and animal models in translational research.[3]

Organoids are three-dimensional (3D), stem cell–derived structures conceptualized in the early 2000s that emerged from advances in stem cell biology and tissue engineering. Organoids, by their definition, mimic the cellular diversity, architectural complexity, and functional attributes of native organs or tissues, making them powerful platforms for studying human development, disease mechanisms, and therapeutic responses *in vitro*.[4] Pioneering work by Sato *et al.*[5] demonstrated that intestinal stem cells could self-organize into 3D structures resembling mini-guts when cultured in a supportive extracellular matrix (ECM) with specific growth factors. This breakthrough laid the foundation for organoid technology, which has since expanded to a wide spectrum of organs or tissues, including brain[6], liver[7], gut[8], kidney[9], and heart[10] organoids, which replicate essential physiological and pathological states.[2]

The OoC technology originated from the convergence of microfluidics and bioengineering in the late 1990s and early 2000s, integrating living cells into microfluidic devices to emulate organ-level functionality and recapitulate dynamic physiological processes such as fluid flow, shear stress, and multi-organ interactions. The first notable OoC system, a lung-on-a-chip, was developed by Donald Ingber's group[11] in 2010, integrating pulmonary epithelial and vascular endothelial cells implanted on both sides of a porous membrane within a microfabricated two-chamber device to replicate the mechanical and biochemical microenvironment of the human lung. The field has evolved rapidly since, with chips designed for the heart, liver, kidney, and multi-organ systems[12], offering precise control over fluid flow, oxygen gradients, and intercellular interactions.[13]

Organoids and OoC systems have unique strengths. Organoids excel in recapitulating the self-organizing capacity of tissues, enabling the study of developmental processes and cellular heterogeneity in a 3D context.[14] However, their static culture conditions limit their ability to simulate physiological dynamics such as blood flow or tissue–tissue interfaces. Conversely, OoC systems provide a dynamic microenvironment, incorporating perfusion, shear stress, and multicellular interactions, closely mimicking *in vivo* conditions.[15] Nonetheless, they rely on simpler cellular arrangements and may not fully capture the intricate tissue architecture of organoids. By acknowledging these complementary attributes, researchers have integrated organoids into OoC platforms.[16] This hybrid approach combines the 3D complexity and cellular fidelity of organoids with the dynamic, physiologically relevant conditions of microfluidic systems, thereby enhancing the realism of *in vitro* models and offering superior predictive power for drug screening, disease modeling, and personalized medicine.

This review focuses on how organoid biology and OoC engineering can be combined with microengineering and sensing to construct more controllable and informative MPS (Figure 1). The scope is organized using four complementary dimensions: biological complexity (cell source, maturation, vascularization, and immune or neural integration); engineering control (geometry, materials, perfusion, shear stress, and mechanical or electrical stimulation); monitoring readouts (electrophysiology, barrier integrity, biochemical sensing, imaging, and omics); and application context (mechanistic studies, efficacy and toxicity testing, personalized medicine, and manufacturing quality control). The organ-based organization is retained to help readers compare representative systems without obscuring this cross-cutting framework. Subsequent sections therefore progress from organoids and OoC models to integrated organoid-on-a-chip systems, microengineering, sensors, and translational challenges.

2. Microphysiological systems: From organoids and organ-on-a-chip to integrated platforms

Microphysiological systems encompass organoids, OoC, and integrated (multi-)organoid-on-a-chip systems. Organoids and OoC contribute complementary biological complexity and engineering control, while multi-tissue platforms extend the analysis to inter-organ interactions and systemic responses.[16,17] These systems may complement traditional 2D cultures and animal models in drug development, disease modeling, toxicology, and personalized medicine when their context of use is adequately validated (Figure 1).

2.1. Organoids

Organoids are defined as self-organizing 3D structures derived from stem cells that replicate key architectural and functional features of native organs at a miniature scale.[4] They differ from simpler 3D structures such as spheroids that lack lineage diversity or structural organization. Organoids emulate complex organotypic architecture and physiology, such as generated intestinal organoids with functional proliferation zones, villus-like structures, and specialized

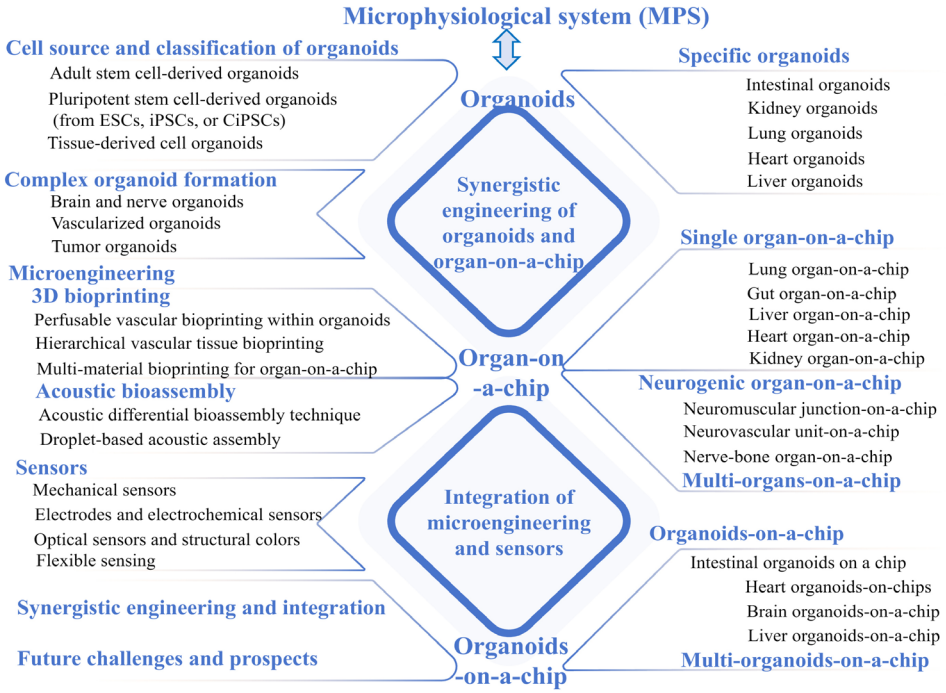


Figure 1. Scope and organization of this review, linking organoid biological complexity, organ-on-a-chip engineering control, microengineering strategies, sensor-based readouts, integrated platforms, and translational challenges
Abbreviations: CiPSC: Chemically induced pluripotent stem cell; ESC: Embryonic stem cell; iPSC: Induced pluripotent stem cell.

epithelial cells, reflecting intestinal function. Moreover, they enable a dynamic analysis of organogenesis, genetic diseases, and therapeutic interventions. Thus, organoids display intrinsic self-organization, spatial polarization, and multicellular complexity; improved organoids have enabled the study of more physiologically relevant systems.[18]

2.1.1. Source and classification of organoids

Advanced technologies have expanded organoid research from upstream biological development to downstream applications in disease modeling, drug discovery, and regenerative medicine. Three main cell sources are used in organoid technology: pluripotent stem cells (PSCs), adult stem cells (ASCs), and tissue-derived cells (TDCs); each has unique advantages and limitations. Additionally, organoids are classified based on their derivation: ASC-derived organoids, PSC-derived organoids, and TDC-derived (especially tumor) organoids.[19] Organoids are improved by incorporating diverse cell types, applying gene-editing tools, and chemical reprogramming for cell fate manipulation technologies to model complex tissues and dynamics.[20]

(a) Adult stem cell–derived organoids

Adult stem cells are lineage-committed stem cells within specific tissues used to form organoids that mimic adult tissue physiology. ASC-derived organoids are established using tissue-resident multipotent stem or progenitor cells, typically modeling epithelial tissues from a single germ layer. Sato *et al.*[5] delineated ASC-derived intestinal crypt-villus structures from leucine-rich repeat-containing G protein-coupled receptor 5 (LGR5)+ cells. These organoids are used for studying adult tissue homeostasis and pathologies, including gastrointestinal disorders and cancers. Because they resemble their tissue of origin, ASC-derived organoids are employed in preclinical models of disease. For example, liver organoids from ASC-like cholangiocytes model liver fibrosis and viral hepatitis.[4] Xu *et al.*[21] established kidney organoids (tubuloids) from CD24+ cells, modeling polycystic kidney disease (PKD) while reproducing tubular-specific cellular architecture. ASC-based systems maintain tissue-specific characteristics and genetic fidelity, but their limited differentiation potential restricts their application primarily to single-germ-layer epithelial tissues.

(b) Pluripotent stem cell–derived organoids

Pluripotent stem cells, including embryonic stem cells (ESCs) and induced pluripotent stem cells (iPSCs), can differentiate into any cell lineage.[22] Their broad potency enables the generation of complex organoids with

multilineage differentiation.[23] ESCs, derived from the inner cell mass of blastocysts, form organoids by culturing them under specific conditions, mimicking organ structure and function, making them valuable for development studies, disease modeling, and drug screening. iPSCs can also be prepared by gene-editing technology with clustered regularly interspaced short palindromic repeats–CRISPR-associated protein 9 (CRISPR-Cas9), which has transformed organoid research by enabling the faithful recreation of disease-associated mutations or highly specific models. This precision genetic modeling allows high-throughput gene knockouts for functional studies. Hendriks *et al.*[24] demonstrated that multiplex CRISPR-based modifications in hepatocyte organoids facilitate target identification and drug development for non-alcoholic fatty liver disease (NAFLD), underscoring the intersection of organoid biology and genetic engineering for creating patient-relevant disease models.

A novel approach by Guan *et al.*[22] uses small molecules to induce PSCs for organoid construction. This chemical induction reprograms somatic cells into a pluripotent state, bypassing genetic manipulation. Chemically induced pluripotent stem cells (CiPSCs) can then be directed to differentiate into multiple lineages, generating complex organoids that resemble native tissues in structure and function. This method simplifies iPSC production while improving reproducibility and scalability, advancing regenerative medicine, disease modeling, and drug discovery. Chemically derived liver progenitor cells (human chemically derived hepatocytes) have also been developed as a source for liver organoids, offering promising models for liver disease, regenerative medicine, and toxicology testing, with applications in treatment and drug development.

Unlike ASC-derived organoids, PSC-derived organoids (from ESCs, iPSCs, or CiPSCs) exhibit broader differentiation potential into all three germ layers, enabling the formation of epithelial and mesenchymal compartments, rendering them suitable for developmental studies and modeling congenital diseases.[25] However, PSC-derived organoids require complex differentiation protocols. Moreover, ethical concerns surrounding ESCs and the complexity of differentiating iPSCs hamper their scalability and reproducibility. These organoids can model early organogenesis, as seen with brain, intestinal, and kidney organoids.

(c) Tissue-derived cell–derived organoids

Fully differentiated cells can transform to a progenitor-like state under appropriate culture conditions, as shown in tumor organoid generation.[26] However, lineage reprogramming and long-term stability of TDC-derived organoids is challenging. Incorporating multiple cell types, such as immune cells, fibroblasts, neural cells, vascular components, and ECM, has been pivotal for enhancing the realism of organoids. Strating *et al.*[27] successfully used fibroblast-enriched co-cultures of colon cancer organoids to induce epithelial-to-mesenchymal transition (EMT), elucidating mechanisms through which cancer-associated fibroblasts contribute to immunosuppressive tumor microenvironments and chemoresistance. Similarly, Schuth *et al.*[28] developed matched pancreatic ductal adenocarcinoma (PDAC) organoid/fibroblast co-cultures, demonstrating that fibroblasts affect tumorigenesis and mediate chemoresistance via cytokine signaling and EMT transcriptional changes. Bioprinting methods enabled the incorporation of vascular structures, as in Liu *et al.*'s[29] multi-material 3D bioprinting of vascularized liver organoids, which provided functional capillary networks to sustain nutrient perfusion and cellular metabolism. These integrated models better mimic the heterogeneity of native tissues and are valuable in oncology and immunology studies.

2.1.2. Specific studies of organoids

(a) Intestinal organoids

Intestinal organoids are 3D structures derived from intestinal stem cells or reprogrammed somatic cells that replicate the architecture and function of the intestinal epithelium *in vitro*. They consist of a polarized epithelial layer with crypt-like domains containing stem and Paneth cells, surrounded by villus-like regions with differentiated enterocytes, goblet cells, and enteroendocrine cells. This self-organized structure mimics the *in vivo* crypt-villus axis, but the number and positioning of crypt-like domains in mouse intestinal organoids cannot be precisely controlled, highlighting inconsistency. Such variability arises from limited understanding of how intrinsic programs interact with microenvironmental cues. Overcoming these challenges requires engineering approaches to guide morphogenesis, imposing order on this unpredictable process and prioritizing novel construction strategies over downstream outcomes.

Intestinal organoids face major challenges in reproducibility and control. The stochastic nature of stem cell self-organization produces variable size, shape, and composition, limiting standardized research. Gjorevski *et al.*[8] addressed this by introducing bioengineered control over organoid formation through tissue geometry *(*Figure 2a*)*. Recognizing that native architectures emerge from epithelial self-organization and external regulators, they used hydrogel photopatterning and microfabrication to dictate initial size and shape. This enabled prediction and guidance of developmental trajectories, particularly crypt formation. They showed that predefined hydrogel microtopography establishes local differences in cell packing and morphology, driving reproducible

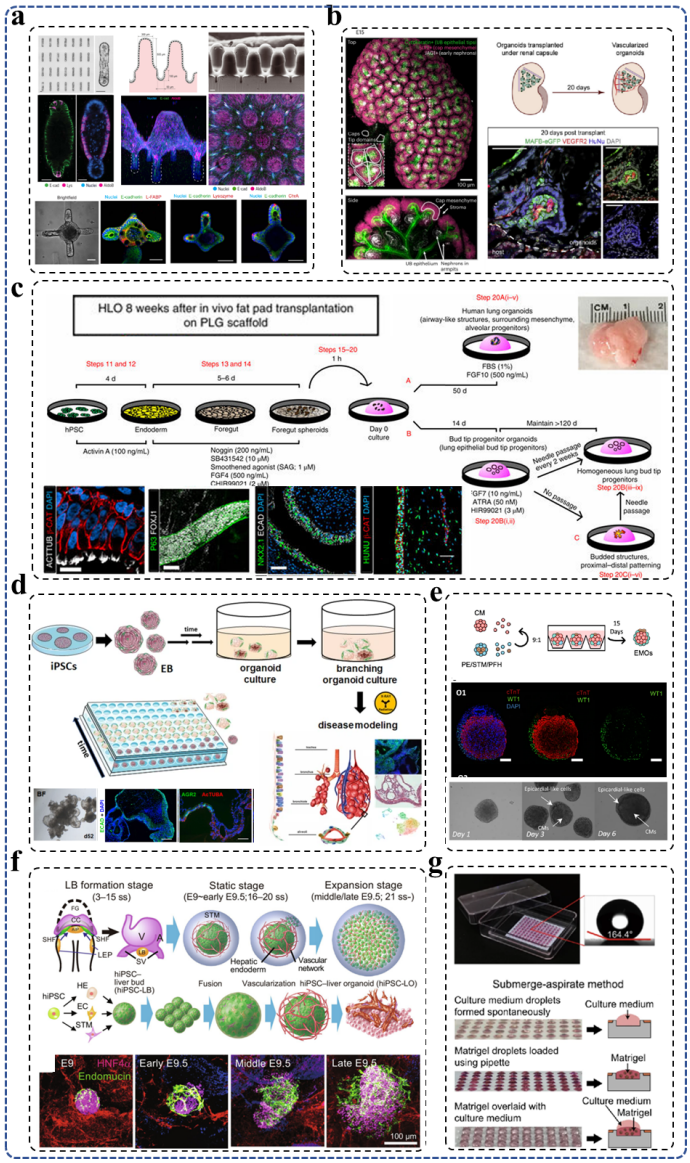


Figure 2. Representative single-organoid studies. (a) Engineered microenvironments for extrinsic control of intestinal organoid development. Reprinted with permission from Gjorevski *et al.*[8] Copyright © 2022 American Association for the Advancement of Science. (b) Overview of kidney organoid development. Reprinted with permission from Prahl *et al.*[9] Copyright © 2024 The Author(s), under exclusive license to Springer Nature Limited. (c) Generation of human pluripotent-stem-cell-derived lung organoids. Reprinted with permission from Miller *et al.*[30] Copyright © 2019 The Author(s), under exclusive license to Springer Nature America, Inc. (d) Matrix-free human lung organoids derived from induced pluripotent stem cells (iPSCs) for lung-injury modeling. Reprinted from Budeus *et al.*[31] (e) Co-culture of pro-epicardium/septal transverse mesenchyme/posterior foregut/hepatic diverticulum (PE/STM/PFH) cells with cardiomyocytes during heart-organoid development. Reprinted from Branco *et al.*[32] (f) Human iPSC-derived liver organoids generated by fusion of liver buds. Reprinted with permission from Tadokoro *et al.*[33] Copyright © 2024 American Association for the Advancement of Science. (g) Integrated superhydrophobic microwell array chip for rapid analysis of lung-cancer organoids. Reprinted from Hu *et al.*[34]

epithelial patterning. These spatial variations activated mechanosensing pathways such as Yes-associated protein (YAP) and Notch, localizing Paneth cell differentiation and suppressing stem cell fates to specify crypt- and villus-like domains. Unlike traditional cultures reliant on random budding, geometry alone yielded macroscopic organoids with accurate crypt-villus architecture. By prioritizing construction precision, this study provides a framework for scalable, reliable intestinal models.

Traditional human organoid cultures fail to replicate the dynamic equilibrium of *in vivo* tissues, often favoring proliferation with limited diversity or differentiation at the cost of scalability. Yang *et al.*[35] developed a tunable human small intestinal organoid (hSIO) system to balance

stem cell self-renewal and differentiation. They proposed that enhancing stem cell "stemness" would amplify differentiation potential under a single culture condition. Using small-molecule modulators of wingless-related integration site (WNT), Notch, and bone morphogenetic protein (BMP) pathways, they optimized intestinal stem cell behavior without artificial gradients. Bromodomain and extraterminal (BET) inhibitors reversibly shifted the balance toward enterocyte differentiation with high proliferation, while niche signal manipulations induced unidirectional differentiation into secretory lineages. The optimized hSIO system yielded organoids with greater cellular diversity (enterocytes, goblet cells, rare Paneth cells) and strong proliferative capacity, overcoming prior limitations by engineering culture conditions rather than post-formation interventions.

Beyond these cornerstone studies, recent efforts have pushed the boundaries of intestinal organoid development through innovative engineering. Zhang *et al.*[36] pioneered a direct reprogramming method using human urine cells to generate intestinal organoids, bypassing the pluripotent stage to reduce tumorigenic risks while preserving structural fidelity to native tissue. Lorenzo-Martín *et al.*[37] introduced a mini-colon model integrating microfabrication and optogenetics, enabling spatiotemporal control of tumorigenesis with organoids exhibiting complex crypt-villus-like patterns. Baghdadi *et al.*[38] explored mechanosensing by knocking out Piezo in mouse organoids, revealing their role in intestinal stem cell self-renewal and differentiation through mechanical cues such as basement membrane stiffness. These studies underscore a trend toward integrating physical constraints, chemical modulators, mechanical cues, or biological tools to refine organoid construction, prioritizing precision and control over traditional self-organization to build robust, reproducible intestinal organoid systems.[35]

(b) Kidney organoids

Kidney organoids are typically derived from human pluripotent stem cells (hPSCs), which differentiate into 3D structures resembling nephron units for studying kidney development and disease. A key aspect of production is mimicking nephron-like structures—proximal and distal tubules, glomeruli, and collecting ducts—with efficiency and scalability. Tran *et al.*[39] achieved a breakthrough by generating thousands of kidney organoids with 1–2 nephron-like structures per unit, using single-cell transcriptomics and immunofluorescence to study nephrogenesis and disease mechanisms. These organoids, patterned through specific signaling pathways, provide insight into processes of human kidney development and disease.

The functional capabilities of kidney organoids, including filtration and reabsorption, are pivotal for modeling renal diseases. Organoids must replicate processes such as blood filtration and selective reabsorption of water, ions, and nutrients. This has been extensively studied in PKD. In Tran *et al.*'s[39] study, *PKD1* and *PKD2* mutations induced cyst formation—a hallmark of PKD. Screening 247 protein kinase inhibitors identified compounds that blocked cysts without impairing growth, showing that kidney organoids can recapitulate disease phenotypes and model therapies. Their ability to maintain filtration and reabsorption even in diseased states highlights their value for studying disease progression and testing drugs. Such systems also allow investigation of how nephron dysfunction, as in PKD, alters kidney function.

A major challenge in kidney organoids is achieving sufficient maturation, particularly in the proximal tubule, essential for solute reabsorption. Vanslambrouck *et al.*'s[40] study addresses this by enhancing the specification of metanephric nephron progenitors, producing elongated and functionally distinct proximal tubules. These organoids demonstrated improved functionality, including albumin and organic cation uptake vital for studying nephron reabsorption, better response to the nephrotoxic agent cisplatin, and increased viral replication when exposed to SARS-CoV-2. This maturation of proximal tubules into their S1, S2, and S3 segments allows for more accurate modeling of proximal tubule–related diseases, such as nephrotoxicity and inherited disorders.

In addition to genetic factors, mechanical forces are essential in kidney development. Incorporating physical stress into organoid cultures could improve structure and function, making them more reliable models for kidney disease and regenerative medicine. Prahl *et al.*'s[9] research on nephron-forming niches shows how mechanical stress, generated by mesenchymal cell packing at ureteric bud tips, impacts nephron development. As these niches pack more tightly, they undergo rhythmic stresses that influence cell fate. Mathematical models further demonstrated that kidney curvature constrains this packing, causing a stiffening transition during embryonic development. Such mechanical factors shape the spatial organization of nephron progenitors and their differentiation into podocytes and tubular cells. These insights inform kidney organoid engineering, particularly the design of artificial models that better mimic *in vivo* tissue behavior (Figure 2b).

Beyond the classic studies of PKD and proximal tubule maturation, efforts to optimize the long-term stability and physiological relevance have contributed to our understanding of kidney organoid functionality, such as studies on the role of specific genes in kidney development. Freedman *et al.*[41] used CRISPR editing to model PKD, confirming the functional defects in *PKD1*

and *PKD2* mutant organoids. Other studies have focused on improving vascularization within kidney organoids to mimic real kidney circulation, essential for filtering blood. Kroll *et al.*[42] developed a perfusable kidney organoid model incorporating endothelial cells to form microcirculation, an essential step toward fully functional organoid systems. These efforts highlight the diverse methodologies used to improve kidney organoid models.

(c) Lung organoids

Lung organoids are 3D cell culture models that mimic the structural and functional characteristics of the developing lung *in vitro*. Their unique morphology and dynamic growth provide insights into lung development and function. The budding growth of lung organoids is a complex process involving differentiation and morphogenesis, driving endoderm induction, foregut patterning, and formation of bronchial and alveolar structures. Notably, lung organoids display highly irregular macroscopic morphologies, reflecting their ability to adapt to the structural and functional features of real lung tissues, making them promising models to study biomechanical strain.

Simulating complex respiratory behaviors—such as dynamic airflow, pressure responses, and biomechanical strain—remains an underexplored aspect of organoid research. Recreating dynamic breathing in lung organoids is key to mimicking physiological function. Some studies have shown bronchial-like cavities within organoids that imitate stretching and contraction, modeling fundamental respiratory processes. Enhancing responses to mechanical strain could support studies of respiratory dynamics in health and disease. Biomechanical strain modeling has also been used to regulate mechanical forces, promoting cellular differentiation and alveolar maturation, and advancing the construction of functional respiratory systems *in vitro*. Despite individual progress in morphology and function, integrated approaches are needed to optimize the consistency of organoids for structural and functional fidelity. Irregular morphology challenges require high-resolution imaging technologies and dynamic monitoring to enhance their modeling accuracy and physiological relevance.

Current protocols for generating lung organoids are time-intensive, requiring optimization to shorten production cycles without compromising biological fidelity. Miller *et al.*[30] introduced a systematic protocol to derive lung organoids from hPSCs, marking a landmark in the field. This multi-step differentiation process mirrors key stages of lung development, including endoderm induction, foregut patterning, and the creation of two organoid types: bud tip progenitor organoids and fetal lung–like organoids. The methodology highlights pathways for improving structural fidelity and cellular characteristics, closely aligning with human fetal lung tissue while addressing challenges of cellular maturity and functional integration (Figure 2c). The generated lung organoids display bronchial- and bronchiolar-like architectures surrounded by mesenchymal tissue and express alveolar-cell markers, providing a platform to study epithelial–mesenchymal interactions during lung development. Bud tip progenitor organoids contain highly proliferative multipotent cells with multilineage differentiation and strong engraftment potential.

Lung organoids have become indispensable for modeling respiratory diseases and developmental processes. Pezet *et al.*[43] developed a pulmonary fibrosis model using induced respiratory airway progenitors (iRAPs) derived from hPSCs, achieving an unprecedented *in vitro* replication of fibrosis pathology. Their protocol generated expandable iRAPs closely resembling terminal bronchiolar and alveolar tissues, with a purification rate of ~98%. These iRAPs differentiated into mature alveolar epithelial type I (AT1) and type II (AT2) cells, creating a reliable platform to study disease mechanisms and therapies. By deleting Hermansky–Pudlak syndrome 1 (*HPS1*) in iRAPs, they reproduced aberrant differentiation features and profibrotic fibroblast recruitment seen in idiopathic pulmonary fibrosis. This model enabled detailed investigation of respiratory airway/terminal and respiratory bronchiole (RA/TRB)-associated populations, transitional AT2 cells, and other pathological features of fibrosis. Its scalability allowed production of large quantities of iRAP-derived cells and revealed lineage relationships among airway progenitors, offering insights into fibrosis dynamics unattainable in animal models.

These diverse studies illustrate the versatility and transformative potential of lung organoids in exploring respiratory diseases. Salahudeen *et al.*[44] developed distal lung organoids to study SARS-CoV-2 infection, demonstrating angiotensin-converting enzyme 2 (ACE2) receptor–mediated mechanisms and identifying club cells as infection targets. Leibel *et al.*[45] used lung organoids to examine multi-strain SARS-CoV-2 tropism and pulmonary innate immune responses triggered by canonical and noncanonical viral pathways, uncovering therapeutic opportunities with exogenous surfactants. Important advances have also been made in modeling chronic lung diseases. Basil *et al.*[46] identified respiratory airway secretory cells as progenitors for alveolar AT2 cells, revealing disrupted differentiation in chronic obstructive pulmonary disease. Jones *et al.*[47] examined injury-induced niches and mesenchymal regulation, showing mesenchymal AF1 cells play a critical role in repair outcomes. Furthermore, Budeus *et al.*[31] developed a matrix-free method to generate iPSC-derived human lung organoids, providing a robust model to study lung injury, particularly radiation-induced damage, and offering new insights into the radiation sensitivity of

different lung cells (Figure 2d).

(d) Heart organoids

Heart organoids are an important advance in regenerative medicine and cardiac modeling, providing unique insights into early heart development and disease. Among human organoid systems, they have progressed rapidly, particularly in mimicking cardiogenesis and myocardial functions. Their defining feature is the ability to generate beating myocardial tissues—essential for understanding cardiac physiology and clinical applications. Early efforts focused on producing cardiomyocyte aggregates with contractility, while combining biochemical cues, self-organized cellular properties, and engineered scaffolds has since improved their reliability as platforms for modeling structural and cellular heart dynamics. Recent advancements now incorporate chamber formation, epicardial layers, and vascular-like networks. This progression positions heart organoids as key tools for investigating congenital heart defects, cardiomyocyte maturation, and myocardial remodeling. The transition from simple contractility to complex systems with cellular interactions and physiological functions underscores their promise in organ regeneration and therapeutic modeling.

Early heart organoids demonstrated rhythmic contractility and myocardial organization, but newer designs, such as the multilineage self-organized organoid model, mark a significant advance. Branco *et al.*[32] recreated the transient pro-epicardium, a critical feature of cardiac embryogenesis, along with septal transverse mesenchyme and posterior foregut structures. Co-culturing these with cardiomyocyte aggregates produced epicardium–myocardium organoids, which recapitulate epicardial layers covering myocardium-like tissues. This model not only enhances structural fidelity but also reveals interactions between epicardial cells and myocardium, including cardiomyocyte proliferation and maturation driven by paracrine signaling. The development of multilineage organoids underscores the role of morphogen pathways and the necessity of 3D environments to better mimic soluble factor gradients pivotal in cardiac differentiation (Figure 2e).

The primary use of heart organoids is in evaluating therapeutic efficacy for cardiac pathologies, particularly myocardial infarction (MI) repair and cardiovascular toxicity. Yang *et al.*[48] developed an engineered cardiac repair model mimicking MI remodeling. This system captures the phased process—from hypoxic stress and cardiomyocyte apoptosis to fibroblast activation and ECM deposition—while also simulating post-MI electrophysiological dysfunction, a hallmark of cardiac failure. Yang's approach quantifies cell fate changes and identifies regulatory pathways including transforming growth factor-beta (TGF-β), Rho-associated coiled-coil-containing protein kinase (ROCK), and WNT signaling. Validation with modulators such as SB431542 (TGF-β inhibitor) and CHIR99021 (WNT activator) highlights the utility of staged modulation to arrest fibrosis and enhance infarct repair. Beyond functional recovery, the model provides a humanized framework for rapid screening of antifibrotic drugs, though its scope is limited to post-ischemic fibrotic repair. Nonetheless, this engineered model offers a valuable assay platform for drug testing and myocardial regeneration in ischemic heart disease.

As heart organoids advance, their relevance for newborn and adult cardiac pathologies—from myocardial defects to chronic infarction—will deepen. Volmert *et al.*[49] introduced self-organized patterned heart organoids closely resembling human embryogenesis at 6 to 10 weeks of gestation. Their study integrated metabolic and retinoic acid signaling gradients to recapitulate chamber formation and anterior–posterior axis patterning. This model produced functional atrial and ventricular cardiomyocytes, organized epicardial structures, and proepicardial organ formation within hollow chambers—features not previously achieved in heart organoids. Demonstrating utility, Kiselev *et al.*'s system emulated congenital heart defects induced by ondansetron exposure, linking the drug to ventricular septal abnormalities. This model represents a technical advance for pharmacological applications and disease modeling by enabling researchers to trace developmental errors and their outcomes.

Heart organoids are transformative tools in regenerative medicine, providing structural and functional replicas for drug screening and congenital heart defect studies; organoid systems are leveraged for high-throughput screening. Mills *et al.*[10] emphasize how bioengineered cardiac organoids can reduce false-positive hits from 2D assays and provide mechanistic insights into drug efficacy and toxicity, precisely identifying the mevalonate pathway's central role in cardiomyocyte proliferation. Thus, reliable platforms to study regenerative strategies without compromising organ functionality are needed. Similarly, Zhang *et al.*'s[50] 3D cardiac tissue sheet demonstrates enhanced contractility and paracrine cytokine secretion for angiogenesis, facilitating ischemic heart disease studies. Additionally, Lewis *et al.*'s[51] hybrid system integrates 2D and 3D approaches to analyze drug-induced cardiotoxicities, underscoring the versatility of organoids as predictive models. However, immature vascularization, restricted electrophysiological mimicry, and the absence of immune cells and neural crest cells are current limitations.

(e) Liver organoids

The liver is a cornerstone of human physiology, orchestrating essential functions such as detoxification and metabolism.

As a parenchymal organ, it depends on hepatocytes—its primary functional cells—to process toxins, metabolize nutrients, and maintain biochemical homeostasis. These hepatocytes are arranged within the liver lobule, a hexagonal unit reflecting the organ's architectural precision. At the lobule's periphery, portal triads—composed of the hepatic artery, portal vein, and bile duct—deliver a dual blood supply rich in oxygen and nutrients, while the central vein drains processed blood into systemic circulation. This vascular network sustains the liver's metabolic activity and underscores its role as a detoxifying powerhouse.

Unlike traditional 2D cultures, organoids aim to recapitulate the liver's 3D complexity, restoring lobular structure and blood supply dynamics to bridge the gap between *in vitro* models and *in vivo* reality, with structural fidelity enhancing functional relevance. Tadokoro *et al.*[33] engineered liver organoids to reflect both structural and functional features of the liver, particularly in fibrosis. Starting with human iPSCs (hiPSCs), they developed liver buds—early fetal liver–like structures—and fused them into larger liver organoids mimicking midgestational fetal liver. This fusion fostered interactions among hepatocytes, endothelial cells, and mesenchymal cells, producing complex structures with hepatocytes, vasculature, and bile ducts after transplantation. The goal was not to replicate adult liver anatomy but to harness fetal liver's regenerative and immunomodulatory properties. When grafted onto chemically induced fibrotic livers in immunocompromised mice, these hiPSC-derived liver organoids integrated with host vasculature and promoted regeneration. A key feature was their ability to reduce fibrosis via M2 macrophage polarization, driven by secretion of macrophage-recruiting and antifibrotic factors—more pronounced in fetal than adult liver. This design leveraged fetal-specific traits such as hematopoiesis to influence the host microenvironment (Figure 2f).

A pragmatic compromise is to sacrifice some anatomical detail for high-throughput analysis. Kimura *et al.*[7] took a distinct yet complementary approach that emphasizes metabolic fidelity, restoring sufficient hepatocyte function to study genetic impacts and probe genotype–phenotype associations in non-alcoholic steatohepatitis (NASH) without prioritizing complex structures such as bile ducts or sinusoids. His team devised a pooled human organoid panel from hiPSC-derived hepatocytes, engineered to emulate steatohepatitis under insulin-insensitive conditions—a reflection of the liver's metabolic role in diabetic states. These organoids were not designed to replicate full lobular architecture but to provide a scalable platform for large-scale phenotyping, focusing on lipid accumulation and inflammation as NASH hallmarks. A key finding was the role of the GCKR-rs1260326:C>T variant, which modulates disease severity depending on metabolic context. Their method differentiated foregut progenitors into hepatic organoids, maintaining hepatocyte identity while exposing them to fatty acid overload to mimic NASH pathology. This setup enabled identification of mitochondrial dysfunction linked to the *GCKR* variant, critical for drug evaluation and disease modeling.

A challenge in liver organoid design is pre-vascularization without compromising parenchymal integrity. Fan *et al.*[52] introduced a nonparenchymal cell grafting strategy to construct hiPSC-derived hepatobiliary organoids (hHBOs) by integrating endothelial and mesenchymal cells at defined differentiation stages. The process began with foregut stem cell spheroids differentiated into hHBOs on a microfabricated chip, avoiding Matrigel for uniformity. Endothelial grafting was optimized at the hepatic maturation stage, when hepatocytes expressed vascular endothelial growth factor (VEGF) and angiopoietins, promoting endothelial invasion and sprouting to mimic sinusoidal development. Mesenchymal cells, notably MRC-5 fibroblasts, enhanced this process, stabilizing vasculature and modestly boosting lipid metabolism via *ASGR1* upregulation, without altering hepatocyte fate. Post-transplantation into mice, these pre-vascularized hHBOs integrated with host vasculature and self-organized into hepatic zones and bile ducts, reflecting the liver lobule's dual blood supply and biliary network.

Beyond these flagship studies, many efforts have enriched liver organoid development, each addressing structural and functional restoration. Leite *et al.*[53] crafted 3D spheroids combining HepaRG hepatocytes and primary human hepatic stellate cells to detect drug-induced fibrosis by maintaining hepatic stellate cell quiescence alongside hepatocyte metabolic competence. This model, responsive to compounds such as allyl alcohol and methotrexate, mirrors the liver's injury-response dynamics without its full lobular architecture. Wu *et al.*[54] scaled up hepatic precursor organoids using human ESCs in bioreactors, embedding low-concentration Matrigel to support expansion while retaining hepatocyte polarity—ideal for drug testing despite heterogeneity risks. Liu *et al.*[55] fabricated decellularized liver scaffolds seeded with hiPSC-derived cells with restored organ-level vasculature and metabolism, prioritizing sinusoidal-like structures for toxicity studies. Wang *et al.*[56] demonstrated that hepatobiliary organoids incorporated functional bile ducts, leveraging polarized hepatocytes to study clearance functions. Utami *et al.*[57] used oxygen-permeable microwells to enhance cytochrome P450 (CYP) activity, refining drug metabolism models. These approaches emphasize restoring key liver features—vascularity, biliary networks, or metabolic zones—tailored to fatty liver and fibrosis modeling; they share a focus on structural ingenuity over experimental minutiae.

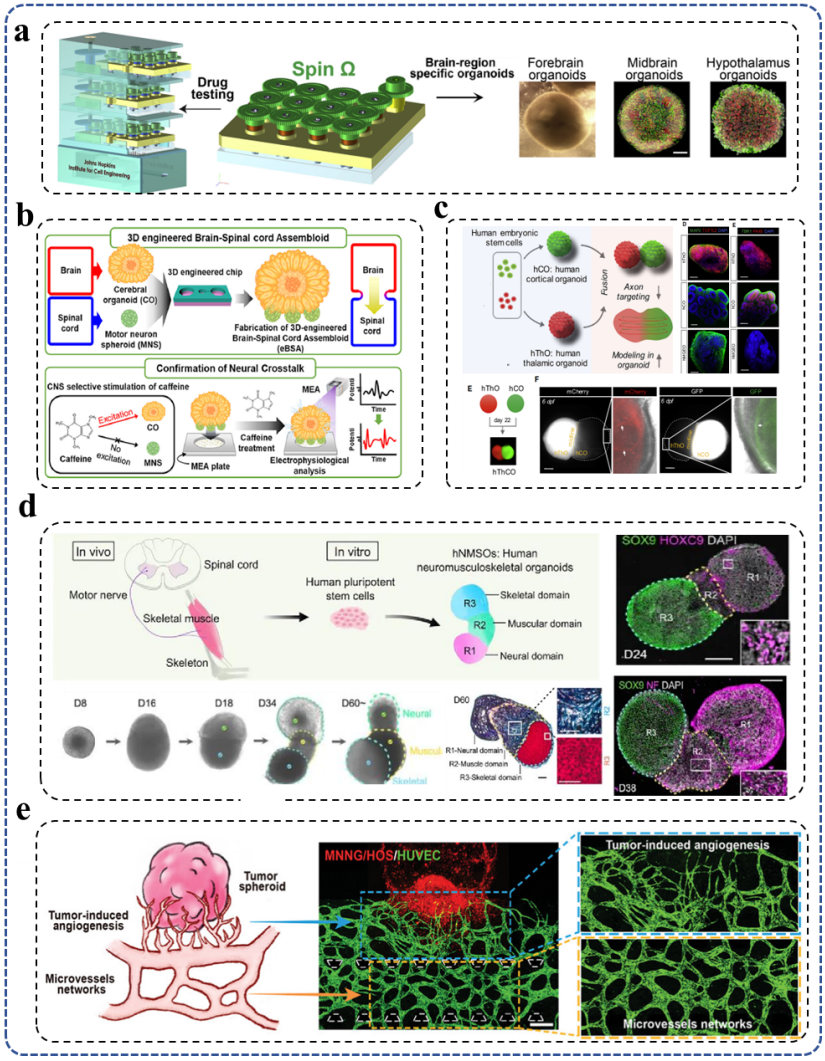


Figure 3. Representative neural and vascularized organoid studies. (a) Brain-region-specific organoids for disease modeling. Reprinted with permission from Qian *et al.*[58] Copyright © 2016 Elsevier. (b) Engineered brain-spinal cord assembloid for electrophysiological analysis of neural signal transfer. Reprinted from Son *et al.*[59] (c) Reciprocal projections in fused thalamic and cortical organoids. Reprinted with permission from Xiang *et al.*[60] Copyright © 2018 Elsevier. (d) Self-organized neuromusculoskeletal tri-tissue organoids derived from human pluripotent stem cells. Reprinted with permission from Yin *et al.*[61] Copyright © 2024 The Author(s). (e) Confocal image of a tumor perivascular niche with heterogeneous microvasculature and a vascularized tumor spheroid (scale bar: 400 μm). Reprinted with permission from Du *et al.*[62] Copyright © 2024 Wiley-VCH GmbH.

2.1.3. Brain and nerve organoids

Brain organoids represent a major advance in modeling the human nervous system, bridging the gap between simplistic cell cultures and the complexity of *in vivo* studies.[59] Derived from iPSCs, these 3D constructs can self-organize into structures mimicking the whole brain or specific regions—forebrain, midbrain, hindbrain, and thalamus. Qian *et al.*[58] developed a miniaturized spinning bioreactor system, SpinΩ, to generate human brain organoids with greater reproducibility and lower cost. Using this system, they cultured forebrain-specific organoids from hiPSCs that displayed key features of human cortical development, including a well-organized outer subventricular zone with neural progenitor cells and organized neuronal subtypes across all six cortical layers. These forebrain organoids also produced γ-aminobutyric acid (GABA)ergic neurons, reflecting features unique to human brain development and absent in rodent models. The versatility of SpinΩ was further demonstrated in generating midbrain and hypothalamic organoids. The forebrain platform was applied to model Zika virus (ZIKV) infection, showing that African and Asian ZIKV strains preferentially infect neural progenitors, causing increased cell death and suppressed proliferation. This reduced neuronal layer volume, resembling the pathological features of human microcephaly. The ability to model ZIKV infection at different stages of cortical

neurogenesis underscores its value for studying brain development and disease mechanisms. Additionally, SpinΩ significantly reduced media volume, making it a cost-effective platform for large-scale, high-throughput applications such as drug screening and disease modeling (Figure 3a).

Brain organoids can generate diverse cell types, including cortical and retinal cells. Their diversity of cell types, from neurons to glial cells, and capacity to form intricate connections akin to neural networks underscore their potential as dynamic systems reflecting developmental principles rather than simple aggregates.[63] Gabriel *et al.*[64] developed an *in vitro* system to engineer brain organoids capable of forming optic vesicles, essential for eye development. Using iPSC-derived brain organoids, they demonstrated the formation of bilateral optic vesicles that matured into complex structures with neuronal and non-neuronal cell types. These optic vesicle–containing brain organoids (OVB-organoids) incorporated retinal progenitor cells, retinal pigment epithelia, lens-like cells, axon-like projections, electrically active neuronal networks, and microglia. Notably, OVB-organoids were light-sensitive, exhibiting photosensitive activity across light intensities, which could reset after transient photobleaching. Bilaterally symmetric optic vesicles formed without artificial signaling centers, underscoring the intrinsic self-patterning capacity of iPSCs. The ability to generate complex, photosensitive structures within 50–60 days opens new opportunities for studying early neurodevelopment and eye disorders. Son *et al.*[59] also presented a 3D-engineered brain–spinal cord assembloid on a multielectrode array (MEA) chip to geometrically align these components with signal transmission across the central–peripheral divide. Assembloids are spatially organized multicellular constructs and organoids that function more like real human tissue and organs produced from diverse cell types (Figure 3b).

Cortical organoids, for example, can differentiate into all brain regions, offering a panoramic view of neurogenesis. Electrophysiological recordings and calcium imaging further demonstrated neuronal maturation and network activity in fused organoids. Xiang *et al.*[60] presented a method for generating region-specific brain organoids with features of the medullary spinal trigeminal nuclei (SpV). Using hPSCs with small mothers against decapentaplegic (SMAD) inhibition and WNT/RA activation, they created SpV-like organoids (hmSpVOs) that exhibited morphological and molecular characteristics of the medullary SpV, including lineage markers and neural connectivity with the thalamus. By integrating hmSpVOs with thalamic organoids, they established a functional SpV–thalamus circuit. Another study explored reciprocal projection loops by fusing human ESC–derived thalamic-like organoids (hThOs) with cortical-like organoids, offering new ways to study thalamocortical interactions. Single-cell RNA sequencing showed that hThOs uniquely expressed thalamic markers, with glutamatergic neurons predominating. When fused with human cortical–like organoids, hThOs extended axons forming thalamocortical projections, while cortical neurons projected back to the thalamus, establishing corticothalamic connections. Immunostaining confirmed synapse formation, mimicking *in vivo* thalamocortical pathways (Figure 3c).

Beyond these milestones, numerous studies enrich the neurosystem organoid landscape. Region-specific organoids, such as those of the spinal cord or fused assemblies (e.g., cortex–optic nerve), allow targeted exploration of functional specialization. Yin *et al.*[61] reported a significant advancement in human neuromusculoskeletal tri-tissue organoids (hNMSOs) with their integration of neural, muscular, and skeletal domains within a single 3D construct. Starting from hiPSCs, they employed a static-to-spinning co-development strategy, using Sonic hedgehog (SHH) signaling and skeletogenic factors to induce simultaneous lineage differentiation. Single-nucleus RNA sequencing and spatial transcriptome profiling confirmed distinct lineages and their spatial organization in hNMSOs. The neural domain acquired a ventral-specific identity and generated motor neurons that innervate skeletal muscles. These organoids self-organized into spatially distinct yet interconnected regions—neural zones with ventral motor neurons, contractile muscle, and supportive skeletal tissue. During the maturation process of hNMSOs, the three tissues showed tissue-specific development (Figure 3d). Functional studies demonstrate that hNMSOs have robust spontaneous electrical activity with functional connections between neural and muscular tissues, motor neurons that innervate skeletal muscle, and skeletal support enhancing muscle maturation. Moreover, hNMSOs provide a valuable model for studying human neuromusculoskeletal crosstalk and related diseases.

2.1.4. Vascularized organoids

The development of vascularized organoids marks a pivotal step in overcoming one of organoid technology's main challenges: establishing a functional vascular network. iPSC-derived organoids are particularly promising due to their pluripotency and ability to differentiate into endothelial cells and mural cells, including pericytes and vascular smooth muscle cells. Without robust vasculature, organoids suffer from limited nutrient and oxygen delivery, often leading to necrosis in larger constructs. Advances in this field highlight the potential of iPSC-derived vascularized organoids to bridge *in vitro* and *in vivo* physiology, offering insights into vascular development and tissue engineering.

Vascularization not only supports cell survival but also enhances physiological relevance by mimicking *in vivo* tissue dynamics, critical for disease modeling and regenerative medicine. A landmark study by Du *et al.*[62] exemplifies engineering approaches to vascularize organoids through a patient-derived tumor organoid (PDTO)-on-a-chip model. This system integrates PDTOs with microfluidic technology to construct a hierarchical, tumor-specific microvascular network, reflecting the structural diversity of clinical tumors. PDTOs were seeded within a multi-channel microfluidic chip alongside endothelial cells, enabling self-assembled vasculature with perfusable lumens and tumor-induced angiogenic sprouting. The model produced a layered architecture, with disorganized angiogenesis near the tumor and organized microvessels distally, closely mimicking *in vivo* tumor vasculature. Microfluidics provided precise microenvironmental control, facilitating nutrient supply and real-time monitoring of tumor–vascular dynamics. This platform prioritized vascular functionality—ensuring perfusion and structural integrity—rather than focusing only on downstream applications. While the study highlighted Notch signaling in tumor cell migration toward vessels, its key contribution was demonstrating a scalable, reproducible method for vascularizing heterogeneous organoids. Particularly relevant for vascular-rich tumors such as sarcomas, this model sets a precedent for strategies emphasizing vascular fidelity and adaptability, offering a versatile tool for studying vascularization across organoid types (Figure 3e).

The process typically begins with mesoderm induction of iPSC aggregates, followed by endothelial differentiation within a 3D matrix such as collagen I–Matrigel to form vessel-like structures. In contrast to engineered systems, Wimmer *et al.*[65] developed a protocol for generating self-organizing 3D blood vessel organoids from hPSCs, emphasizing intrinsic cellular mechanisms over external manipulation. The process begins with mesoderm induction of hPSC aggregates, followed by differentiation into endothelial networks and pericytes within a collagen I–Matrigel matrix, yielding organoids that recapitulate human microvasculature within 2–3 weeks. The vascular networks feature endothelial cell–lined vessels supported by mural cells, forming a scalable system expandable in suspension culture. A key feature is integration with host vasculature upon transplantation into immunocompromised mice, where organoids matured into functional arteries, arterioles, and veins connected to mouse circulation. This self-assembly leverages the developmental potential of hPSCs, bypassing biofabrication tools such as bioprinting yet achieving a perfusable vascular system. The focus is on construction—optimizing differentiation cues and matrix composition—rather than post-formation analyses, making it a foundational technique for vascularizing organoids such as brain or liver models. While lacking active flow *in vitro*, its transplantability suggests a path toward functional perfusion, offering a complementary strategy to engineered approaches and underscoring the versatility of hPSC-derived systems in vascular organoid research.

This self-organizing capacity enables hierarchical vascular networks resembling native microvasculature, forming the basis for functional organoids. Another approach to vascularization involves co-culturing vascular and organ-specific organoids, as in the development of vascularized brain organoids. In this strategy, vascular organoids are fused with brain organoids, cultivating endothelial and neural lineages together to form blood–brain barrier (BBB)-like structures. Vascular organoids rich in endothelial cells are embedded with brain organoids in a supportive matrix, allowing spontaneous vascular branching and integration with neural tissue. The resulting vascularized brain organoids show selective permeability characteristic of the BBB, supported by microglial cells that enhance functionality through immune responses and synapse phagocytosis. Unlike bioprinted or microfluidic systems, this method relies on cellular self-organization, augmented by cues such as VEGF to promote endothelial differentiation and vessel formation. The study emphasized construction over experimental outcomes, focusing on building a robust vascular network that supports neurogenesis without requiring active perfusion *in vitro*.[66]

While diverse in execution, they share a focus on constructing functional vasculature, with variations in complexity and scalability suited to different organoid applications. Achieving a perfusable, stable vascular system remains a technical hurdle, requiring innovative engineering strategies. Beyond these examples, several studies have advanced vascularization strategies with distinct methods. Liu *et al.*[67] used genetic engineering by introducing an inducible ETS variant transcription factor 2 (ETV2) into kidney organoids, achieving robust endothelialization that enhanced nephron maturation without external scaffolds. Skylar-Scott *et al.*[68] utilized orthogonal differentiation of stem cells to co-develop vascular and neural lineages in cortical organoids, generating spatially organized vascular networks via cell aggregation. Holloway *et al.*[69] optimized culture conditions to maintain endogenous endothelial cells in intestinal organoids, resulting in vascularized constructs with organ-specific identity through intrinsic mechanisms. Additionally, 3D bioprinting has emerged as a powerful engineering tool, with applications in liver and breast tumor organoids, where precise deposition of endothelial cells and biomaterials forms perfusable vascular channels. These approaches illustrate techniques ranging from self-assembly to bioengineering that address the challenge of vascularizing organoids.[70]

2.1.5. Tumor organoids

Patient-derived tumor organoids preserve important histological and genetic features of their source tumors, but conventional expansion can be too slow and material-intensive for clinical drug selection. Hu *et al.*[34] addressed this limitation by coupling lung cancer organoids with an integrated superhydrophobic microwell array chip (InSMAR-chip). As shown in Figure 2g, the device contains 108 microwells of approximately 440 nL each, allowing passage-0 organoids to be distributed into isolated 3D cultures and exposed to multiple drugs without prolonged expansion. The miniaturized workflow generated drug-response results within one week while maintaining organoid growth, viability, and parental-tumor characteristics. Agreement with genomic alterations, xenograft responses, and available clinical outcomes illustrates how microengineering can convert organoid heterogeneity from a practical barrier into a rapid, patient-specific testing opportunity.

Despite varied origins, their shared strength is recapitulating tumor heterogeneity and microenvironmental features, laying a foundation for downstream studies. Papargyriou *et al.*[71] developed a branched organoid model for PDAC, embedded in collagen gels, that effectively recapitulated the phenotypic diversity and heterogeneity observed *in vivo*. Derived from patient tumor tissues, these organoids exhibited morphologies linked to transcriptional programs such as EMT, reflecting PDAC subtypes and cellular states. The study showed that organoids captured both intertumoral and intratumoral heterogeneity, with epithelial and mesenchymal phenotypes displaying distinct responses to chemotherapy and radiotherapy. Using Morphologic Organoid Phenotypic Heterogeneity Mapping (MOrPHeMap), the authors quantified this diversity and identified phenotype-specific therapeutic targets, such as mitogen-activated protein kinase kinase/rapidly accelerated fibrosarcoma (MEK/RAF) inhibitors that reprogrammed mesenchymal organoids into a uniform phenotype. This finding highlights PDAC's notorious drug resistance, potentially driven by phenotypic plasticity, with organoids providing a platform to dissect these mechanisms. Unlike mutation-driven models, this approach emphasizes dynamic phenotypic changes, underscoring organoids' superiority in simulating complex disease progression. Nonetheless, the model's limited microenvironmental representation suggests the need for immune cell co-cultures to enhance clinical relevance.

Compared to 2D cell lines, their 3D structure more closely mimics *in vivo* conditions, reducing genetic drift from prolonged passaging. Glioma organoids from samples often pose challenges in tissue acquisition and culture. Peng *et al.*[72] proposed an individualized patient tumor organoid (IPTO) model for central nervous system tumors, including glioma, by culturing patient-derived tumor explants in iPSC-derived cerebral organoids. Within 10 days, IPTOs were generated with a higher success rate than traditional methods. Validated through histopathology, genomics, and single-cell RNA sequencing, IPTOs preserved cellular heterogeneity, molecular features, and the microenvironment of parental tumors, accurately predicting patient responses to chemotherapy (e.g., temozolomide) and targeted therapies, including resistance mechanisms. IPTOs avoid dissociation-induced spatial heterogeneity, combine rapid establishment with microenvironment retention, and are particularly suited for diverse central nervous system tumors, especially given glioma's invasive nature.

Tumor organoids share key features: high-throughput cultivation, pronounced heterogeneity, and close resemblance to parental tumors. These attributes make them pivotal for drug screening, disease mechanism studies, organoid biobanks, and bioinformatics-assisted drug development. *Rao et al.*[73] established liver cancer organoids with a 40.9% success rate, tailoring chemotherapy for intrahepatic cholangiocarcinoma via drug sensitivity testing. Jia *et al.*[74] used single-cell transcriptomics to reveal molecular subtype heterogeneity in breast cancer organoids, with implications for lung cancer. Xu *et al.*[75] developed a high-throughput screening platform, identifying seven drug candidates in cervical cancer organoids, showcasing efficiency applicable to drug development. Mo *et al.*[76] constructed a colorectal cancer liver metastasis organoid biobank, capturing heterogeneity and predicting chemotherapy responses to liver cancer. Liu *et al.*[77] paired lung cancer organoids with single-cell RNA sequencing to dissect immunotherapy responses in the microenvironment. Across cancer types, these studies underscore organoids' high-throughput and heterogeneity advantages. They signal a shift from isolated models to integrated platforms, particularly for bioinformatics-aided drug development, though success rates and microenvironment simulation remain challenges requiring interdisciplinary solutions.

2.2. Organ-on-a-chip and human multi-organ-on-a-chip systems

Organ-on-a-chip platforms are microfluidic systems that use micro- and nanoscale fabrication and controlled fluid flow to emulate selected human-organ functions *in vitro*.[1,78] Depending on scope, OoC platforms can be classified as single-organ devices or multi-organ systems. Single-organ devices reproduce selected liver, kidney, gut, or cardiac functions using organ-specific microarchitectures.[79] Multi-organ systems connect distinct tissue modules to model inter-organ communication, systemic responses, and pharmacokinetic (PK)–pharmacodynamic (PD)

interactions, including drug–drug interactions.[80,81]

Common configurations include single-layer channels for simple organ models, double-layer channels for barrier tissues (e.g., BBB), and hydrogel-channel types for mimicking ECM environments.[82] The transition from single-organ to multi-organ OoCs requires careful engineering of features such as vascular systems, nutrient gradients, and dynamic fluid communication to ensure proper functional interdependence.[83] Closed-chamber multi-organ systems minimize dead volumes for stable perfusion but limit accessibility, whereas open-access systems allow manual interaction with cultures but suffer from dead volume constraints.[82,84] Although their clinical use faces challenges such as scalability, standardization, and inter-model validation,[83] they could provide better cost-effective systems for predictive toxicology, disease modeling, and pharmaceutical development.[79] Innovations such as incorporating microfluidic-controlled perfusion, artificial intelligence (AI) for real-time monitoring, and advanced imaging technologies have improved the precision and reproducibility of OoCs.[78,85]

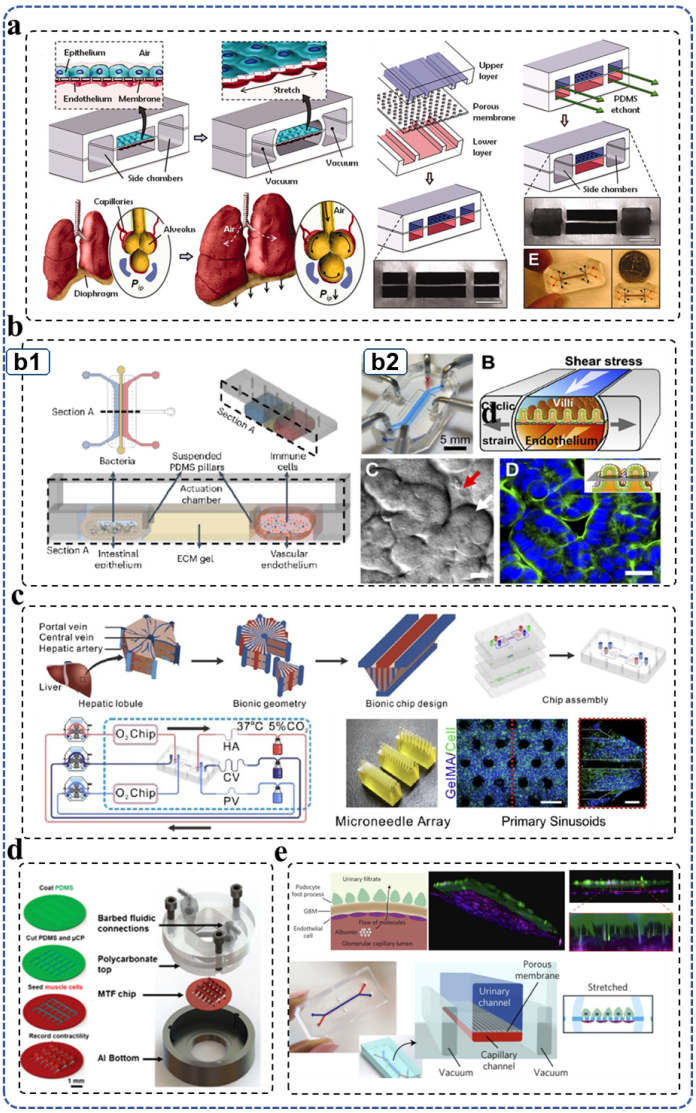


Figure 4. Studies of single-organ-on-a-chip devices. (a) Biologically inspired design of a human breathing lung-on-a-chip microdevice. Reprinted with permission from Huh *et al.*[11] Copyright © 2010 American Association for the Advancement of Science. (b) Gut-on-a-chip models. (b1) A human induced pluripotent stem cell–derived gut-on-a-chip with intestinal epithelial and vascular endothelial channels separated by an ECM-like gel. Reprinted from Ballerini *et al.*[86] (b2) A human gut-on-a-chip device and associated phenotype changes induced by microbiome and mechanical deformation. Reprinted from Kim *et al.*[87] (c) Design and operation of the microneedle-assisted hepatic acinus chip. Reprinted from Li *et al.*[88] (d) High-throughput heart-on-a-chip and fluidic microdevice for *in vitro* heart-function studies. Reprinted with permission from Agarwal *et al.*[89] Copyright © 2013 The Royal Society of Chemistry. (e) Modeling the human glomerular capillary wall with an organ-on-a-chip microfluidic device. Reprinted with permission from Musah *et al.*[90] Copyright © 2017 Macmillan Publishers Limited, part of Springer Nature.

2.2.1. Single-organ-on-a-chip

(a) Lung organ-on-a-chip

Lung-on-a-chip technology reproduces key structural and physiological features of the human alveolar–capillary interface. It enables dynamic interactions between alveolar epithelium and vascular endothelium under air–liquid interface conditions and can incorporate cyclic strain to mimic breathing. These controlled mechanical and fluidic cues support studies of gas exchange, inflammation, infection, inhalation toxicity, and therapeutic response.[91] Combining an air–liquid interface with mechanical actuation therefore makes lung-on-a-chip a useful model of both pulmonary physiology and disease.

One of the earliest breakthroughs in lung-on-a-chip came from Huh *et al.*[11] in 2010, presenting a biomimetic microsystem that replicated the human alveolar–capillary interface, the critical unit for gas exchange. Using microfabrication, the team created a microfluidic device with a porous, flexible membrane separating two microchannels. Human alveolar epithelial and pulmonary microvascular endothelial cells were cultured on opposite sides, forming functional monolayers. Cyclic strain applied to the membrane mimicked alveolar stretching during breathing. The system enabled studies of biological responses to stimuli such as bacterial infection and inflammation. It also simulated infection responses, showing neutrophil migration and engulfment of *Escherichia coli* on the epithelial surface. Mechanical strain was further shown to enhance inflammatory and toxic responses of lung cells to silica nanoparticles, a common inhalation toxicity model (Figure 4a).

Mimicking the spherical geometry of the cell's natural microenvironment improves the physiological fidelity of cell culture based on a biomimetic morphology of a 3D respiratory epithelial tissue structure.[92,93] Huang *et al.*[94] introduced a biomimetic alveolar lung-on-a-chip model that replicates the 3D structure and physiological functions of human pulmonary alveoli. Notably, a 3D porous hydrogel made of gelatin methacryloyl (GelMA) with an inverse opal structure, which mimics the sac-like pores and interconnecting windows of alveolar sacs, was used. The GelMA scaffold, fabricated using sacrificial alginate microbeads, features uniform, interconnected pores with a stiffness (~6.23 kPa) similar to that of native lung tissue, providing a physiologically relevant microenvironment for cell growth. This structure supports the formation of a functional epithelial monolayer when seeded with primary human alveolar epithelial cells, which exhibit high viability and form tight junctions, essential for alveolar barrier function. The model is integrated into a poly(dimethylsiloxane) (PDMS) chip that simulates cyclic breathing motions through mechanical actuation, applying 8% strain to mimic physiological alveolar expansion. This dynamic environment promotes cell spreading, proliferation, and the maintenance of *in vivo*-like behaviors.

More recent innovations range from viral infections and cancer therapeutics to inflammatory and fibrotic diseases.[95] Si *et al.*[96] developed a human airway-on-a-chip platform lined with bronchial epithelia to study viral infection dynamics and drug efficacy. In an influenza A–infected airway-on-a-chip, nafamostat co-administered with oseltamivir extended the treatment window. Moreover, amodiaquine was identified as an effective therapeutic for SARS-CoV-2 infection, demonstrating the platform's potential for antiviral screening. Deinhardt-Emmer *et al.*[97] used a human alveolus-on-a-chip to show that secondary Staphylococcus aureus infection after influenza damages the endothelial barrier. Building on this, Zhang *et al.*[98] utilized a similar alveolar-on-a-chip to replicate SARS-CoV-2-induced lung injury, showing that epithelial cells were more susceptible to viral infection than endothelial cells. The addition of immune cells allowed the targeted viral infection model to recapitulate immune infiltration and inflammatory cytokine release, with remdesivir treatment mitigating barrier disruption and viral replication.

Lung-on-a-chip systems are recreating human-relevant respiratory physiology and responses, with vascular integration offering insights into endothelial damage and immune-cell interactions. Thacker *et al.*[99] used a vascularized lung-on-a-chip to show how SARS-CoV-2 infection triggers endotheliitis and persistent inflammatory responses marked by interleukin 6 (IL-6) secretion; tocilizumab reduced but did not fully prevent barrier loss. Dasgupta *et al.*[100] modeled acute radiation–induced lung injury and reproduced DNA damage, inflammatory cytokine upregulation, and barrier dysfunction, enabling tests of lovastatin and prednisolone. More recently, Ringquist *et al.*[101] developed an immune-competent lung-on-a-chip that reproduced major features of the human severe-influenza response, providing an appropriate infection-model context for the previously uncited study.

(b) Gut organ-on-a-chip

Gut-on-a-chip (GoC) technology represents a major advance in *in vitro* modeling of the human intestine, aiming to replicate its physiological, mechanical, and biochemical dynamics. The intestine is essential for nutrient absorption, barrier function, microbiota interactions, and drug metabolism. GoC studies highlight the importance of dynamic flow for maintaining constant shear stress during cell differentiation, enhancing polarization and tight junction formation with crypt-villus-like structures.[102] Guo *et al.*[103] developed a single-layer GoC model using Caco-2 cells cultured under dynamic shear flow with a porous membrane and ECM support. This enabled formation of

a highly polarized, compact monolayer expressing tight junction proteins and elevated differentiation markers such as villin and sucrase–isomaltase. Compared to static systems, this model greatly improved drug metabolism studies related to nutrient absorption and barrier function.

Conventional models such as 2D cultures or animal systems often fail to capture its structural, cellular, and functional complexity. Beyond single-layer designs, double-layer GoC systems enhance physiological relevance by separating luminal and vascular compartments. Grassart *et al.*[102] used such a platform to study *Shigella* infection, revealing how mechanical forces such as flow and peristalsis enhance bacterial invasion by leveraging the microenvironment, including crypt-like epithelial structures. Shim *et al.*[104] incorporated villi-like 3D collagen scaffolds into a double-layer device, achieving improved gut barrier function and enzymatic activity under fluidic shear stress. Jing *et al.*[105] further demonstrated a gut-vessel microfluidic system where intestinal epithelial cells were co-cultured with vascular endothelial cells under peristaltic motion, resulting in functional microvilli, glycocalyx layer formation, and successful bacterial co-culture.

Gut-on-a-chip has provided new insights into microbiome-mediated intestinal inflammation, serving as a platform for modeling intestinal diseases and testing therapeutic interventions. Kim *et al.*[87] presented a GoC model incorporating microbiome, immune cells, and mechanical deformation to explore bacterial overgrowth and inflammation. The model mimics human intestinal pathophysiology, enabling long-term *in vitro* culture of epithelium, immune cells, and commensal microbes—crucial for studying diseases such as ileus and inflammatory bowel disease (IBD). The study showed that mechanical deformation is essential for intestinal health, as the absence of peristalsis-like motion led to bacterial overgrowth resembling IBD and ileus. It also revealed that immune cell interactions with endotoxins or non-pathogenic microbes stimulated proinflammatory cytokine production, contributing to epithelial injury and barrier dysfunction, key to understanding the inflammatory processes driving these diseases (Figure 4b).

Gut-on-a-chip platforms address limitations by simulating fluid flow, peristalsis, and oxygen gradients through microfluidics. Advances in GoC technology have facilitated the study of intestinal microbiome interactions, supported by oxygen gradients and mechanical forces, enabling insights into gut physiology and drug effects.[106,107] Ballerini *et al.*[86] developed a GoC model that simulates the human intestinal environment, incorporating human fecal microbiota and peristaltic-like movements to investigate microbiome–host interactions and predict responses to immune checkpoint inhibitors in melanoma patients. By integrating human intestinal organoids, microvascular endothelial cells, and patient-derived fecal samples, the system supported multiomic analysis, revealing epithelium-specific biomarkers and microbial factors linked to clinical outcomes. The findings indicated that the microbiome of non-responders to immune checkpoint inhibitors had reduced capacity to buffer cellular stress and self-renew, while specific microbial and soluble components correlated with clinical features. This GoC platform not only recapitulates microbiome–host interactions but also provides insights into molecular mechanisms influencing therapeutic responses, enabling identification of prognostic biomarkers and potential therapeutic targets.

Gut-on-a-chip devices have also been applied to model intestinal diseases and screen therapies. Wu *et al.*[108] developed an intestine-on-a-chip integrated with machine learning to screen probiotics for enteritis relief, identifying *Bifidobacterium longum* as the most effective strain for reducing inflammation and enhancing epithelial integrity. Shin *et al.*[109] reported a patient-derived intestinal organoid–based device that recapitulates disease-specific differentiation patterns under dynamic biomechanical conditions, demonstrating its potential for personalized disease modeling, including Crohn's disease and colorectal cancer. While GoC platforms provide improved physiological relevance compared to traditional models, challenges remain in standardization and scalability for high-throughput applications. Donkers *et al.*[110] highlighted the broad design variability in GoC systems and underscored the need for integrated approaches to optimize preclinical drug development and disease modeling. Özkan *et al.*[111] emphasized the potential of GoC systems in personalized medicine, particularly for understanding gut microbiota interactions, disease mechanisms, and testing therapeutic interventions.

(c) Liver organ-on-a-chip

Liver-on-a-chip platforms combine controlled perfusion with multicellular 3D culture to reproduce key aspects of hepatic transport, metabolism, and vascular organization. Photocontrolled porous scaffolds and co-cultures with endothelial and stromal cells have improved albumin secretion, urea synthesis, CYP expression, and the stability of long-term hepatotoxicity models.[112,113] Li *et al.*[88] further developed a microneedle-assisted hepatic acinus chip (Figure 4c). Its acinus-inspired culture region connected portal-vein, hepatic-artery, and central-vein pathways through microneedle-generated sinusoid-like channels with radii of 100–200 μm. The three inlet streams were operated at 2, 1, and 1 mL/min, respectively, and the perfusable microsystem remained stable during 7–14 days of culture. This design improved intratissue flow, cell viability, microstructure formation, and hepatic metabolic function, while also showing that channel dimensions and flow partitioning must be reported when liver-on-a-chip

performance is compared across platforms.

The liver, a highly vascularized organ, makes *in vitro* modeling challenging. Vascularization is essential for improving the biological accuracy of liver-on-a-chip systems, together with its complexity—arising from diverse cell types including hepatocytes, Kupffer cells, hepatic stellate cells, cholangiocytes, and endothelial cells. To address this, Ya *et al.*[114] developed a liver lobule-on-a-chip with self-assembled, perfusable hepatic sinusoid networks using microfluidic-guided angiogenesis, resulting in higher metabolic activity and prolonged hepatocyte function. Lee *et al.*[115] created an implantable vascularized liver-on-a-chip that supported liver bud maintenance and modeled inflammatory and fibrotic progression during NAFLD. This model proved predictive in *in vitro* and *in vivo* studies. For hepatocellular carcinoma, Özkan *et al.*[116] engineered a vascularized hepatocellular carcinoma-on-a-chip system, incorporating tunable collagen matrices and liver-specific cells to analyze chemoresistance and treatment efficacy under physiologically relevant conditions. Matsumoto *et al.*[117] further replicated hepatic zonation by employing oxygen gradients in microfluidic devices to simulate zonal liver functions, including xenobiotic metabolism and carbohydrate processing.

The liver, a metabolically active organ, is central to drug detoxification, nutrient metabolism, and immune response. Liver-on-a-chip systems effectively model liver diseases and evaluate potential therapies. Chhabra *et al.*'s[118] shear device enabled the modulation of cytokine environments to regulate endothelial–hepatocyte interactions, facilitating studies on regenerative responses. Nawroth *et al.*[119] designed a triculture liver-on-a-chip to study alcohol-associated liver disease, recapitulating key markers such as lipid accumulation, oxidative stress, and bile canaliculi remodeling under ethanol exposure, with potential for patient-specific research. These platforms have also advanced studies on liver regeneration and drug-induced liver injury (DILI). For DILI research, Hou *et al.*[120] developed a stacked array on a chip to investigate idiosyncratic DILI mechanisms, identifying cytokine-driven macrophage polarization as a critical factor. Such models enhance our understanding of drug toxicity and liver repair mechanisms.

(d) Heart organ-on-a-chip

Heart-on-a-chip (HoC) technology integrates human-relevant cardiac tissue engineering and microfluidics to model cardiac physiology and pathology. It bridges the gap between simplistic cell cultures and the physiological complexity of the human heart, replicating myocardial structure and function, and is invaluable for studying cardiovascular diseases, a leading cause of mortality worldwide. HoC platforms have shown versatility in recapitulating cardiac microenvironments. Zhao *et al.*[121] engineered chamber-specific cardiac microtissues from hiPSCs, creating atrial- and ventricular-specific tissues with distinct drug responses and electrical conductivity. This platform also facilitated long-term modeling of diseases such as left ventricular hypertrophy and targeted drug testing and disease-specific modeling. Similarly, Veldhuizen *et al.*[122] advanced HoC by co-culturing hPSC-derived cardiomyocytes with cardiac fibroblasts in a microfluidic platform that provided controllable microenvironments. This biomimetic approach, incorporating anisotropic architecture, enhanced tissue maturation and synchronous contractions, closely mimicking native myocardium.

Genetic and patient-specific disease models have further expanded HoC capabilities. Park *et al.*[123] developed an optogenetic HoC model to study catecholaminergic polymorphic ventricular tachycardia, a genetically driven arrhythmia. Using precise genetic editing, the system reproduced hallmark events such as diastolic Ca^{2+} waves and reentrant rhythms, enabling identification of molecular mechanisms, including the role of ryanodine receptor phosphorylation in arrhythmogenesis. For ischemic heart disease, Gaballah *et al.*[124] established a hypoxic HoC model using hPSC-derived cardiomyocytes to study oxygen deprivation. The system demonstrated hypoxia-induced arrhythmias, sarcomere disorganization, and impaired Ca^{2+} handling. The therapeutic potential of the antiarrhythmic drug levosimendan was observed, as it mitigated arrhythmias and preserved sarcomere integrity under hypoxic stress, positioning HoC as a preclinical tool for ischemic heart disease studies. Liu *et al.*[125] complemented this work by integrating bioelectronics into a HoC model for real-time monitoring of cardiac electrophysiology. This platform revealed hypoxia-induced tachycardia and arrhythmias, provided insights into ion-channel behavior during acute hypoxia, and enabled detailed electrophysiological analyses.

Heart-on-a-chip platforms typically combine microfluidic chip fabrication with engineered cardiac microtissues, mimicking key aspects of human MPS while providing controllable microenvironments and real-time feedback. Microfluidic systems have advanced 3D cardiac tissue modeling, improving physiological relevance. Chen *et al.*[126] reviewed innovations in HoC technology, highlighting progress in microfluidic chip fabrication and real-time feedback systems. These 3D microtissues show superior mechanical and electrical properties compared to monolayer cultures, providing a reliable platform for modeling cardiac responses to drugs and environmental stimuli. Wu *et al.*[127] further emphasized integrating HoC with blood vessel-on-a-chip systems, enabling studies of cardiac–vascular interactions. This approach is especially valuable for investigating cardiovascular

disease mechanisms and supporting high-throughput drug screening.

Hence, HoC platforms provide physiologically relevant models for studying cardiac biology, disease mechanisms, and therapeutic interventions. Their ability to integrate patient-derived cells, replicate tissue-specific responses, and enable real-time monitoring underscores the versatility and clinical potential of HoC technology in cardiovascular research and personalized medicine. Despite progress, challenges remain in fabricating scalable, high-throughput HoC systems that replicate complex cardiac physiology, including large vessels and valves. Recent innovations such as bilayer membrane microfluidic devices and vascularized networks for tissue perfusion offer promising solutions by improving oxygen and nutrient delivery to cardiac tissues.[126] These systems refine the *in vitro* microenvironment and enhance HoC functionality for pharmaceutical research. Agarwal *et al.*[89] presented a high-throughput HoC system using semi-automated fabrication to create submillimeter thin-film cantilevers from soft elastomers. Engineered with anisotropic cardiac microtissues mimicking ventricular laminar architecture, these cantilevers allow calculation of systolic and diastolic stresses from deflection during contraction. The microdevice, made from autoclavable materials, ensures reusability and compatibility with optical and electrical assays for cardiac contractility. Its ability to test drug effects, such as isoproterenol, is enhanced by scalability and reproducibility, making it a promising tool for pharmacological studies, particularly with rare or expensive cell sources (Figure 4d).

(e) Kidney organ-on-a-chip

The development of kidney OoC systems represents a promising innovation in biomedical engineering, providing dynamic *in vitro* models to mimic the complex structure and functions of the human kidney, especially the glomerulus. This platform offers a robust tool for studying glomerular diseases, drug screening, and personalized medicine, providing insights into kidney disorder mechanisms and possible interventions.[128] These devices integrate human cells within microfluidic environments to reproduce tissue morphology, organ-level function, and disease phenotypes. Kidney OoC systems often use microfluidic platforms to recreate the kidney's dynamic environment. Musah *et al.*[90] developed a glomerulus-on-a-chip (GOAC) made of flexible PDMS with two parallel microchannels separated by a porous PDMS membrane (Figure 4e). This structure mimics the tissue–tissue interface of the glomerular capillary wall. HiPSC-derived intermediate mesoderm cells were cultured in the top channel and differentiated into podocytes *in situ*, while primary human glomerular microvascular endothelial cells were seeded on the opposite side. Cyclic suction applied to hollow chambers flanking the channels mimicked the stretching and relaxation of living glomeruli. The chip reproduced the differential molecular filtration of the glomerular wall, retaining albumin in the vasculature while allowing inulin to pass into the urinary space. These features make the GOAC a powerful tool for studying renal mechanisms and diseases.

Recent advances have enabled the recreation of kidney filtration processes, critical for understanding renal physiology and pathophysiology. A key feature of kidney OoCs is their ability to replicate renal filtration, selectively handling small molecules such as urea and creatinine while retaining macromolecules such as albumin. Petrosyan *et al.*[129] presented a GOAC model that mimics the human glomerular filtration barrier (GFB) using human podocytes and glomerular endothelial cells in a microfluidic platform. Unlike models with artificial membranes, this GOAC allows direct podocyte–endothelial interaction, essential for reproducing native GFB structure and function. The chip's three-channel system co-cultures human podocytes and glomerular endothelial cells on a collagen I matrix, enabling formation of a functional GFB with ECM components such as collagen IV and laminin. The GOAC shows selective permeability, filtering inulin while retaining albumin, similar to *in vivo* function. It also responds to pathological conditions, including hyperglycemia, nephrotoxic agents such as puromycin aminonucleoside, and sera from membranous nephropathy patients, with albumin leakage proportional to clinical proteinuria levels.

Simulating filtration and blood purification holds strong potential for advancing knowledge of kidney diseases and therapeutic strategies. A major advantage of kidney OoC systems is their potential for disease modeling. Mou *et al.*[130] designed a device incorporating a biomimetic ultrathin membrane made from electrospun silk fibroin to establish an epithelial–endothelial interface. This platform supports differentiation of hiPSCs into glomerular cells, including podocytes and endothelial cells, essential for forming the kidney's filtration barrier. Integration of these cells enabled the development of a functional GOAC with *in vivo*-like cell structure, tissue organization, and selective molecular filtration. The fenestrae regulate biomolecule passage by size and charge, simulating kidney function in a controlled setting. These devices allow real-time study of disease progression and therapeutic testing in a more physiological context than 2D cultures or animal models. This functionality is especially valuable for modeling glomerular injury and diseases such as proteinuria, often arising from glomerular damage.

The importance of 3D architecture and vascularization in kidney OoC systems provides new insights into kidney function and disease mechanisms. Lin *et al.*[131] advanced this field by developing a 3D vascularized proximal tubule (3D VasPT) model that mimics native kidney structure and function. The model features adjacent conduits lined

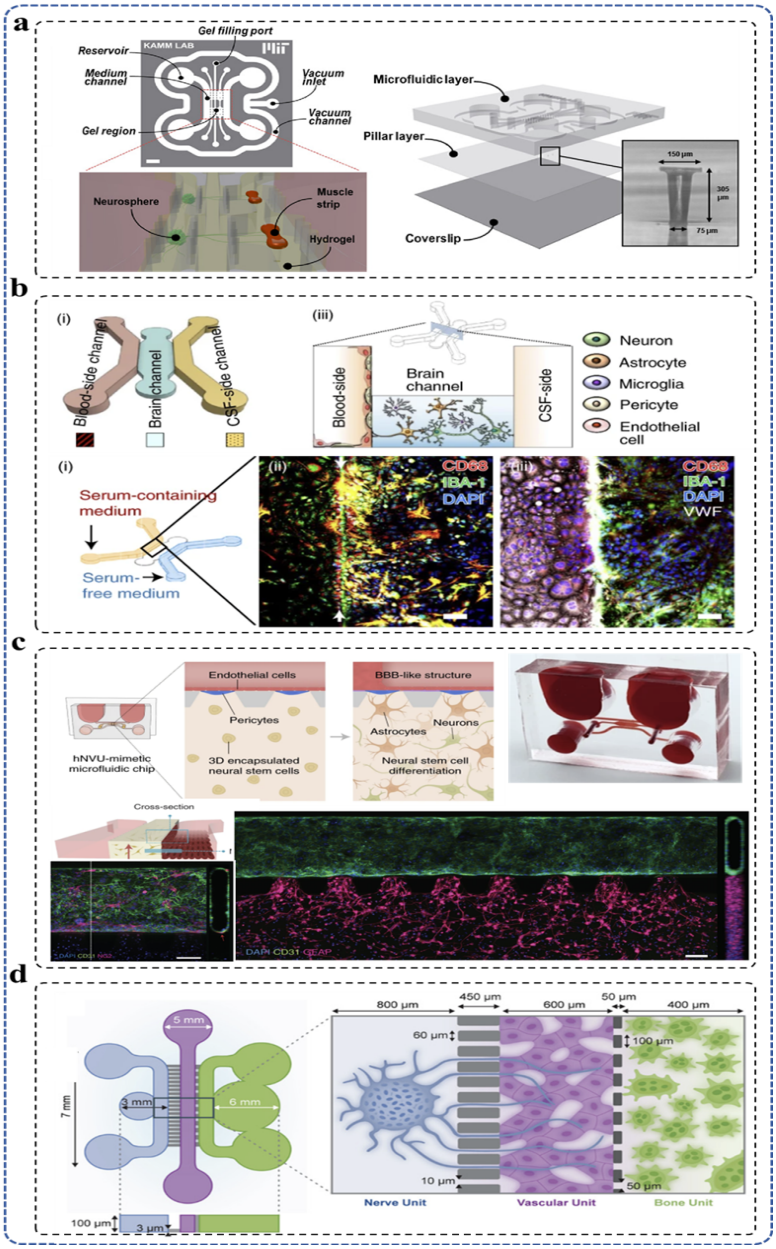


Figure 5. Representative neurogenic organ-on-a-chip models. (a) Microfluidic co-culture of muscle bundles and neurospheres. Reprinted from Uzel *et al.*[132] (b) Microfluidic neurovascular-unit model for blood–brain-barrier characterization. Reprinted with permission from Lyu *et al.*[133] Copyright © 2021 The Author(s), under exclusive license to Springer Nature Limited. (c) Three-dimensional microfluidic human neurovascular-unit chip. Reprinted with permission from Kim *et al.*[134] Copyright © 2021 The Author(s), under exclusive license to Springer Nature Limited. (d) Neurovascular-bone chip integrating nerve, vascular, and bone units. Reprinted with permission from Neto *et al.*[135] Copyright © 2022 The Authors.

with confluent epithelium and endothelium, embedded in a permeable ECM, and integrated with a closed-loop perfusion system. This design enables co-culture of proximal tubule epithelial cells and glomerular microvascular endothelial cells, supporting active solute reabsorption through tubular–vascular exchange. The 3D VasPT demonstrates key renal functions, including albumin uptake and glucose reabsorption, and allows study of epithelial–endothelial crosstalk under normal and hyperglycemic conditions. Its ability to recapitulate *in vivo* renal physiology makes it a valuable platform for drug screening, disease modeling, and pharmacological studies.

2.2.2. Neurogenic organ-on-a-chip

The relationship between neurons and their target organs or cells is fundamental to biological function. Neurons control tissues including muscle, heart, blood vessels,

and bone through synaptic connections and signaling pathways. This regulation maintains homeostasis, enables rapid responses to environmental changes, and coordinates complex physiological processes. Disruptions in neural interactions can cause severe pathologies such as neuromuscular disorders, cardiovascular disease, and impaired bone remodeling. Understanding neuron–organ interactions is therefore essential for both basic science and therapeutic development. OoC technology—particularly models integrating neural components with specific organ systems such as neuromuscular junctions (NMJs), neuro-cardiac coupling, neurovascular units (NVUs), and neuro-bone—offers a powerful *in vitro* platform to replicate these interactions. By mimicking direct cell-to-cell communication and microenvironmental cues, these systems provide new insights into the dynamic interplay between neurons and their target tissues.

(a) Neuromuscular junction-on-a-chip

Neuromuscular junctions are essential for motor function, acting as the interface between motor neurons and skeletal muscle fibers. NMJ degeneration is linked to neurodegenerative diseases such as amyotrophic lateral sclerosis and spinal muscular atrophy. Recent advances in bioengineering and OoC techniques offer new ways to study these processes. Compartmentalized designs mimic the body's physical separation between spinal cord and limb, allowing observation of motor neuron axonal outgrowth and remote muscle innervation. This approach more accurately replicates *in vivo* neuromuscular interactions and provides a platform for studying NMJ pathology and repair in both basic and translational research.[136]

The study of human neuromuscular function and disease has traditionally relied on animal models due to challenges in direct human research. Ionescu *et al.*[137] developed a simplified *in vitro* model to explore molecular communication between motor neurons and muscle cells using a compartment-containing microfluidic system. This platform enabled the formation of functional *in vitro* NMJs and imaging techniques to measure axon outgrowth and NMJ activity, clarifying the complex cellular mechanisms involved in the structure and function of NMJs. However, this study relied on mouse models, which may not fully represent human physiology.

To better study NMJ formation, maturation, and degeneration, human-specific tissue-engineered NMJ models have been developed. Uzel *et al.*[132] created a microfluidic platform integrating myoblast-derived muscle strips and motor neurons differentiated from mouse ESCs within a 3D hydrogel. Incorporation of optogenetic control enhanced the versatility of NMJ studies: photosensitizing ESCs with channelrhodopsin made motor neurons optically excitable, allowing spatiotemporal control of neuronal activation. This approach enabled selective excitation of motor neurons or muscle cells, providing more refined NMJ analysis than traditional chemical stimulation methods. The system's design allows the use of light to explore complex processes such as NMJ maturation, synaptic adaptation, and muscle remodeling, providing insights into the role of activity in plastic synaptic changes. The system also used compliant micropillars to anchor muscle strips, offering a noninvasive way to measure muscle contraction and force generation. This feature is particularly valuable in drug screening, where muscle activity serves as a marker of treatment efficacy. The ability to quantitatively assess neuromuscular function, along with opportunities for further engineering, makes this system promising for advancing NMJ pathology research, high-content screening assays for neuromuscular diseases, and applications in soft robotics (Figure 5a).

Interspecific differences limit the translation of animal model research into clinical practice. To address this, Vila *et al.*[138] further developed a bioengineered, allogeneic, patient-specific human NMJ model. Unlike previous studies, this study focused on creating standardized, objective, and quantitative methods to detect and diagnose disease. The platform combines tissue engineering, optogenetics, microfabrication, optoelectronics, and video processing, making it well-suited for diagnosing and evaluating novel therapies for myasthenia gravis, an antibody-mediated autoimmune disease. Yamamoto *et al.*[139] proposed a human neuromuscular tissue microfluidic model developed in a human 24-well plate format. This study marks progress in mimicking human tissues on microfluidic devices.

(b) Neurovascular unit organ-on-a-chip

The NVU—comprising brain microvascular endothelial cells (BMECs), pericytes, astrocytes, neurons, and the ECM—is essential for maintaining BBB integrity and cerebral homeostasis. NVU-on-a-chip models provide powerful tools for studying brain diseases, pathogen penetration, and the neurorestorative potential of therapies. Lyu *et al.*[133] developed a microfluidic stroke model with an integrated NVU to evaluate stem cell therapies for ischemic stroke. The system incorporated BMECs, pericytes, astrocytes, neurons, and microglia, enabling investigation of post-stroke recovery and the role of stem cell types in neurorestoration. Results showed that human neural progenitor cells and human neural stem cells promote recovery mainly by enhancing NVU structural and functional integrity rather than direct neuronal replacement. This highlights the importance of restoring NVU functionality in post-stroke recovery, focusing on gliogenesis, vessel development, and immune regulation. The model also allows assessment of stem cell behavior across the BBB, making it a valuable tool for preclinical stem cell–based therapy trials. Collectively, these OoC

models support more personalized, high-throughput testing of NVU-targeted interventions and provide a powerful platform for neurodegenerative disease research and drug screening (Figure 5b).

These models recapitulate the brain's vascular environment, including functional BBB formation, NVU cellular interactions, and responses to external stimuli such as pathogens or therapeutic agents. Kim *et al.*[134] developed a human NVU-on-a-chip that mimics BBB structure and function by integrating human neural stem cells, BMECs, and brain pericytes. Using optimized hydrogel composition and fluidic systems, the platform recreated brain-like conditions to study microbial penetration, focusing on the neurotropic behavior of *Cryptococcus neoformans*. The system showed that the pathogen crosses the BBB without disrupting tight junctions, potentially via transcytosis. This model enables real-time study of pathogen dynamics and microbial–BBB interactions, expanding opportunities for infectious disease research and therapeutic drug testing (Figure 5c).

(c) Nerve-bones organ-on-a-chip

The neurovascularized bone chip (NVB chip) was developed to model interactions between the nervous system, vasculature, and bone tissue under inflammatory conditions. It incorporates three compartments—neuronal, vascular, and bone—that mimic crosstalk among sensory neurons, endothelial cells, and osteoclasts. The NVB chip is a compartmentalized microfluidic device with three interconnected channels for neuronal, vascular, and bone cells. The neuronal compartment, containing dorsal root ganglion explants, is separated from the vascular and bone compartments by microgrooves that permit axonal projections but block somal components. The vascular unit, formed with a collagen/fibrin hydrogel, supports endothelial cells in a 3D configuration mimicking capillary structures. The bone unit, seeded with osteoclasts, lies adjacent to the vascular compartment. This design places neuronal terminals in proximity to endothelial and bone cells, enabling study of nerve–vascular–bone interactions under physiological and inflammatory conditions. The NVB chip provides a versatile platform for investigating inflammatory bone diseases such as osteoarthritis and rheumatoid arthritis, mimicking the complex interplay among nerves, vessels, and bone in a controlled *in vitro* environment.

This model seeks to unravel mechanistic interactions in inflammatory bone diseases such as osteoarthritis. Beyond modeling osteoclasts, the NVB chip examines inflammation's effects on neuronal function, particularly pain perception. Under inflammatory conditions, sensory neurons in the neuronal compartment show increased axonal sprouting toward the vascular and bone units, suggesting heightened pain responses. This effect is linked to upregulated neurotrophic factors such as brain-derived neurotrophic factor (BDNF), secreted by endothelial cells under inflammatory signals. Interactions between osteoclasts and endothelial cells may further promote nerve sprouting through additional pro-inflammatory factors. This model provides insight into neurovascular modulation of bone pain and serves as a platform to test anti-inflammatory therapies. Using a microfluidic approach, the NVB chip provides a powerful tool to study bone inflammation, pain perception, and nerve–bone interactions in disease progression (Figure 5d).[135]

2.2.3. Multi-organ-on-a-chip

Multi-OoC platforms represent a major innovation in OoC technology, enabling the modeling of inter-organ interactions and systemic physiology *in vitro*. Chen *et al.*[140] revealed the interaction between tissues under normal and inflammatory conditions by integrating the liver and intestinal multi-organ platform and demonstrating the potential of this system to mimic complex *in vivo* processes (Figure 6a). They also provided physiologically and inflammation-relevant evidence of gut–liver crosstalk through long-term (>2 weeks) maintenance of hepatic (e.g., albumin, bile acid metabolism) and intestinal (e.g., barrier integrity) functions in baseline interaction or cytokine responses. This integrated multi-tissue platform can synergistically enhance and generate insights useful for understanding inflammatory organ crosstalk and complex pathophysiological processes.

Leveraging advanced microfluidics, autologous organ models, and real-time biomonitoring, these systems allow the evaluation of complex pharmacological and pathological processes beyond the scope of single-organ models. Schimek *et al.*[141] proposed a chip-based system mimicking the transport function of the human cardiovascular system for integrating biovascularization into a multi-organ microarray (Figure 6b). The system-on-a-chip interconnects two standard tissue culture compartments and further vessel branching and vessel diameter reduction down to a microvessel scale realized by a two-photon laser ablation technique. The layout ensures physiological fluid-to-tissue ratios and generates pulsatile shear stress in a widely adjustable physiological range within a microchannel circuit entirely covered with endothelial cells using a peristaltic on-chip micropump. This system provides indicative long-term experiments that revealed stable performance to mimic the human circulatory system over two and four weeks and has the potential application for future establishment of human-on-a-chip systems. Continued progress in vascular integration, immune modeling, and long-term culture will expand their applicability and clinical relevance, marking a

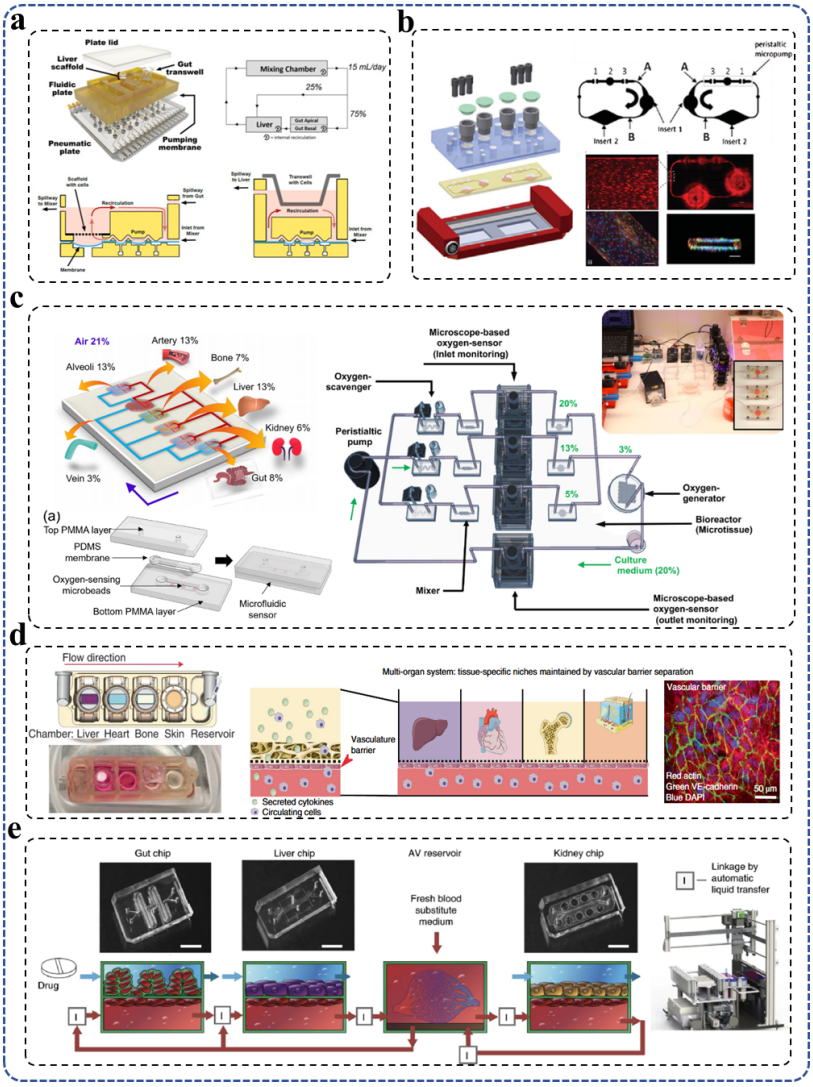


Figure 6. Representative multi-organ-on-a-chip systems. (a) Multi-microphysiological system platform containing immune-competent gut and liver models. Reprinted from Chen *et al.*[140] (b) Multi-organ-on-a-chip layout with an integrated human dermal microvascular endothelial cell microvasculature. Reprinted with permission from Schimek *et al.*[141] Copyright © 2013 The Royal Society of Chemistry. (c) Automated closed-loop oxygen-controlled multi-organ platform containing artery, bone, liver, kidney, and gut modules. Reprinted with permission from Jiang *et al.*[142] Copyright © 2024 The Author(s). (d) Integrated multi-organ chip containing liver, heart, bone, and skin tissues. Reprinted with permission from Ronaldson-Bouchard *et al.*[17] Copyright © 2022 The Author(s), under exclusive license to Springer Nature Limited. (e) First-pass multi-organ system containing gut, liver, and kidney chips. Reprinted with permission from Herland *et al.*[143] Copyright © 2020 The Author(s), under exclusive license to Springer Nature Limited.

transformative step in precision medicine. [144]

Multi-OoC systems also support disease modeling and systemic toxicity assessment across tissues. Kim *et al.*[145] used 3D cell printing and tissue-derived ECM to reconstruct organ-specific microenvironments in a type 2 diabetes model. Wagner *et al.*[146] demonstrated dynamic multi-organ culture for long-term substance testing. Jiang *et al.*[142] introduced closed-loop oxygen control for connected microtissue modules, enabling tissue-specific regulation of a critical metabolic variable.

A central challenge in multi-OoC design is that different tissues require different oxygen levels, whereas conventional platforms are commonly exposed to a single incubator condition. Jiang *et al.*[142] addressed this problem with the closed-loop modular platform shown in Figure 6c. Miniaturized optical oxygen sensors continuously measured the inlet and outlet of each tissue module, while oxygen-scavenging and oxygen-generating components adjusted the shared medium. The system independently maintained oxygen levels between 4% and 20% across connected modules and demonstrated that oxygen conditions alter tissue-specific drug metabolism. Thus,

the contribution of their work is not simply the addition of another multi-organ circuit, but the introduction of feedback control as a means of maintaining tissue-specific physiology within a coupled system.

Linked OoC systems have expanded GoC's capabilities by enabling multi-organ interactions. Ronaldson-Bouchard *et al.*[17] developed a tissue-chip system that interlinks mature human heart, liver, bone, and skin tissues through recirculating vascular flow, enabling multi-organ interactions and the recapitulation of interdependent organ functions, maintaining phenotypic stability over four weeks and enhancing the prediction of drug responses (Figure 6d). Milani *et al.*[147] introduced a gut–liver-on-a-chip device to study mycophenolate mofetil metabolism, capturing the contribution of intestinal and hepatic systems in the drug's pharmacokinetics and metabolic conversion. This coupled system emphasized the interplay between intestinal permeability and hepatic metabolism. Similarly, Sakai *et al.*[148] developed a small intestine–liver platform using hiPSC-derived intestinal epithelial cells and primary hepatocytes to explore co-culture effects, showing enhanced function for both cell types under perfusion. GoC technology has transformed investigations of intestinal physiology, drug metabolism, microbiota-host interactions, and disease modeling. Continued efforts to refine device designs, integrate multiple organ systems, and incorporate patient-derived materials will further extend the applicability of this emerging technology.

The development of Multi-OoCs is driven by the need for comprehensive models that replicate whole-body dynamics. Nguyen *et al.*[149] combined human kidney and liver organoids via microfluidic channels to study the biodistribution and therapeutic efficacy of mesenchymal stromal cell–derived extracellular vesicles. This system successfully recapitulated human physiological responses and allowed in-depth analysis of extracellular vesicle accumulation and recovery from kidney injury, showcasing the potential of multi-OoC models for systemic therapy evaluation. Li *et al.*[150] developed an intestine–kidney-on-a-chip to investigate the nephrotoxicity associated with intestinal drug absorption, highlighting how drug combinations influence toxicity and absorption, demonstrating the platform's predictive power in evaluating drug-induced side effects.

The application of multi-OoCs to drug metabolism and absorption has advanced understanding of inter-organ interactions. Kurniawan *et al.*[151] demonstrated this with a gut–liver MPS, which revealed crosstalk mechanisms modulating drug metabolism. Co-culturing iPSC-derived intestinal cells with primary human hepatocytes enhanced CYP activity through metabolic interactions involving arachidonic acid, underscoring the role of organ crosstalk in hepatic metabolism and improving *in vitro* prediction of drug responses. Shah *et al.*[152] introduced a multi-OoC platform combining the HuMiX GoC and Dynamic42 liver-on-a-chip to simulate the gut–liver axis. This system provided insights into host–microbe interactions at the gastrointestinal interface, emphasizing multi-OoC utility for studying microbiome-driven drug effects and disease mechanisms.

These multi-OoC platforms can simulate the complex interplay of organ systems, accelerating drug discovery and improving human-specific disease modeling. Wang *et al.*[153] developed an MPS integrating alveolus and BBB chips to model the neurological effects of SARS-CoV-2 infection. Direct BBB exposure to the virus caused mild disruption, while medium from the infected alveolus chip induced more severe BBB damage, including endothelial dysfunction, pericyte detachment, and neuroinflammation. Transcriptomic analysis revealed altered actin cytoskeleton expression in brain endothelial cells and increased inflammatory gene expression in glial cells. The study further showed that low viral loads in the lungs can trigger early cerebral microvascular damage, suggesting systemic inflammation, rather than direct viral invasion, drives COVID-19 neurological symptoms. This lung–brain MPS highlights the BBB's role in relaying peripheral inflammation to the brain and provides a platform to investigate extrapulmonary complications.

Unlike single-organ systems, which replicate individual functions, multi-OoCs recreate physiologically accurate connections and crosstalk among organs, making them highly relevant for studying PK, PD, and drug-induced toxicity. Gao *et al.*[154] used a microfluidic co-culture model to study macrophage–cardiomyocyte interactions in inflammation-mediated myocardial injury. This approach revealed metabolic pathways driving oxidative stress and inflammation, enabling precise drug screening and identification of cardioprotective compounds. Ronaldson-Bouchard *et al.*[17] further advanced multi-OoC technology by integrating heart, liver, bone, and skin tissues within a vascularized flow system. This platform recapitulated doxorubicin's PK and PD profiles, identified early microRNA biomarkers of cardiotoxicity, and maintained tissue-specific phenotypes for four weeks, demonstrating superior predictive accuracy for systemic drug effects compared to isolated tissues.

Multi-OoC models are increasingly used to assess systemic effects of drug absorption, metabolism, and toxicity, improving preclinical testing. Herland *et al.*[143] presented a multi-OoC platform that predicts human PK and PD from *in vitro* data. The system integrates fluidically coupled OoCs representing gut, liver, kidney, and bone marrow to mimic first-pass absorption, metabolism, and excretion. Using computational models with experimental input, they accurately predicted PK parameters for orally administered nicotine and intravenously injected cisplatin.

Predictions of organ toxicities were validated against patient data. This coupled model offers a more realistic simulation of human drug behavior, with potential for enhanced drug discovery, trial design, and personalized medicine. The study also underscores the importance of endothelial barriers in replicating physiological processes, marking a step forward in *in vitro*-to-*in vivo* translation for drug development (Figure 6e).

2.3. Integration of (multi-)organoid-on-a-chip

2.3.1. Motivation for integration

Organoids represent a major advance for mimicking human organ-specific, multilineage cellular composition and functions. However, their lack of perfusable vasculature and limited environmental control reduce physiological relevance. Conversely, OoC systems excel at regulating microenvironmental stimuli, such as fluid flow and mechanical forces, but fall short in replicating complex tissue architecture and diversity. Integrating these approaches offers the opportunity to overcome such deficiencies and develop platforms that better emulate human physiology.[155] Organoids provide biologically relevant cellular composition, while OoCs contribute geometric precision, perfusion, and mechanical stimuli to mimic organ-level interactions. Integration could vascularize organoids, improving nutrient delivery and reducing necrotic core formation, a critical limitation of traditional models.[16] Beyond structural gains, providing flow and electrical or mechanical stimuli in OoC-integrated systems helps create more physiological microenvironments.[156]

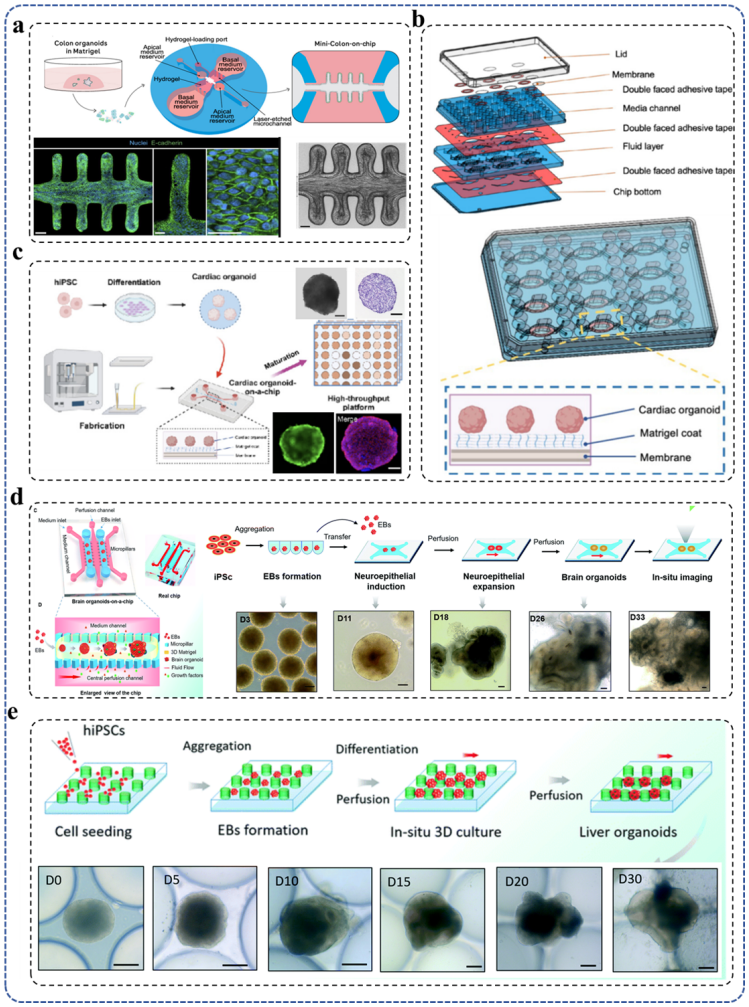


Figure 7. Representative organoid-on-a-chip systems. (a) Bioengineered human mini-colons supporting colonic epithelial homeostasis. Reprinted with permission from Mitrofanova *et al.*[157] Copyright © 2024 The Author(s). (b,c) Cardiac organoid-on-a-chip platform used to evaluate polystyrene-nanoplastic–induced cardiotoxicity. Reprinted with permission from Zhang *et al.*[158] Copyright © 2024 American Chemical Society. (d) Perfusable chip for three-dimensional culture and differentiation of brain organoids. Reprinted with permission from Wang *et al.*[159] Copyright © 2018 The Royal Society of Chemistry. (e) On-chip differentiation and generation of functional liver organoids from hiPSCs. Reprinted with permission from Wang *et al.*[160] Copyright © 2018 The Royal Society of Chemistry.

2.3.2. Representative organ-specific organoid-on-a-chip

(a) Intestinal organoid-on-a-chip

Kasendra *et al.*[161] established a primary human small intestine-on-a-chip using biopsy-derived organoids, combining donor-derived epithelium with controlled luminal flow. Workman *et al.*[162] developed iPSC-derived intestinal organoid-on-a-chip with multiple epithelial subtypes and cytokine responsiveness, although tubular geometry and mesenchymal, neural, and immune compartments remain difficult to reproduce. Nikolaev *et al.*[163] created perfusable scaffold-guided mini-intestines with continuous removal of dead cells and regenerative capacity. The iFlow platform further introduced self-assembled vasculature for studying immune-cell recruitment during colon inflammation, while luminal accessibility remained a limitation.[164]

Mechanically engineered devices have further enhanced modeling accuracy. Kim *et al.*[87,107] developed a GoC that can be coupled with a porous microfluidic setup and imitated peristalsis-like motion, enabling long-term bacterial co-culture and functional studies of inflammation and bacterial overgrowth. Sontheimer-Phelps *et al.*[165] developed a colon-on-a-chip, reproducing the bilayered mucus structure needed for barrier function and mucus hydration signaling during inflammation. The integration of microbiota into OrgoC platforms has also been pivotal. Trujillo-de Santiago *et al.*[166] and Ballerini *et al.*[86] highlighted microbiota-on-a-chip systems' role in studying host–bacterial interplay, using advanced fabrication methods and stem cell technologies to recreate these dynamic interactions.

(b) Heart organoid-on-a-chip

The development of heart organoid-on-a-chip (Heart-OrgoC) is emerging as a promising approach for modeling cardiac function and pathology. Combining stem cell–derived cardiac organoids with OoC technology improves structural and functional fidelity while enabling precise control of microenvironmental factors. Heart-OrgoC systems integrate electrical and mechanical stimuli to simulate native cardiac dynamics, as shown by micropatterned cardiac organoids that promote vascular network formation and contractile function through geometric confinement.[167,168] Shirure *et al.*[169] highlighted that vascularized cardiac organoids generated on microfluidic platforms can reproduce human heart functions and dynamic tissue perfusion *in vitro*, extending their use in disease modeling and drug testing. Min *et al.*[170] refined this approach by incorporating cardiac fibroblasts, endothelial cells, and cardiomyocytes derived from hiPSCs within a perfusable ECM, achieving maturation and effective drug screening.

Bioprinting methodologies have been instrumental in replicating the geometric and functional complexity of the heart. Kupfer *et al.*[171] fabricated electromechanically functional chambered organoids through bioprinted hiPSC constructs, advancing the field toward functional macroscale cardiac tissues suitable for disease modeling and therapeutic applications. However, challenges remain in achieving complete spatial differentiation and physiologically relevant ejection fractions in chambered structures.[169] Efforts to improve the scalability and consistency of cardiac organoids are reflected in advances by Hoang *et al.*[168], where micropatterning facilitated the reproducible engineering of multilineage cardiac organoids for developmental toxicity testing. These approaches underscore the versatility of Heart-OrgoCs as platforms that support both foundational research and clinical translation.

The utility of Heart-OrgoCs in cardiotoxicity studies is illustrated by Mathur *et al.*[172], who developed cardiac MPS capable of predicting drug-induced toxicity with human-specific responses, bypassing the interspecies extrapolation limit of animal models. Concurrently, Zhang *et al.*[158] applied a hybrid approach integrating OoC technology with cardiac organoids to study nanoplastic-induced cardiotoxicity, uncovering stage-specific mechanisms such as oxidative stress and fibrosis, and revealing heightened toxicity under pathological conditions (Figure 7b and 7c). Likewise, Mills *et al.*[167] combined human cardiac organoids with high-throughput techniques to identify potential therapeutics, including BET inhibitors effective against SARS-CoV-2-induced cardiac dysfunction.

Overall, heart-OrgoCs have made significant progress in replicating cardiac functionality, structural organization, and responses to pathological stimuli. Remaining challenges—such as achieving fully vascularized, multi-chambered constructs with native physiological parameters—present opportunities for further integration of bioprinting, microfluidics, and tissue engineering. These systems are poised to advance cardiac disease modeling, drug discovery, and regenerative medicine.

(c) Brain organoid-on-a-chip

Brain OoCs (BOoCs) combine organoid technology with microfluidics, creating a biomimetic environment that overcomes limitations of conventional brain organoid models, such as variability, immaturity, and lack of vasculature. These systems enable precise microenvironmental control for advanced studies in neurodevelopment and related disorders. Wang *et al.*[159] engineered a perfusable BOoC platform to generate hiPSC-derived 3D brain organoids by incorporating 3D Matrigel within an OoC system in a controlled manner. The top layer of the chip consisted of two parallel culture chambers

for the 3D culture and formation of brain organoids, separated by a central channel that served as the fluid flow passageway, which contained trapezoidal pillar array structures for interconnection.

Under perfusion, the brain organoids displayed neural differentiation, regionalization, and cortical organization that captured key features of early human brain development (Figure 7d). Compared with static culture, fluid flow increased the expression of cortical-layer markers T-box brain transcription factor 1 (TBR1) and COUP-TF-interacting protein 2 (CTIP2), linking the engineering intervention directly to enhanced developmental patterning. Perfusion also supported extended culture and reduced the transport limitations associated with conventional static organoids. However, the platform did not recreate a functional vascular or immune compartment, and excessive shear or unstable flow could introduce new variability. Appropriate quality-control readouts therefore include organoid size, viability, cortical marker expression, regional organization, and flow stability rather than maturation claims based on morphology alone.

Similarly, researchers from the same team used micropillar array chips to generate uniform hiPSC-derived brain embryoid bodies, facilitating studies of neurodevelopment and breast cancer-derived exosome effects on the carcinogenesis of brain organoids.[173]

A study reported the development of a BOoC platform that generates multiple signaling gradients to induce forebrain organoids with distinct dorsal–ventral structures, closely mirroring human brain development.[174] Unlike traditional methods, which struggle to form gradients and organized regions, this BOoC uses a multi-layer microfluidic chip to precisely control molecular gradients without shear forces, fostering more structured growth. Temperature-responsive hydrogels provide stable 3D support, enhancing *in vivo*-like development and long-term culture viability. This approach advances neurodevelopmental and disease modeling by creating more realistic, controlled environments for brain organoid research.

A key application of BOoC systems is modeling prenatal environmental exposures, such as nicotine or drugs, which are difficult to study *in vivo*. Wang *et al.*[175] showed that nicotine exposure induced premature differentiation and disrupted cortical structure in BOoC, showcasing the platform's power in revealing developmental anomalies caused by teratogenic substances. Similarly, Cui *et al.*[176] utilized a cortical organoid-on-a-chip to demonstrate how valproic acid exposure inhibits neuronal differentiation and impairs regional organization. The transcriptomic similarities of these valproic acid–exposed organoids to autism patient brains underline the platform's promise in studying neurodevelopmental disorders such as autism. Beyond environmental exposure models, organoid-on-a-chip platforms are instrumental in addressing mechanical and biophysical phenomena in brain development. Karzbrun *et al.*[177] leveraged a confined microfabrication setup to mimic surface folding and wrinkling, elucidating the opposing forces of cytoskeletal contraction and nuclear expansion during tissue morphogenesis. This model recapitulates the biophysical basis of gyrification and smooth-brain pathologies, providing insights into related neurodevelopmental disorders.

Integration of immune dynamics with the BOoC system has strong potential for studying brain aging and neuroimmune interactions. Ao *et al.*[178] developed a microphysiological platform combining dynamic flow with cortical organoids exposed to monocytes, showing that aged monocytes promoted aging marker expression in organoids and demonstrating the platform's utility for modeling immune-mediated brain aging and related diseases. However, advancing functional maturation of brain organoids remains a challenge. Incorporating endothelial cells into microfluidic designs is essential for vasculature formation. For example, cerebral organoids fused with vascular organoids recapitulate neovascular interactions, addressing necrotic core formation when growth surpasses the millimeter scale.

(d) Liver organoid-on-a-chip

Liver organoid-on-a-chip provides controlled perfusion during stem-cell differentiation and long-term 3D culture, helping overcome diffusion and functional limitations of static systems. Ma *et al.*[179] designed a perfused liver-on-a-chip for efficient *in situ* culture of 3D hepatic spheroids, demonstrating how device geometry can support stable spheroid perfusion. Wang *et al.*[160] formed embryoid bodies, induced hepatic differentiation, and generated hepatocyte- and cholangiocyte-containing organoids within the micropillar chip shown in Figure 7e. Perfused cultures showed improved viability, expression of *SOX17*, *FOXA2*, *ALB*, and *CYP3A4*, and albumin and urea production relative to static culture. Dose- and time-dependent acetaminophen toxicity linked engineering control to drug-testing performance. Remaining bottlenecks include functional vasculature, physiologically faithful zonation, and long-term stability; useful quality-control outputs include oxygen, albumin, urea, CYP activity, and tissue viability.

Liver organoid-on-a-chip technologies represent an interdisciplinary innovation that combines microengineering and stem cell biology. These systems show strong potential as platforms for drug toxicity screening, disease modeling, and personalized medicine. Wang *et al.*[180] modeled NAFLD using hiPSC-derived liver organoid-on-a-chip with induced pathological features,

such as lipid droplet formation, triglyceride accumulation, and expression of fibrogenic markers, through sustained exposure to free fatty acids in perfused 3D cultures. This platform has provided new insights into the progression mechanisms of NAFLD. Furthermore, the integration of liver organoids into microfluidic systems allows for dynamic studies of inter-organ crosstalk and the effects of spatial heterogeneity on zonation-related drug metabolism, which remain critical challenges in liver modeling.[181]

Their ability to replicate complex liver functions and pathologies continues to expand, though challenges such as vascularization and zonation require further refinement to approach clinical and industrial applicability. PSC-derived liver organoids exhibit improved structural and functional characteristics compared to static culture systems. The integration of liver progenitor–derived organoids into on-chip platforms promotes advanced features such as bile canaliculi formation and higher CYP expression levels, demonstrating the advantages of perfusion culture for mimicking *in vivo*-like microconditions.[16] Despite these advancements, limitations remain, such as the lack of functional vasculature within organoid systems. While pre-vascularized liver spheroids and microfluidic systems with perfusable vascular beds have been developed, functional cellular fenestrae, characteristic of liver sinusoidal endothelial cells, are often lacking, which hinders fully recapitulating physiological liver processes.[182] With the advent of differentiation protocols for liver sinusoidal endothelial cells, replacing endothelial cells such as human umbilical vein endothelial cells (HUVECs) may further enhance the physiological relevance and zonation in liver-on-a-chip systems.[183]

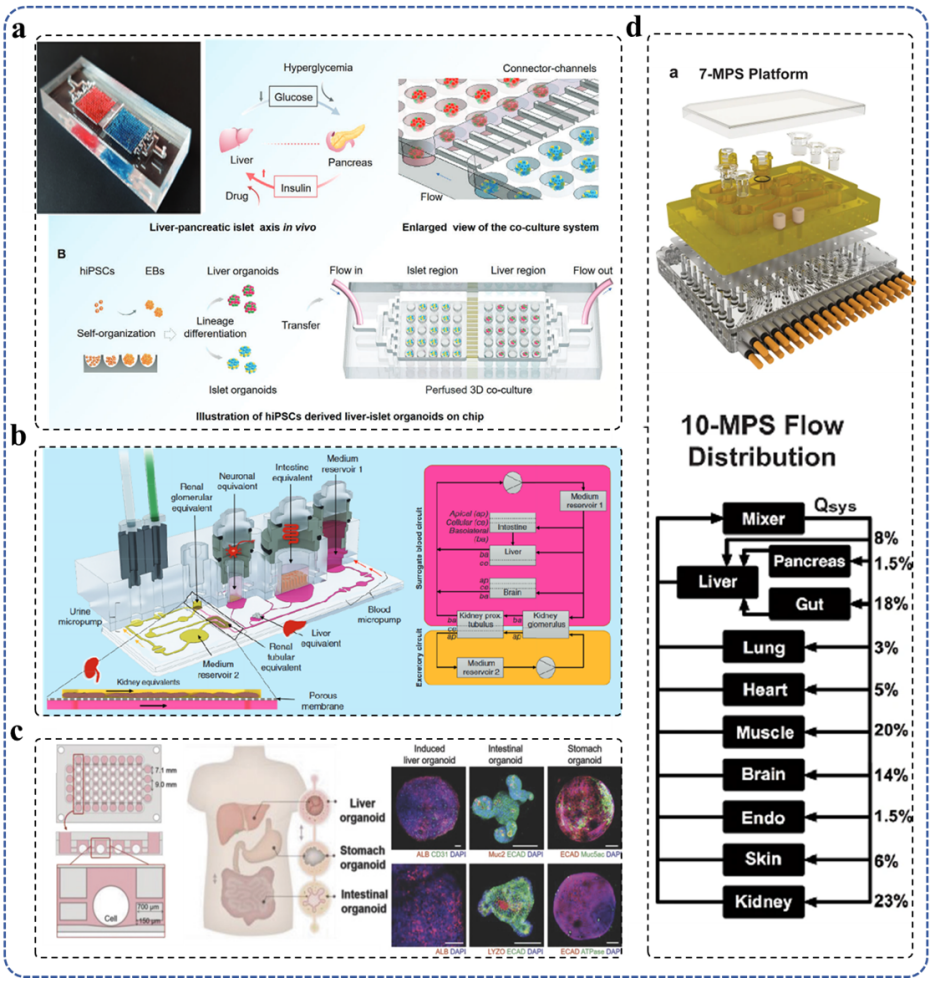


Figure 8. Representative multi-organoid and interconnected microphysiological system (MPS) platforms. (a) Human induced pluripotent stem cell (hiPSC)-derived multi-organoid-on-a-chip model of the human liver–pancreatic–islet axis. Reprinted from Tao *et al.*[184] (b) Autologous hiPSC-derived four-organ chip. Reprinted from Ramme *et al.*[185] (c) High-throughput microfluidic integration of three-dimensional induced hepatic tissue with internal organoids. Reprinted with permission from Jin *et al.*[186] Copyright © 2018 Wiley-VCH. (d) Seven- and 10-MPS platforms and their flow-partitioning architecture. Reprinted from Edington *et al.*[187]

2.3.3 Multi-organoid-on-a-chip

Multi-organoid-on-a-chip systems place two or more self-organized tissues in connected but controllable microfluidic compartments to examine inter-organ signaling, metabolism, and toxicity. Unlike multi-OoC platforms built primarily from engineered tissue modules, these systems emphasize the cellular diversity and developmental organization of organoids while using flow to regulate communication between them. Representative applications include liver–islet metabolic crosstalk, autologous multi-tissue culture, and metabolism-dependent drug toxicity; their shared engineering challenges are physiological scaling, common medium compatibility, flow partitioning, and reproducible organoid quality.

A critical advancement in multi-organoid-on-a-chip systems has been recreating physiological vasculature and fluid flow to mimic *in vivo* communication. Ronaldson-Bouchard *et al.*[17] developed a vascular flow–linked system integrating mature heart, liver, bone, and skin tissues separated by an endothelial membrane. This system modeled doxorubicin PK and cardiotoxicity, emphasizing the importance of controlled vascular communication. Wikswo *et al.*[188] highlighted scaling and systems biology as essential components for maintaining physiological ratios and designing universal culture media for multi-organ systems, with particular focus on mHu (milliHuman) and μHu (microHuman) models. Schutgens *et al.*[189] further demonstrated the adaptability of kidney tubuloids cultured in a microfluidic system replicating epithelial transport, highlighting their potential for personalized nephrotoxicity assays. Such improvements ensure that organoids retain specific phenotypic and functional characteristics over time.

Multi-organoid-on-a-chip systems have enabled exploration of metabolic inter-organ interactions, such as the liver–islet axis. Tao *et al.*[184] developed a microengineered multi-organoid system from iPSC-induced liver–islet organoids that recapitulates glucose-stimulated insulin secretion and glucose metabolism (Figure 8a). The system contains two compartmentalized regions that enable 3D co-culture of liver and islet organoids for up to 30 days through a connected microchannel network under circulatory perfusion conditions. The multi-organoids exhibited favorable growth of both liver and islet organoids and improved their tissue-specific functions, facilitating increased glucose utilization and sensitive glucose-stimulated insulin secretion. The multi-organoid-on-a-chip recapitulates the human-relevant liver–islet axis under both physiological and pathological conditions. It displays decreased glucose transport capacity and mitochondrial dysfunction under high-glucose conditions for utility in type 2 diabetes modeling, as well as alleviation after metformin treatment for utility in therapeutic testing. Aizenshtadt *et al.*[190] presented a pump-less islet–liver-on-a-chip that reproduces features of metabolic crosstalk under physiological and high-fat diet conditions, providing new insights into the mechanisms of type 2 diabetes and metabolic dysfunction-associated steatotic liver disease.

These systems offer powerful tools for translational research, disease modeling, and precision medicine. The gut–liver–brain interaction is associated with systemic diseases, such as neurodegeneration. Trapecar *et al.*[191] established a gut–liver–brain chip focused on Parkinson's disease, revealing that microbiome-associated short-chain fatty acids promoted pathology-associated pathways in the brain while influencing immune-specific interactions across tissues; they also used a gut–liver–lipocyte chip to explore IBD, showing paradoxical inflammatory effects of short-chain fatty acids depending on T-cell involvement, clarifying the role of metabolism, immunity, and injury.[192] Koenig *et al.*[193] developed a brain–liver chip that combines BBB models with liver organoids to study drug permeability and metabolism, enabling simultaneous monitoring of parent drug and metabolites across organ compartments. These innovations demonstrate the capability of multi-organoid-on-a-chip systems to model the intricate interplay along inter-organ axes.

Multi-organoid systems can be used to predict drug efficacy and off-target toxicity. McAleer *et al.*[12] demonstrated the on-target effects and metabolism-dependent cardiotoxicity of tamoxifen using linked human liver, bone-marrow, and cardiac organoid modules. Yin *et al.*[194] established a liver–heart organoid-on-a-chip with hiPSC-derived tissues to evaluate the cardiotoxicity of antidepressants after hepatic metabolism, highlighting metabolism-dependent effects of clomipramine on cardiac function. Li *et al.*[150] developed an intestine–kidney chip for assessing drug absorption and nephrotoxicity, enabling organ-specific toxicity testing within a connected platform.

These multi-organoid MPS will enhance patient-specific disease modeling and enable quicker, more accurate, cost-effective testing of drugs and clinically relevant pharmacological assessments by reducing inter-donor variability. Ramme *et al.*[185] developed a four-organ chip integrating brain, liver, intestine, and kidney tissues derived from a single donor's iPSCs, which shared the same genetic background. The four-organ chip was designed to host cell culture spaces for intestinal organoids, liver spheroids, renal organoids, and neurospheres in an arrangement mimicking the *in vivo* situation. The successful co-culture of the four autologous tissue models in one common medium deprived of tissue-specific growth factors allowed crosstalk studies over two weeks. The four organ models were placed in distinct compartments to host cell culture spaces for neurospheres, liver spheroids, intestinal organoids, and renal organoids. This dynamic fluidic circulation is adjusted

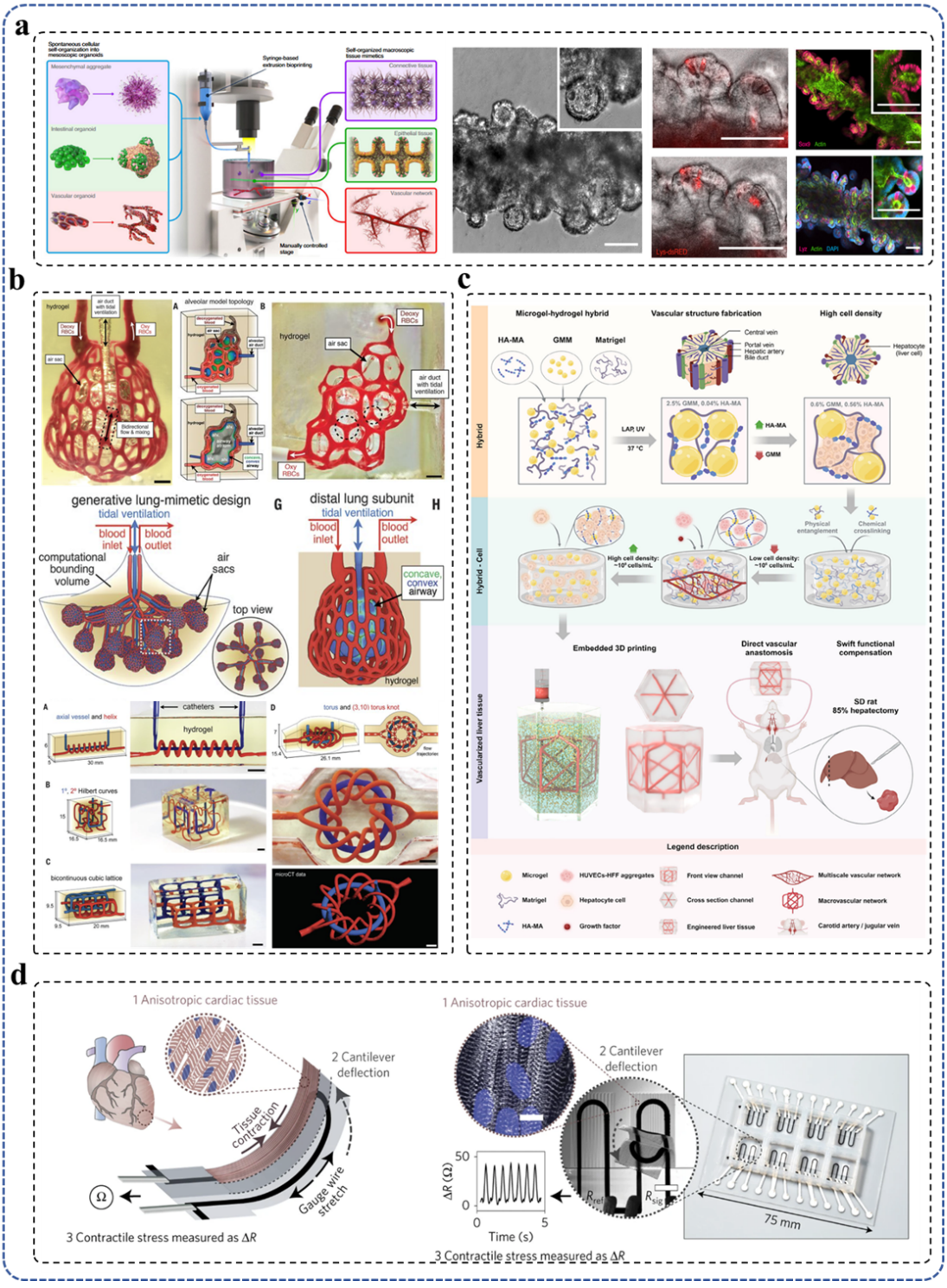


Figure 9. Representative 3D-bioprinting strategies for organoids and engineered tissues. (a) Bioprinting-assisted tissue emergence using self-organizing building blocks. Reprinted with permission from Brassard *et al.*[195] Copyright © 2020 The Author(s), under exclusive license to Springer Nature Limited. (b) Multivascular networks and functional intravascular topologies in biocompatible hydrogels. Reprinted with permission from Grigoryan *et al.*[196] Copyright © 2019 The Authors, some rights reserved; exclusive licensee American Association for the Advancement of Science. (c) Microgel–hydrogel hybrid for mechanically stable, cell-dense vascularized liver tissue. Reprinted with permission from Wang *et al.*[197] Copyright © 2025 Wiley-VCH GmbH. (d) Multimaterial 3D printing of instrumented cardiac microphysiological devices. Reprinted with permission from Lind *et al.*[198] Copyright © 2016 Springer Nature Limited.

to enable physiological nutrition and oxygen supply similar to human blood circulation, connecting the organs and mimicking the *in vivo* situation of the human body (Figure 8b).

Many studies have attempted to establish a multi-organ model by integrating other internal organoids using the high-throughput microfluidic array platform. The liver plays a major role in drug metabolism; the intestine and the stomach play important roles in drug absorption and the metabolism of xenobiotics. Jin *et al.*[186] developed a 3D vascularized liver organoid model using induced hepatic cells and simultaneously integrated intestinal and stomach organoids for drug screening and toxicology testing. The induced hepatic cells, generated via nonviral direct reprogramming of mouse embryonic fibroblasts, were co-cultured with human endothelial cells in a decellularized liver ECM hydrogel. This model was incorporated into a microfluidic device, a triculture multi-organ model of induced hepatic tissues, stomach organoids, and small intestinal organoids co-cultured with HUVECs, creating a dynamic, *in vivo*-like environment that supported cell functionality. The 3D liver organoids showed enhanced hepatic functions, including albumin secretion, urea production, CYP activity, and drug responses, making it a promising platform for high-throughput screening (Figure 8c).

Multi-organoid MPS can mimic complex biological processes and enable crosstalk involving organ–organ interaction, system homeostasis, and PK. Edington *et al.*[187] demonstrated an approach to co-culture multiple multi-organoid MPS linked together physiologically on open-system, reusable microfluidic platforms for quantitative study of a range of compounds or drugs (Figure 8d). They described three different platform designs mixing chambers up to 4-way, 7-way, and 10-way with independently programmable flow rates and internal re-circulation to enhance nutrient exchange. The on-board pneumatically driven pumps were used to provide precise control of drug distribution and flow partitioning over both intra- and inter-MPS. They reported the first co-culture of seven interacting MPS, adding brain, heart, and pancreas to the initial four platforms (liver/immune, lung, gut/immune, and endometrium), and maintained functional cultures for three weeks. Using this seven-way system, they studied the PK of diclofenac, finding strong agreement between predicted and measured drug concentrations. A subsequent 10-way MPS platform, incorporating kidney, skin, and skeletal muscle in addition to the seven MPS, operated successfully for four weeks. Its success relied on 26 pumps and robust design features that minimized contamination risks. Future efforts should prioritize scaling laws, universal medium compatibility, and refined vascular integration to broaden their translational applications.

3. Integration of microengineering and sensors in organoids and organ-on-a-chip

3.1. Integration of microengineering

Integration of microengineering, such as 3D bioprinting and acoustic bioassembly, with OoC models improves biomimicry and dynamic organoid behavior, bridging the gap between organoids and OoC systems.[199] 3D bioprinting strategies are gaining significant attention due to their ability to precisely control the spatial arrangement of cells or organoids. Bioprinting technologies are generally classified into three categories: inkjet-based bioprinting[200–202], extrusion-based bioprinting[203–205], and photocuring bioprinting[206–208], based on fundamental printing principles with cell-containing biomaterials. In particular, volumetric bioprinting is one of the cutting-edge photocuring bioprinting techniques, and drawing inspiration from holography and multi-angle projection techniques enables the rapid construction of centimeter-scale 3D sophisticated structures within tens of seconds.[209–211] 4D bioprinting further improves this field by adding the temporal dimension based on stimuli-responsive printing ink, allowing constructs to dynamically evolve under controlled stimuli.[212,213] 3D and 4D bioprinting have revolutionized the scalability, reproducibility, and complexity of organoids and provided an essential tool for disease research and regenerative medicine.[214] Acoustic bioassembly excels in creating heterocellular architectures with high cell density, overcoming conventional bioprinting's limitations in cellular rearrangement after deposition. Overall, the convergence of advanced technologies into organoids/OoC systems has significantly enhanced their precision, dynamic control, and physiological relevance.[215]

3.1.1. Bioprinting-assisted tissue emergence

The spatial control afforded by 3D bioprinting enables precise integration of multiple cell types and ECM components, essential for mimicking *in vivo* architectures.[216,217] Brassard *et al.*[195] introduced bioprinting-assisted tissue emergence (BATE), combining stem cells and organoid-forming cells with ECMs to guide large-scale tissue self-organization and create centimeter-scale tissues that feature complex structures, such as lumens, vasculature, and intestinal epithelia, with *in vivo*-like features, including crypts and villi. They utilized a syringe-based extrusion system, which, combined with microscopy-based bioprinting, allowed precise control over cellular density, tissue geometry, and the placement of multiple cell types. By controlling the geometry, BATE enabled tissues to self-organize into functional structures, mimicking organ development of various tissues, including epithelial, vascular, and connective tissues, successfully forming self-organized intestinal tubes, fibrous structures, and vascular networks. BATE was used to construct multi-tissue models, such as

gastrointestinal tubes that contained both intestinal and gastric zones. The results demonstrated the potential of BATE for creating highly relevant tissue models that can be used for drug discovery, diagnostics, and regenerative medicine, providing a scalable and reproducible method for engineering complex tissue structures with functional relevance to *in vivo* systems (Figure 9a).

(a) Bioprinting perfusable vasculature within organoids

Integration of periosteum-derived organoids with 3D-printed scaffolds illustrates how printed architectures can support vascularized bone regeneration.[218] More generally, perfusable vascular models are needed to improve nutrient and oxygen transport in large engineered tissues. Grigoryan *et al.*[196] used food dyes as photoabsorbers in stereolithographic printing to create intricate, perfusable vascular topologies within biocompatible hydrogels. The printed networks supported flow, red-blood-cell oxygenation, intervascular nutrient delivery, tidal ventilation in lung-like structures, and engineered liver tissues (Figure 9b).

To address the challenge of limited nutrient and oxygen supply in organoid cores, a study introduced an approach to enhance human brain organoid growth and integration by printing meshed microporous vessels.[219] By using two-photon polymerization 3D printing technology, it created artificial vessels with dense micropores to improve nutrient delivery, overcoming the common issue of hypoxia and apoptosis that restrict organoid size and maturation. These 3D-printed vessels supported greater proliferation, reduced cell death, and enabled the growth of larger, more mature organoids. The vascularized organoids showed enhanced neuronal differentiation and calcium signaling, indicating improved maturation. The vessels also promoted the fusion of multi-regional organoids, including cortex, striatum, and medial ganglionic eminence, facilitating cell migration and neuronal projections. This method offers a promising platform for simulating brain development, studying neurological disease, drug screening, and advancing complex brain organoid engineering.

(b) Embedded bioprinting of hierarchical vascular tissue

In large-scale tissue engineering, constructing vascular networks that withstand physiological pressures is key for successful implantation.[220] Building upon their previous research, Wang *et al.*[197] addressed the limitations of current extrusion-based 3D printing, which struggles to replicate complex hierarchical vascular structures, and the mechanical inadequacy of existing bio-inks. Their work introduces a novel approach using crosslinkable microgels to enhance the mechanical stability of the bio-ink. By integrating these microgels into a soft GelMA-based bio-ink, they successfully created a material that provides an ideal microenvironment for encapsulated HUVECs and induces the spontaneous formation of microvascular networks. The material's robust functionality enabled implanting the 3D-printed multi-branched tissue into a rat model, where it was directly connected via surgical anastomosis to the rat's carotid artery and jugular vein. This proof of concept showed that the engineered tissue could withstand the shear stress of blood flow, marking a significant step forward in fabricating large, vascularized tissues and offering a new path for treating organ failure in the future (Figure 9c).

In the treatment of acute liver failure, where a substantial number of functional cells are required, high-cell-density 3D bioprinting is promising and key to successful rapid vascularization.[221] However, conventional hydrogels lack the mechanical strength to withstand the shear forces of physiological blood flow.[222] Addressing this challenge, Wang *et al.*[223] developed a novel heterogeneous microgel–hydrogel hybrid bio-ink capable of encapsulating high-cell-density hepatocytes and supporting the embedded bioprinting of hierarchical vascular structures. By optimizing the ratio of microgels to biomacromolecules, this composite forms a covalently crosslinked network that provides the necessary mechanical stability to resist blood flow shear and facilitates direct vascular anastomosis, ensuring efficient nutrient and oxygen exchange. They illustrated the overall strategy, which involves using this novel composite to construct implantable vascularized liver tissue for rapid functional compensation. The study validated the material's efficacy in an animal model, offering a new direction for tissue regenerative therapy.

Other research teams have also made remarkable contributions in the field of 3D bioprinting. Xu *et al.*[224] developed a double-network dynamic hydrogel to address the mechanical instability of traditional dynamic hydrogels during 3D printing. This novel bio-ink, composed of a dynamic hydrogel and a covalently crosslinked non-dynamic hydrogel network, maintains structural integrity and facilitates vascular morphogenesis through its unique matrix dynamics, providing a new strategy for tissue vascularization. Duan *et al.*[225] focused on bone tissue regeneration, using 3D bioprinting to fabricate pre-vascularized bone organoids for the rapid reconstruction of cranial bone defects. By combining mesenchymal stromal cells, HUVECs, and osteogenic microparticles, they successfully achieved rapid *in situ* vascularized bone formation, offering a highly effective solution for critical-sized bone repair. Li *et al.*[226] leveraged human CiPSCs to create functional hepatocyte organoids, which were then bioprinted into a hepatic tissue model. This model demonstrated significant therapeutic efficacy in a mouse model of liver failure, highlighting its potential for clinical research in liver regenerative medicine. In a groundbreaking integration of bioelectronics and bioprinting, Kong *et*

al.[227] developed an implantable biohydrogel battery. This innovative device possesses mechanical properties that match biological tissues and can generate dual-mode currents to support both tissue regeneration and cardiac pacing, offering a promising solution for next-generation transient bioelectronics.

(c) Multi-material bioprinting for organ-on-a-chip

Multi-material bioprinting offers additional possibilities for creating heterogeneous, hierarchical tissue structures.[228] Lind *et al.*[198] introduced a novel approach for fabricating instrumented cardiac MPS using multimaterial 3D printing. The device integrates soft strain gauge sensors within micro-architectures that guide cardiac tissue self-assembly, enabling non-invasive electronic monitoring of contractile stress *in vitro*. Using six functional inks, the team printed complex, multilayer cantilever structures that supported laminar cardiac tissues derived from human and neonatal rat cardiomyocytes. These devices generated high-fidelity functional tissues and provided continuous readouts of contractile strength, offering a platform for long-term studies of cardiac function and drug responses. They also enabled real-time tracking of contractile development over weeks and detailed dose–response studies with drugs such as verapamil and isoproterenol. This 3D printing method simplifies fabrication of customized devices, reduces the complexity of traditional methods, and opens new possibilities for cardiac tissue engineering, toxicology testing, and personalized medicine (Figure 9d).

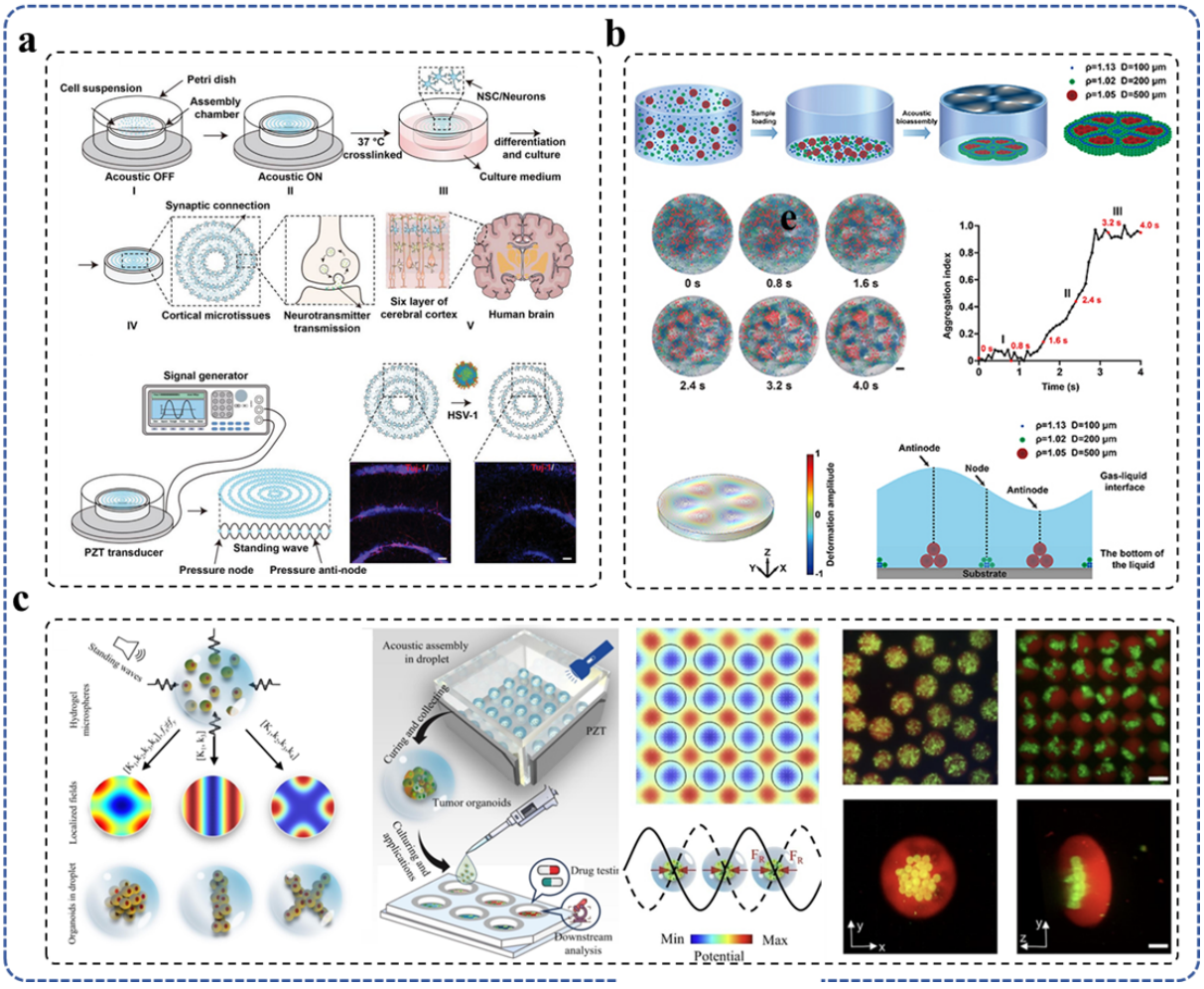


Figure 10. Representative acoustic bioassembly strategies. (a) Acoustic assembly of human cerebral-cortex-like microtissues from human induced pluripotent stem cell (hiPSC)-derived neural progenitors and neurons. Reprinted with permission from Wang *et al.*[229] Copyright © 2023 Wiley-VCH GmbH. (b) Size- and density-dependent acoustic differential bioassembly of spatially defined heterocellular architectures. Reprinted from Gu *et al.*[230] (c) Acoustically tunable intradroplet organoid assembly for high-throughput tumor-model construction. Reprinted with permission from Wang *et al.*[231] Copyright © 2024 Elsevier B.V.

3.1.2. Acoustic bioassembly

Traditional bioprinting and bioassembly methods, such as extrusion and inkjet printing, excel at depositing cells in controlled patterns but often fail to reproduce the closely packed, spatially defined heterocellular architectures of natural tissues. Sonic assembly, which uses acoustic waves to manipulate and assemble cellular structures, has emerged as a powerful technique for fabricating 3D tissue architectures. Acoustic forces, particularly bulk acoustic waves, can precisely and non-invasively pattern cells. Wang *et al.*[229] demonstrated that acoustic bioassembly can generate six-layer concentric tissue architectures resembling the cytoarchitecture of the human cerebral cortex. In this approach, hiPSC-derived neural progenitors and neurons were assembled using acoustics, then differentiated and cultured. The resulting tissue model reproduced key features of human cortical tissue, including synaptic connections and neuroelectrophysiological activity, providing a platform to study neurodegenerative diseases (Figure 10a).

(a) Acoustic differential bioassembly technique

An acoustic bioassembly approach addresses limitations of other 3D tissue engineering methods by enabling the construction of structured, functional tissues that retain integrity over time. Gu *et al.*[230] introduced an acoustic differential bioassembly technique that manipulates Faraday waves to position different cell types within a single construct (Figure 10b). This method leverages cell size and buoyant density to differentially assemble cells beneath nodal or antinode regions, forming complementary or sandwich cytoarchitectures. For example, hiPSC-derived liver spheroids and endothelial cells were organized into hexagonal patterns mimicking hepatic lobules, with spheroids at nodal regions and endothelial cells at antinodes. This spatial arrangement enhanced liver-specific functions, including albumin secretion and urea production, demonstrating the method's ability to recapitulate tissue functionality. The process is rapid, requiring only seconds, and avoids sequential printhead alternation typical of traditional bioprinting. Its high-throughput capability and tunability position acoustic bioassembly as a promising alternative for constructing physiologically relevant tissue models.

(b) Droplet-based acoustic assembly

Acoustic bioassembly excels in creating heterocellular architectures with high cell density using a droplet-based platform to construct tumor spheroids and other cellular aggregates (Figure 10c).[231] The system uses acoustic waves to pattern droplets containing cells into defined 3D structures. Researchers formed diverse configurations, including spherical, linear, and cross-shaped structures by adjusting frequency and amplitude. This method's high throughput and flexibility enabled the generation of thousands of organoid models in a short time, with consistent size and high viability. The droplets were crosslinked into hydrogel-based scaffolds mimicking ECM, essential for cell survival and function. Results showed this approach markedly improved tumor model formation efficiency compared to traditional methods. This droplet-based acoustic assembly thus provides an effective platform for drug screening and disease modeling, with applications in oncology and tissue engineering. Together, these studies highlight the versatility and promise of sonic assembly for developing functional, complex tissue models. While challenges in scale, vascularization, and data universality remain, the synergy of acoustic and AI-driven workflows offers a strong foundation for future advances in regenerative medicine.

3.2. Integration of sensors in organoids and organ-on-a-chip systems

The integration of sensors into OoC systems revolutionizes *in vitro* organ modeling by enabling real-time and non-invasive monitoring of biochemical, biophysical, and biomechanical cues. This facilitates the dynamic evaluation of organoid functionality and microenvironment interactions.[78] Key sensor categories in OoC platforms include mechanical sensors, electrochemical sensors, optical sensors, and flexible sensing, each tailored to specific bioanalytical needs based on target signals and sensing principles.[232,233] Zhang *et al.*[234] developed an integrated modular platform for OoC systems that incorporates physical, biochemical, and optical sensors, enabling dynamic and automated monitoring of organoid microenvironments to enhance drug screening and personalized medicine. The system operates within a custom-designed benchtop incubator, maintaining appropriate conditions for the experiment, pneumatic valving powered by nitrogen controlled via a MATLAB-driven Wago controller, and integrates electrochemical sensors for real-time biomarker detection. Physical sensing, including flow rate monitoring and detection of channel blockages, is achieved with a data acquisition card and LabVIEW software. The platform is designed to be modular, with components such as microbioreactors for organoids, electrochemical sensors, and fluid reservoirs interconnected for seamless fluid flow. This innovative approach allows for *in situ*, automated monitoring of both biophysical and biochemical parameters over extended periods, offering significant improvements over traditional models for drug screening and OoC research.

3.2.1. Mechanical sensors

Mechanical sensors and actuators are important for reproducing and quantifying blood-vessel shear stress, lung expansion, and cardiac contraction. Mechanical cues

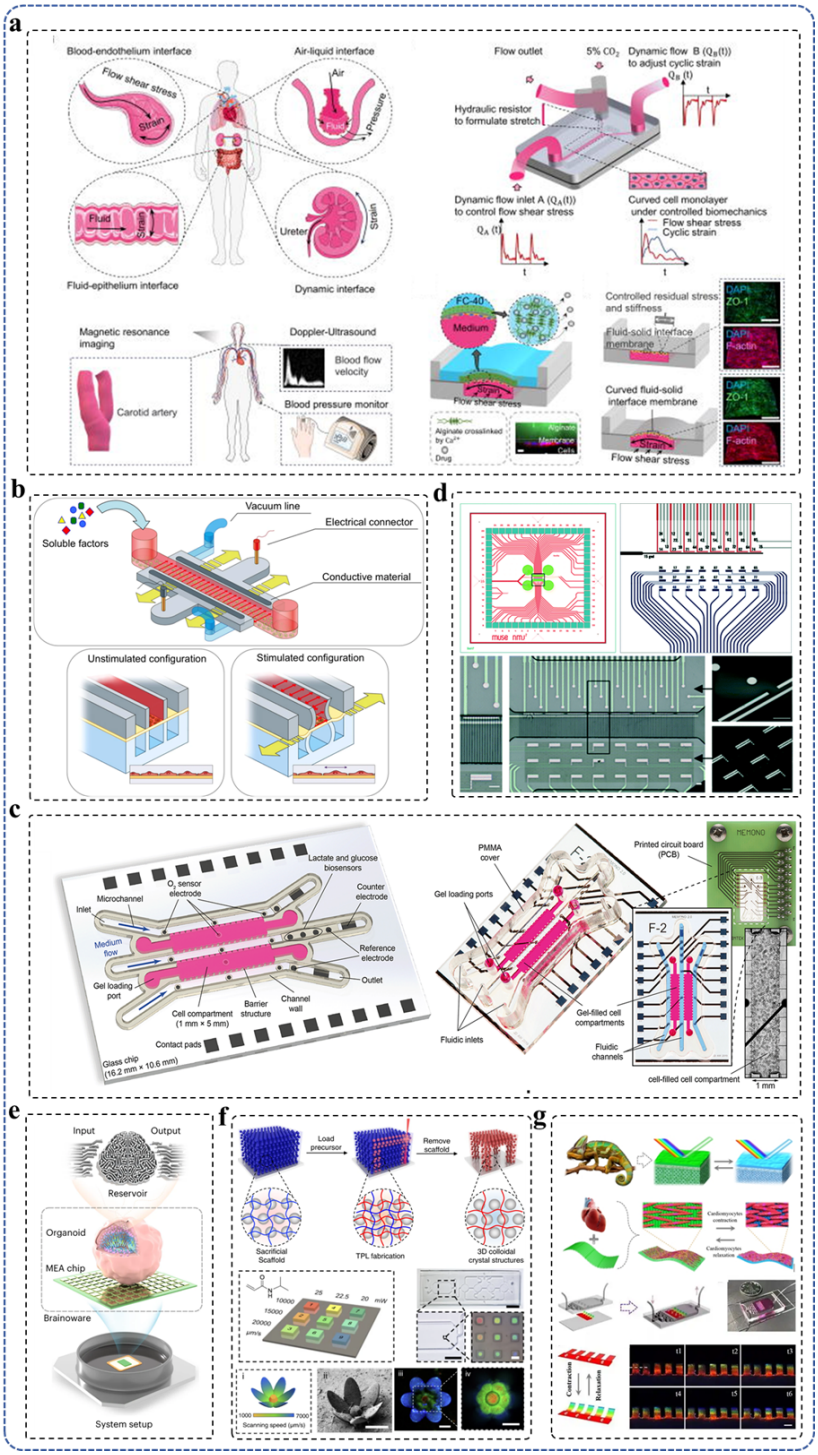


Figure 11. Representative microengineering, stimulation, and sensing strategies in organoid and organ-on-a-chip systems. (a) Fluid–solid dynamic curved interface and drug-release design in a microfluidic organ chip. Reprinted with permission from Su *et al.*[235] Copyright © 2024 AIP Publishing. (b) Microfluidic platform for controlled electromechanical cell stimulation. Reprinted from Pavesi *et al.*[236] (c) Sensor-glass chip with integrated electrochemical microsensors and microchannels for multi-analyte monitoring. Reprinted from Dornhof *et al.*[237] (d) Custom microelectrode-array design for a human neuromuscular-junction chip. Reprinted with permission from Duc *et al.*[238] Copyright © 2021 The Royal Society of Chemistry. (e) Brainoware setup coupling a brain organoid to a high-density multielectrode array (MEA). Reprinted with permission from Cai *et al.*[239] Copyright © 2023 The Author(s), under exclusive license to Springer Nature Limited. (f) Sacrificial-scaffold-mediated two-photon lithography process for colloidal crystals and microhydrogels. Reprinted from Liu *et al.*[240] (g) Engineered cardiomyocyte tissue integrated with a biohybrid structural-color hydrogel film. Reprinted with permission from Fu *et al.*[241] Copyright © 2021 American Association for the Advancement of Science.

such as shear, compression, and cyclic strain can alter organoid growth and maturation.[242] Gut models have used controlled basolateral flow and deformation to regenerate 3D epithelial architecture and villus-like structures.[243] Dynamic mechanical control therefore supports studies of tissue remodeling, PK, and disease mechanisms. More broadly, the convergence of neural regulation and mechanobiology provides a systems-level framework for studying interactions between the nervous system and peripheral organs.[244]

Dynamic curved interfaces between tissues and body lumens are common *in vivo*, but reproducing their geometry and mechanical environment *in vitro* remains challenging. Su *et al.*[235] developed a microfluidic organ chip containing two fluid–solid curved interfaces, including a deformable PDMS membrane that enabled controlled cyclic strain and flow-induced shear stress. The platform was used to examine Piezo1 expression, calcium signaling, and YAP nuclear translocation in endothelial and epithelial cells under combined mechanical stimuli. Analytical modeling, numerical simulation, particle image velocimetry, and optical coherence tomography were used to characterize the mechanical environment. The system also reproduced location-specific conditions at a carotid bifurcation, illustrating how controllable curved interfaces can support mechanobiology studies and site-specific drug testing (Figure 11a).

Mechanical stimulation influences the cell microenvironment and drives stem cell differentiation processes. Combining these simulations, OoC systems can reproduce complex native microenvironments and delineate the individual or synergistic effects of each stimulation on the function, differentiation, development, or regeneration of the tissue or organ. Pavesi *et al.*[236] developed a microfluidic cell stimulator with integrated mechanical sensors to deliver simultaneous mechanical, electrical, and biochemical stimuli to human bone marrow mesenchymal stem cells, enabling detailed analysis of cellular responses. The multilayer PDMS device includes a pneumatic layer for mechanical stretching, a conductive layer for applying a uniform electric field, and a fluidic layer for biochemical delivery, with strain values calibrated to physiological levels via vacuum pressure regulation. Optimized through finite element method analysis, the platform allowed precise control over each stimulus, showing that mechanical stimulation induced morphological changes and actin cytoskeletal reorientation perpendicular to strain. The device also enabled cell harvesting for quantitative reverse transcription polymerase chain reaction, demonstrating upregulated cardiac myocyte marker expression under mechanical and electrical stimuli, with mechanical strain exerting a stronger effect. Compatible with fluorescence imaging, this system provides a versatile tool for studying mechanotransduction, offering insights into stem cell differentiation and tissue engineering (Figure 11b).

To assess mechanical stress in cardiac tissues, researchers developed pneumatic microfluidic platforms to simulate cardiac hypertrophy under controlled conditions. These devices enable the high-throughput evaluation of mechanical stress, drug effects, and tissue phenotypes in real time. [245,246] Lind *et al.*[198] developed an instrumented cardiac microphysiological device featuring embedded mechanical sensors to measure single-cell contractile stresses within laminar cardiac tissues. The device integrates soft strain gauges, composed of carbon black–filled thermoplastic polyurethane, within multilayer cantilevers to provide non-invasive electronic readouts of tissue mechanics. These sensors, with a gauge factor of 2.51 ± 0.09, enabled precise monitoring of contractile stresses (7–15 kPa) in neonatal rat ventricular myocytes and hiPSC-derived cardiomyocytes over extended periods. The platform supported real-time analysis of drug responses, including the inotropic effects of verapamil and isoproterenol, and tracked contractile development of hiPSC-derived cardiomyocyte tissues over 28 days, revealing increased twitch stress and sarcomere maturation. Validation against optical tracking confirmed the reliability of sensor readouts, underscoring their utility in mechanobiology. This approach advances the study of single-cell mechanics in engineered tissues, offering a robust tool for drug screening and tissue engineering.

Cardiac MPS can quantify contractile forces and pharmacological responses using compliant hydrogels and microfabricated structures.[247,248] Soft force-sensing diaphragms enable sensitive, non-invasive measurements of cardiac-organoid contraction under dynamic stimulation and drug exposure.[246] These devices form part of a broader transition from endpoint assays toward instrumented spheroid- and organoid-on-a-chip platforms.[249]

3.2.2. Electrodes and electrochemical sensors

Electrode sensing enables stimulation and recording in neuromuscular and neural systems, while electrochemical sensors can track pH, oxygen, glucose, lactate, and other soluble biomarkers. Enzyme-functionalized amperometric sensors integrated into microfluidic culture networks support continuous metabolic measurements.[250] Device architecture, materials, and flow design determine sensor accessibility, stability, and biological compatibility.[251] In GoC systems, potentiometric sensing has been used to monitor Hg(II) transport under dynamic exposure conditions.[252]

Electrode sensing employs microelectrodes to interface with biological tissues, enabling the study of cellular responses. In human NMJ research, Duc *et al.*[238] developed a microfluidic platform integrated with custom MEAs

to stimulate motor neuron axons and record muscle action potentials (Figure 11d). Their MEA contained 59 electrodes tailored for human NMJ-on-a-chip platforms, with distinct sets for motor neuron cell bodies, axons, and muscle fibers. Rectangular muscle electrodes (200 × 60 μm), aligned with microstructured grooves, ensured precise recording of muscle activity, while axon electrodes stimulated motor neuron axons crossing microchannels. Stimulation with four pulses at 1 Hz reliably triggered muscle action potentials, revealing diverse responses such as "on–off" patterns and fatigue, indicative of functional synapse formation. This approach surpasses calcium imaging in sensitivity, providing a robust tool for studying NMJ disruptions.

Similarly, Cai *et al.*[239] employed high-density MEAs in their Brainoware system to interface with brain organoids, enabling reservoir computing through spatiotemporal stimulation and neural activity recording (Figure 11e). Brainoware mounted brain organoids on high-density MEAs to perform adaptive reservoir computing, processing spatiotemporal electrical inputs that elicited nonlinear dynamics and fading memory in organoid neural networks. Stimulation with bipolar pulses (200 mV, 300 μs) enabled unsupervised learning, demonstrated by improved speech recognition accuracy (from 51 to 78%) and Hénon map prediction (regression score rising from 0.356 to 0.812) after training. This work highlights electrode sensing's potential to mimic brain functionality for AI hardware and underscores its role in bridging *in vitro* models with functional analysis.

Integrated electrodes can quantify both soluble biomarkers and electrophysiological activity in disease-specific MPS. Son *et al.*[59] developed an engineered brain–spinal cord assembloid in which cerebral organoids and motor-neuron spheroids were connected and monitored using MEAs. Caffeine increased neural spiking in the motor-neuron region only when the cerebral component was present, supporting functional signal transfer through the assembloid.

Nicolas *et al.*[253] developed the OrganoTEER instrument to measure transepithelial electrical resistance (TEER) in perfused epithelial tubules within the OrganoPlate platform, advancing electrochemical sensor technology for barrier function analysis. The system evaluated 40 Caco-2 intestinal and renal proximal tubule epithelial cultures grown against an ECM, eliminating the need for artificial membranes. TEER measurements, conducted via a multielectrode setup, showed high sensitivity, detecting a 50% reduction in Caco-2 TEER values after exposure to inflammatory cytokines and rapid barrier disruption within 40 minutes of staurosporine treatment, outperforming fluorescent leakage assays. Time-lapse monitoring over 25 hours under flow conditions further validated the system's real-time capability. This electrochemical approach provides a robust tool for high-throughput, membrane-free TEER analysis, enhancing studies of epithelial barrier dynamics in OoC systems for drug development and disease modeling.

Multi-analyte electrochemical sensing can continuously track oxygen, glucose, and lactate in matrix-based 3D tumor cultures. Dornhof *et al.*[237] integrated amperometric oxygen and enzyme-based glucose/lactate sensors into a microfluidic platform containing triple-negative breast-cancer stem-cell spheroids. The system monitored metabolic responses to hypoxia and drug exposure for approximately one week, providing continuous information unavailable from endpoint assays (Figure 11c). Biosensor-integrated OoC reviews further emphasize calibration, long-term stability, and automated sampling as prerequisites for pharmacological use.[254]

3.2.3. Optical sensors and structural colors

Optical sensors based on fluorescence, luminescence, photonic structures, and light scattering enable spatially resolved analysis of tissue remodeling and molecular interactions. Organic field-effect transistors provide a complementary route for chemical and biomolecule sensing.[255] AND-gated DNA nanosensors have visualized glutathione and apurinic/apyrimidinic endodeoxyribonuclease 1 (APE1) in cells and organoids, supporting selective fluorescence imaging of tumor-associated molecular states.[256] Ordered micro- and nanoscale hydrogels can also organize cancer-on-a-chip cultures and provide optically accessible structured matrices.[257] Hydrogel-based microfluidic scaffolds are widely used in 3D tissue engineering, including cartilage models, although the scaffold itself is not necessarily a sensor.[258]

Optical biosensors can convert molecular secretion or tissue remodeling into non-invasive readouts. Localized surface plasmon resonance sensors have been used for *in situ* monitoring of insulin secretion in islet-on-a-chip systems.[259] Light-scattering biosensing has quantified tissue-level remodeling in an inflammatory synovium-on-a-chip.[260] Thyroid-on-a-chip platforms provide a complementary endocrine example in which organoid function and endocrine-disruption responses are measured in a controlled microenvironment.[261] Structural-color barcodes and related photonic materials offer additional routes for label-free visualization in biomimetic culture platforms.[262]

Structural colors arise from interactions between light and periodic micro- or nanoscale architectures rather than from molecular pigments. Cardiomyocyte-driven deformation of anisotropic inverse opals can shift photonic bandgaps and thereby translate contraction into an optical signal.[263] Ordered colloidal and hydrogel microstructures

can be fabricated through scaffold-mediated printing approaches (Figure 11f).[240] Photonic-crystal cellular-force microscopy similarly uses optical spectral shifts to quantify vertical forces in living cells over time.[264] These approaches illustrate how material structure can provide label-free mechanical readouts for tissue models.

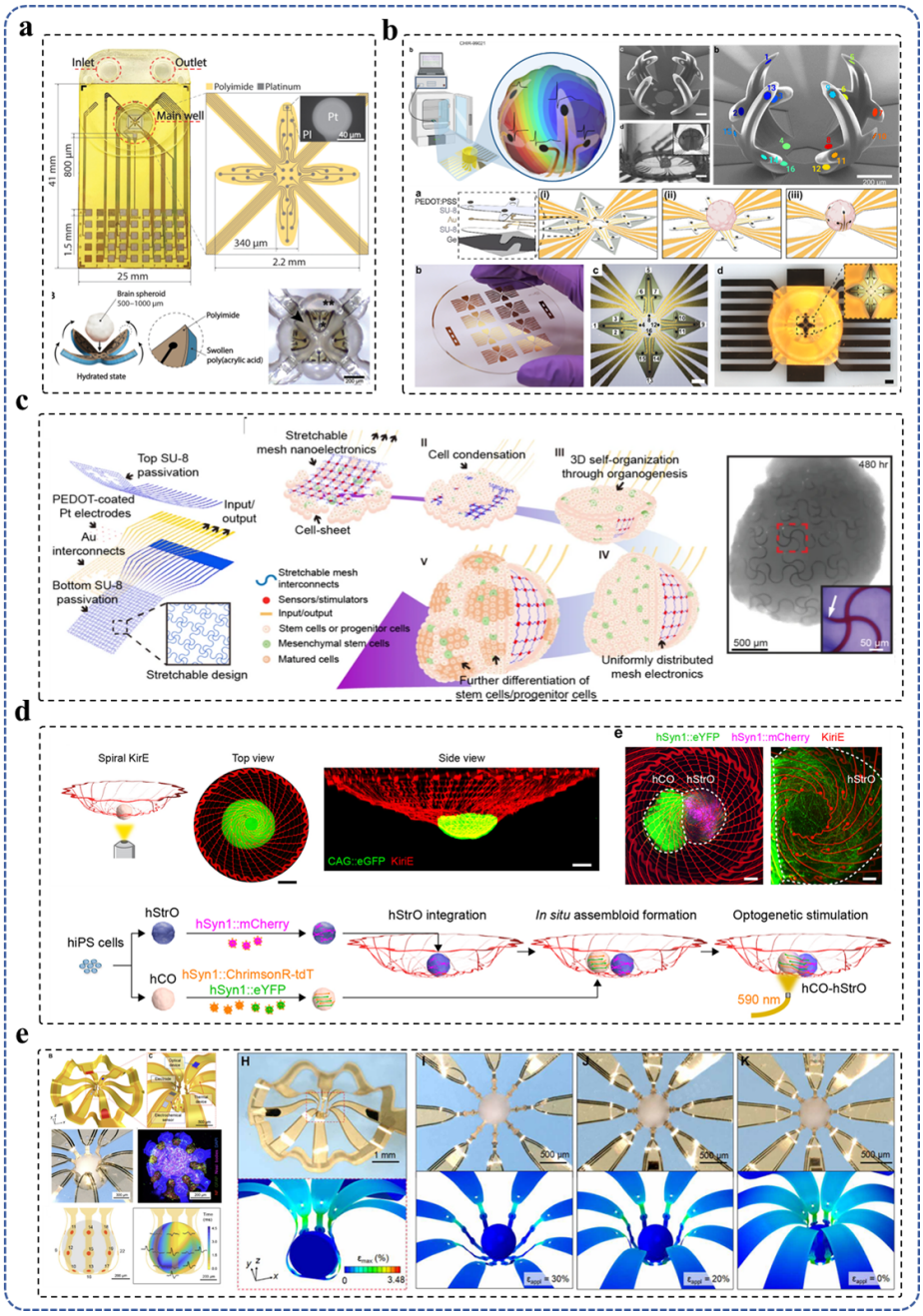


Figure 12. Flexible bioelectronic interfaces for three-dimensional organoid monitoring. (a) Hydrogel-actuated e-Flower multielectrode array (MEA) for brain-spheroid electrophysiology. Reprinted with permission from Martinelli *et al.*[265] Copyright © 2025 American Association for the Advancement of Science. (b) Shape-adaptive shell MEAs for three-dimensional spatiotemporal electrophysiology of cardiac organoids. Reprinted with permission from Choi *et al.*[266] Copyright © 2025 Wiley-VCH GmbH. (c) Stretchable electronics for three-dimensional organoid interfacing. Reprinted from Lee and Liu.[267] (d) Kirigami electronics enabling long-term recording from suspended human cortical organoids. Reprinted with permission from Yang *et al.*[268] Copyright © 2024 The Author(s), under exclusive license to Springer Nature America, Inc. (e) Three-dimensional multifunctional neural interfaces for cortical spheroids and assembloids. Reprinted with permission from Park *et al.*[269] Copyright © 2021 American Association for the Advancement of Science.

Structural colors are increasingly being applied in advanced sensing technologies. Incorporation of the hydrogel into a microfluidic platform established a "HoC" with microphysiological visuality, allowing real-time monitoring of cardiomyocyte behavior through color shifts. Fu *et al.*[241] developed a biohybrid structural color hydrogel by integrating engineered cardiomyocyte tissues with inverse opal GelMA films, enabling autonomic regulation of structural colors (Figure 11g). These films were fabricated using silica colloidal crystal templates, where etched silica nanoparticles produced ordered nanoporous structures exhibiting photonic bandgap properties, reflected as vivid colors. Cultured cardiomyocytes aligned on the GelMA substrate generated cyclic elongation and contraction, dynamically altering the nanostructure and causing synchronous photonic bandgap shifts (e.g., reflection peaks from 605 to 570 nm), mimicking chameleon-like color regulation. Validation with isoproterenol stimulation confirmed its potential for drug screening and biological research. This hydrogel's sensitivity to cellular forces, translating them into observable optical signals, provides a stable and durable platform for studying cardiac pathophysiology and advancing structural color-based sensing in OoC applications.

3.2.4. Flexible sensing

Flexible sensing technologies enable conformable interfaces for bioelectronics and structural monitoring.[270,271] Data-driven inverse design can optimize the geometry and sensitivity of flexible pressure sensors, while programmed microlattice architectures provide a route to controllable 3D curved mesosurfaces.[272,273] These design strategies are relevant to shape-adaptive organoid interfaces because they connect material architecture with mechanical conformity, sensitivity, and device integration.

When 2D planar MEAs are used to monitor the electrical activity of 3D organoids, their limited spatial structure imposes significant constraints on signal acquisition. Recently, flexible electrodes based on shell MEAs have addressed this limitation. Huang *et al.*[274] designed a solvent-responsive, self-folding shell MEA that exploits the reversible solubility of SU8 in acetone and water to achieve precise encapsulation of brain organoids. The device's three channels aligned with distinct brain regions discharged simultaneously, and it successfully detected increased neuronal excitability following glutamate stimulation. In comparative studies, mature brain organoids cultured on shell MEAs and conventional 2D MEAs revealed that only a few electrodes in 2D MEAs captured electrophysiological activity. While the spike duration recorded by both systems was similar, the shell MEA detected more spikes with a higher signal-to-noise ratio, demonstrating greater functional completeness relative to 2D MEAs.

A key advantage of the shell MEA is that it secures brain organoids without chemical or biological fixation, relying instead on the mechanical properties of its flexible electrodes. Inspired by soft microgrippers, Martinelli *et al.*[265] introduced a flower-shaped MEA (e-Flower) that can detect spontaneous neural activity across the submillimeter brain spheroids' surface (Figure 12a). The e-Flower can envelop spheroids; its actuation mechanism leverages the swelling properties of polyacrylic acid hydrogel by the sole addition of cell culture medium. The e-Flower does not require additional solvents and equipment to record electrophysiology for preformed 3D tissues after grafting a swelling hydrogel to a polyimide substrate hosting the electrical interconnects. The e-Flower demonstrated its potential for comprehensive neural signal recording by achieving a curvature with a value tunable by the hydrogel cross-linker concentration and choice of reswelling media. Organoid-encapsulating shell MEAs with programmable and shape-adaptive features are presented as novel technology that enables comprehensive 3D electrophysiological mapping. Choi *et al.*[266] demonstrated on-chip-fabricated devices using shell MEAs that feature customizable geometries and electrode layouts tailored to cardiac organoids' unique morphology for 3D spatiotemporal electrophysiology (Figure 12b). The shell MEAs displayed the long-term spatiotemporal field potential dynamics in spontaneously beating cardiac organoids by generating conduction velocity maps and high-resolution 3D isochrones. This advanced bioelectronic interface-based platform enables high-content 3D spatiotemporal functional analysis of electrophysiological findings for cardiac disease modeling and pharmacological screening.

Flexible sensing has revolutionized bioelectronics, particularly in interfacing with 3D biological constructs such as organoids. Stretchable electronics enable chronic organoid interfacing, supporting long-term and stable monitoring. Lee and Liu[267] emphasized the development of stretchable electronics for electrophysiological recording from brain organoids, advancing organoid intelligence for computational models and illustrating how structural flexibility drives functional innovation (Figure 12c). These studies highlight organoid/electronics hybrids, or "cyborg organoids," which maintain conformal contact despite morphological changes during development. This capability enables single-cell resolution recordings across 3D volumes, a significant improvement over rigid planar electrode arrays. To enhance mechanical compatibility, they advocate for intrinsically soft materials, such as elastomers combined with conductive nanomaterials such as graphene or carbon nanotubes. These materials minimize mechanical mismatch with soft tissues, ensuring chronic stability. Integration with multimodal profiling

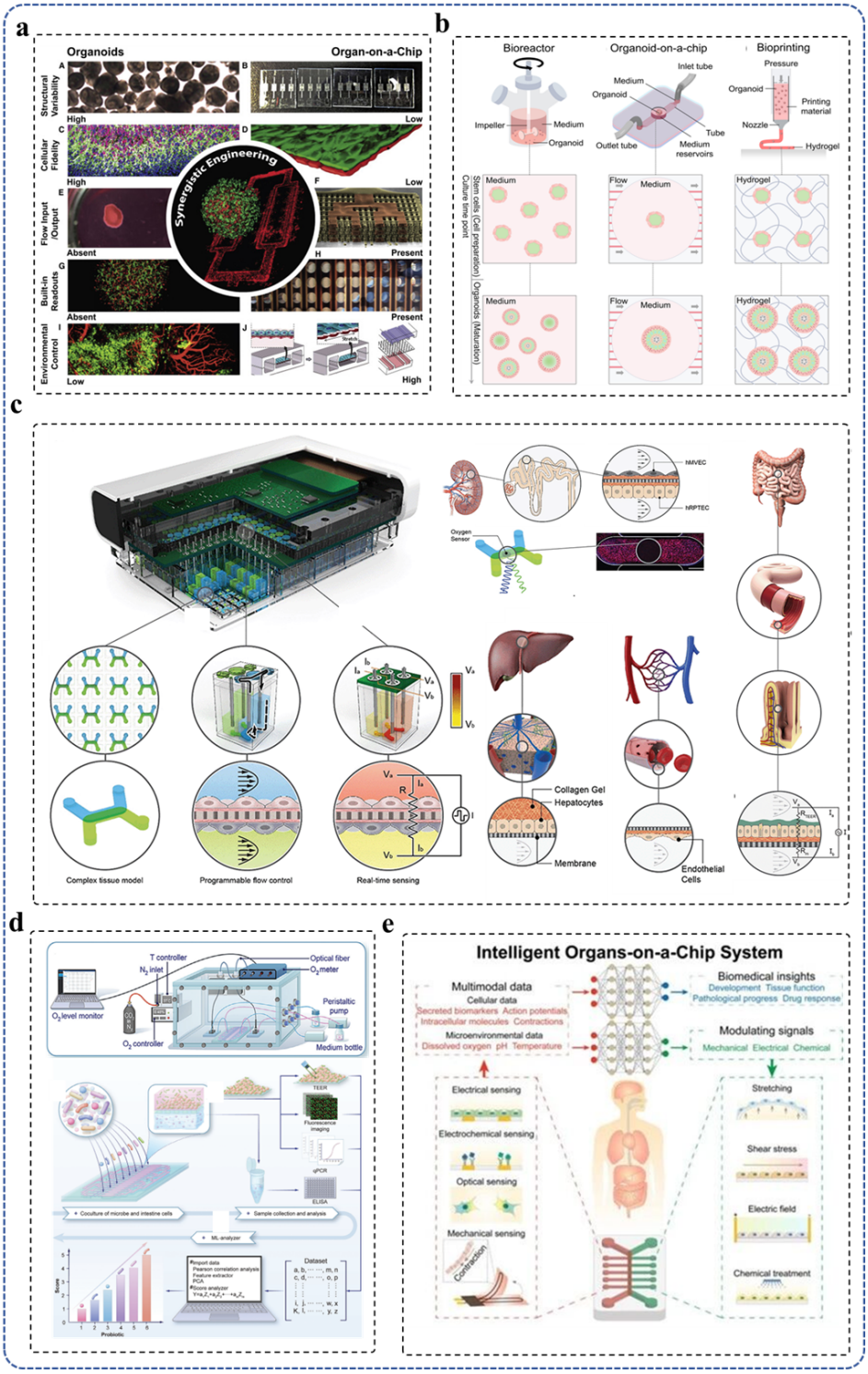


Figure 13. Synergistic engineering and integration. (a) Synergistic engineering of organoids and organ-on-a-chip. Reprinted with permission from Takebe *et al.*[275] Copyright © 2018 Elsevier. (b) Construction and cultivation methods of organoids based on bioreactor, organoid-on-a-chip, and 3D bioprinting. Reprinted with permission from Li *et al.*[276] Copyright © 2025 De Gruyter Brill. (c) High-throughput organ-on-a-chip platform with integrated real-time sensing in drug development workflows. Reprinted with permission from Azizgolshani *et al.*[277] Copyright © 2025 Royal Society of Chemistry. (d) An intelligent intestine-on-a-chip for rapid screening of probiotics with relief-enteritis function. Reprinted with permission from Wu *et al.*[108] Copyright © 2025 Wiley-VCH GmbH. (e) Intelligent organ-on-a-chip systems with comprehensive *in situ* bioanalysis. Reprinted with permission from Li *et al.*[278] Copyright © 2024 Wiley-VCH GmbH.

techniques, such as in situ sequencing, further expands the ability to uncover molecular underpinnings of cellular function, underscoring the power of flexible sensing in biological research.

Modeling neural development and disease by realizing the full potential of organoids and assembloids will require long-term, minimally invasive recording of electrical activity. Inspired by the art of kirigami, Yang *et al.*[268] introduced a novel platform termed "kirigami electronics" (KiriE) for chronic recording from cortical organoids (Figure 12d). KiriE transitions from 2D to a 3D basket-like structure, allowing accommodation of organoids in suspension for up to 120 days without compromising their morphology or cytoarchitecture. This design ensures minimally invasive and long-term monitoring, addressing limitations of conventional penetrating electrodes. They demonstrated KiriE's versatility by integrating it with optogenetic and pharmacological manipulations, successfully capturing corticostriatal connectivity in assembloids. The spiral or honeycomb patterns of KiriE provide structural adaptability, making it a robust tool for studying neural development and disease phenotypes, thus advancing flexible sensing applications in neuroscience.

Microfabricated 3D frameworks have been used as a qualitatively distinct type of multifunctional neural interface to spheroids or assembloids. Their complex architectures, high performance, and high-resolution features with optical, electrical, chemical, and thermal interfaces highlight the design versatility to control geometries, shapes, and sizes to match organoids/spheroids. Park *et al.*[269] introduced a mechanically compliant, multifunctional 3D mesostructure (3D MMF) as a flexible sensing interface for cortical spheroids and assembloids (Figure 12e). Formed through controlled buckling of 2D precursors, these frameworks integrate microelectrodes, light-emitting diodes, and thermal actuators, enabling simultaneous electrical, optical, and thermal interactions. This multifunctionality supports high-fidelity recording of neural activity across spheroid surfaces, surpassing traditional 2D microelectrode arrays. The 3D MMF adapts to spheroid growth through elastic deformation of its elastomeric substrate, maintaining soft contact with minimal tissue damage. Park *et al.* demonstrated its utility in studying synchronized bursting events and neurite bridge dynamics in assembloids, providing insights into neural connectivity and recovery. This platform exemplifies how flexible sensing integrates diverse functionalities for comprehensive neural interfacing.

Sensor selection should begin with the physiological question rather than the sensing mechanism. Mechanical sensors are suited to force, deformation, and flow-related questions; electrochemical sensors provide sensitive measurements of electrophysiology, barrier integrity, and soluble metabolites; optical approaches enable spatially resolved, often label-compatible observation; and flexible interfaces improve contact with growing 3D tissues but introduce fabrication and calibration complexity. Online monitoring is most valuable when the biological state changes rapidly, or sampling would disturb the microenvironment. For closed-loop operation, sensor outputs can be used to adjust flow, oxygenation, or stimulation, but drift, biofouling, material incompatibility, and signal crosstalk require reference measurements and periodic recalibration.[78,232-234,237,265-269]

4. Synergistic engineering: integrated design, monitoring, and applications

Synergy in MPS is achieved when biological complexity, engineering control, and measurement capability are co-designed around a defined physiological question. Simply placing an organoid in a microfluidic device is not sufficient; the integrated system should demonstrate a measurable gain in maturation, function, reproducibility, predictive performance, or experimental control relative to either component alone. Table 1 compares how these complementary features produce distinct gains and limitations across major MPS classes.

4.1. Co-design of biological complexity and engineering control

Organoids and OoC platforms are complementary rather than interchangeable. Organoids provide self-organized multicellular architecture, whereas OoC devices provide spatial control, perfusion, mechanical or electrical cues, and experimental access. Their integration should therefore align organ-specific cell hierarchies with microscale geometry, transport, stimulation, biocompatible sensing, reproducibility, and scalable manufacturing (Figure 13a).[275]

Bioprinting and acoustic assembly offer complementary routes for controlling tissue geometry. Bioprinting enables material and cell placement but must balance resolution, throughput, and cell viability; acoustic assembly rapidly patterns dense cellular structures but requires careful control of scale, material properties, and post-assembly maturation. Tunable hydrogels can provide mechanical and biochemical cues while supporting vascular or compartmentalized structures. Compared with conventional 3D culture, organoid-on-a-chip systems add controlled transport and stimulation, whereas 3D bioprinting adds reproducible spatial organization (Figure 13b).[276]

4.2. Sensor-enabled monitoring and quality control

Sensor integration must balance miniaturization and sensitivity with biocompatibility, signal stability, and minimal disturbance of the cultured tissue. Long-term measurements require controls for drift, biofouling,

Table 1. Comparative framework for synergistic engineering across microphysiological system classes

Platform class	Biological organization	Engineering and monitoring	Synergistic gain	Main limitation	Representative use and evidence
Conventional organoids	Self-organized multicellular 3D tissues	Limited perfusion; mostly endpoint readouts	Captures development and patient heterogeneity	Batch variability, diffusion limits, incomplete maturation	Developmental and patient-specific disease modeling.[14,18]
Single-organ-on-a-chip	Defined tissue interfaces and selected cell types	Controlled flow, strain, gradients, and accessible sensors	Reproduces dynamic organ-level functions	Reduced self-organization and cellular diversity	Barrier, toxicity, and pharmacology studies.[1,15,82]
Organoid-on-a-chip	Self-organized organoids within engineered compartments	Perfusion plus mechanical, electrical, or biochemical cues	Links biological complexity to controllable maturation and function	Vascularization, standardization, and long-term stability	Mechanistic development and functional drug testing.[16,159,160]
Multi-organ-on-a-chip	Linked tissue modules representing different organs	Shared circulation, scaling rules, and optional closed-loop control	Captures inter-organ PK/PD and systemic responses	Medium compatibility, flow scaling, and validation complexity	Systemic toxicity and drug disposition.[17,142,143]
Multi-organoid-on-a-chip	Two or more organoid modules, potentially donor-matched	Compartment-specific culture with controlled interconnection	Combines patient-specific biology with inter-organ communication	Co-maturation, batch effects, and unequal tissue demands	Metabolic-axis and multi-tissue safety studies.[184,185,187]
Sensor-enabled closed-loop MPS	Applicable across single- and multi-tissue systems	Continuous sensing linked to adaptive flow, oxygen, or stimulation	Turns measurements into reproducible feedback control	Drift, biofouling, calibration, and signal crosstalk	Adaptive screening, quality control, and automation.[234,277,278]

Abbreviations: MPS: Microphysiological systems; PD: Pharmacodynamics; PK: Pharmacokinetics.

calibration, and signal crosstalk. Azizgolshani *et al.*[277] developed a 96-device OoC platform with programmable flow, optical access, and integrated electrical and oxygen sensing for liver, vascular, gastrointestinal, and kidney models (Figure 13c). This architecture illustrates how sensor outputs can support standardized release criteria and higher-throughput drug-development workflows.

4.3. Intelligent screening and translational applications

Inflammatory bowel disease, including ulcerative colitis and Crohn's disease, involves dysregulated immune responses and disturbances in the gut microbiota. Wu *et al.*[108] developed a high-throughput intestine-on-a-chip with controlled oxygen conditions, intestinal cell–probiotic co-culture, barrier measurements, inflammatory readouts, and an unsupervised machine-learning score analyzer. The system ranked 12 *Bifidobacterium* strains for their ability to relieve enteritis-associated phenotypes, illustrating how microfluidic standardization and multimodal analysis can accelerate functional probiotic screening (Figure 13d).

Integrated MPS combines tissue architecture, dynamic microenvironments, and continuous measurement to support more reproducible functional characterization (Figure 13e).[278] When validated sensor outputs are linked to actuators, closed-loop control can adjust flow, oxygen, or stimulation in response to tissue state. In drug screening, disease modeling, and personalized medicine, these systems may improve mechanistic resolution and human relevance; however, predictive claims require comparison with clinical or established preclinical data.

5. Discussion: challenges and future prospects

5.1. Challenges of organoids

The reproducibility of organoid research is a critical determinant of experimental credibility, yet remains challenged by system complexity and biological variability. Donor cell heterogeneity—including inter-donor variation and intra-individual iPSC-derived discrepancies—significantly influences organoid formation dynamics and phenotypic outcomes. Genetic and epigenetic diversity within donor populations further compounds these challenges. Current organoid culture methods are labor-intensive, rely on costly reagents, animal-derived ECM components, and non-standardized protocols. Culture

conditions, such as ECM composition (e.g., Matrigel vs. synthetic hydrogels), introduce batch-dependent morphological and functional variation. Synthetic hydrogel-based ECM scaffolds show promise but require further optimization for industrial-scale production and regulatory compliance. Additional factors, including media formulation inconsistencies, oxygen gradient fluctuations, and growth factor concentration disparities, also compromise repeatability.

Bioreactor-integrated approaches and automated cultivation technologies aim to improve throughput and reduce manual intervention; however, these remain in early stages and require significant refinement to achieve clinical-grade manufacturing standards. To address these issues, standardized protocols, automated cultivation systems, and quantitative imaging analytics are essential for reducing user-induced variability and improving reproducibility.

Current organoid models predominantly reflect fetal or developmental tissue stages rather than mature adult physiology, lacking integrated systems such as vasculature, neural networks, and immune components. This developmental immaturity restricts their use in studying adult-onset disease pathogenesis. Firstly, vascularization deficiency remains a fundamental limitation in organoid systems, restricting nutrient diffusion, promoting necrotic core formation, and thereby limiting long-term viability and maturation. Conventional organoid systems face restricted nutrient and oxygen diffusion gradients that hinder tissue maturation and long-term sustainability. A critical obstacle in organoid development is mitigating necrotic core formation in volumetric specimens. Advanced vascularization strategies, such as endogenous vascular network self-assembly or pre-vascularized scaffold integration, have improved assembloid systems by enhancing tissue viability. Likewise, the absence of neural integration reduces physiological complexity in neuro-organoid models. Technical inefficiencies also persist in tumor-derived organoid establishment, including low success rates and difficulties in purifying malignant cells during expansion. Bioengineering innovations—including 3D bioprinting architectures, microfluidic OoC integrations, and multicellular co-culture platforms—are being developed to overcome these limitations, though challenges in scalability and technical complexity remain unresolved.

Clinical translation of organoid technologies faces complex regulatory and logistical barriers. Scaling production to meet clinical-grade specifications requires quality assurance, biosafety protocols, and reproducibility metrics.[279] Utilization of animal tumor-derived matrices (e.g., Matrigel) introduces biocompatibility complications because they fail to meet Good Manufacturing Practice criteria. In parallel, advances in synthetic ECMs have reduced batch variability traditionally associated with animal-derived hydrogel matrices.[280] Establishing international consensus on regulatory frameworks for organoid-based diagnostic and therapeutic applications is imperative to realize their clinical potential. Organoid research has ethical implications spanning donor consent protocols to ontological status considerations. Conventional biobanking paradigms employing consent/anonymization dichotomies prove inadequate for organoid repositories given their genetic donor linkage, creating personalized medicine privacy risks.[281] Furthermore, commercialization processes and equitable access to organoid-derived innovations necessitate robust governance architectures with explicit benefit allocation mechanisms.[282,283] Implementing transparent policies addressing donor engagement, consent granularity, and commercialization boundaries remains crucial for upholding ethical standards in organoid research.[284]

5.2. Challenges of organoids/organ-on-a-chip

Organ-on-a-chip systems face major challenges in replicating the full physiological complexity of human organs. Vascularization remains a key bottleneck, as establishing robust vascular networks is essential for mimicking organ-specific perfusion, oxygen gradients, and drug distribution. While multi-OoC platforms have demonstrated feasibility for PK–PD modeling, optimizing nutrient transport and metabolite clearance is critical to enhance inter-organ physiological relevance. The lack of standardized culture media formulations or harmonized hiPSC protocols often leads to cellular dedifferentiation and functional decline during long-term culture. In addition, polymeric substrates such as PDMS adsorb small molecules, undermining reproducibility in drug screening models. Operational barriers—including high production costs and limited throughput—further constrain adoption in resource-limited environments.

Scaling organoid and OoC production for high-throughput applications also presents technical challenges. Current OoC designs face limitations due to microfluidic complexity and non-physiological media-to-cell ratios. Open-well configurations and 3D bioprinting strategies offer scalable integration without sacrificing biological fidelity. Automation of cell culture protocols further supports standardization while increasing drug screening throughput. Integrated OoC systems hold strong potential for individualized therapeutic strategies. Recent progress highlights human-on-a-chip platforms capable of concurrent multi-organ functional modeling. These systems aim to replicate holistic physiological responses, improve translational accuracy, and reduce reliance on animal models. However, scaling introduces technical challenges, including cell sourcing standardization,

medium optimization, and interconnectivity adaptation.

Operational quality control should combine morphology, composition, function, and stability rather than relying on a single endpoint. Minimum metrics should include size distribution and structural features, cell-type composition and spatial organization, organ-specific functional outputs, barrier or electrical performance where relevant, and the duration of stable culture. Major sources of variability include donor and cell batches, ECM lots, flow and shear conditions, PDMS adsorption, bubbles, and sensor drift. Alignment across laboratories therefore requires reference materials, standard curves, predefined acceptance ranges, minimum reporting standards, and cross-platform benchmarking. These measures convert reproducibility from a general aspiration into a documented release criterion for research and manufacturing workflows.[279,280]

To make current reporting gaps directly visible, Table A1 records the seven requested engineering and biological parameters for representative chip-based and bioprinted platforms. Reported values were checked against the cited primary studies; "not reported" denotes an applicable parameter for which no explicit value was found, whereas "not applicable" identifies platforms without the relevant structural element. A panel-level audit of scale bars and objective magnifications for every reused microscopy block is provided in Table A2; metadata that were not reported or could not be assigned unambiguously are flagged individually.

5.3. Future prospects

Regulatory policy should be described as a pathway for qualified new approach methodologies, not as a universal replacement of animal studies. Section 3209 of the Consolidated Appropriations Act, 2023 (often called the FDA Modernization Act 2.0) broadened the statutory concept of a nonclinical test so that scientifically valid *in vitro*, *in silico*, and other non-animal methods may be used; it did not prohibit animal studies or designate organoids and OoC systems as preferred preclinical models.[285,286] The 118th-Congress FDA Modernization Act 3.0 (S. 5046) passed the Senate on December 12, 2024, but the House did not pass it before that Congress ended, so the 2024 bill did not become law.[287] On April 10, 2025, the Food and Drug Administration (FDA) released a roadmap for reducing animal testing in preclinical safety studies. The program begins with monoclonal antibodies and proposes phased expansion to other product classes, using fit-for-purpose validation, defined contexts of use, and weight-of-evidence assessment.[288] Organoids and OoC systems may therefore contribute regulatory evidence when they are sufficiently reliable, standardized, and relevant to the specific safety or efficacy question; they should not be presented as automatically replacing all animal studies.

The synergistic engineering of organoids and OoC, along with their integration with microengineering and sensing, makes it possible to more accurately simulate human physiological and pathological states, providing stronger support for drug development and disease research. The future of this field lies in the seamless integration and synergy of many technologies. The combination of organoids and OoC with AI and big data technologies has brought new opportunities to biomedical research and precision medicine. The integration of organoid-on-a-chip with AI enables image analysis and processing of organoids. Integrating with machine learning algorithms, it achieves a more efficient and higher-quality organoid construction method by identifying the spatial structure of matrix gels, fine-tuning cell culture conditions, identifying active inducing factors, and evaluating external stimuli. AI-assisted precise fluorescence coloring of grayscale organoid images from bright-field microscopy can be performed to identify and characterize cell type–specific information, helping researchers better observe and analyze the development of organoids and their responses to drugs. Digital twin organ models combined with experimental data from organoids can perform virtual simulations of real organs for disease prediction and diagnostic assistance and develop more precise treatment plans.

The integration of organoid-on-a-chip with big data analysis provides rich materials and data support for drug development and disease research. Organoid models can obtain multi-level data on the growth, development, and drug responses under different conditions, covering information on genes, proteins, cells, and tissues. In disease research, organoids simulate disease states in multi-OoC systems; macroscopic big data analysis integrates multi-source data and different factors on the occurrence and development of organ diseases to mine potential patterns and conduct in-depth exploration of disease mechanisms and the development of new treatment strategies. In drug development, analyzing a large amount of organoid drug test data can be used to predict the efficacy and safety of drugs, explore the mechanism of drug action, and screen drug targets. Personalized treatment plans can also be developed for patients by analyzing the vast amount of data generated from organoids with AI and integrating clinical data and treatment experiences from big data. These advanced systems will not only deepen our understanding of *in vivo* and *in vitro* human biology but also open up new avenues for the development of novel therapeutics and personalized healthcare solutions.

6. Conclusion

Organoids and OoC systems provide complementary strengths: organoids reproduce self-organized multicellular architecture, whereas chips enable controlled perfusion,

mechanical stimulation, inter-tissue communication, and continuous measurement. Their integration with bioprinting, acoustic assembly, and embedded sensors can improve maturation, reproducibility, and functional assessment, but added complexity does not by itself establish physiological relevance. Translation will require standardized cell sources and matrices, fit-for-purpose quality-control metrics, stable long-term culture, transparent reporting of engineering parameters, and validation against clinical or established preclinical data. Sensor-enabled and computationally assisted platforms may support adaptive experiments and higher-throughput screening, provided that calibration, drift, biofouling, and model bias are controlled. Progress therefore depends on co-designing biological complexity, engineering control, and measurement around clearly defined questions. With rigorous benchmarking and responsible governance, these systems can strengthen disease modeling, drug development, and personalized medicine while complementing, rather than universally replacing, existing preclinical approaches.

Acknowledgments

Graphical abstract created with BioRender.

Funding

F.Y. Zheng acknowledges support from the National Key Research and Development Program of China (2025YFF0511602), the Beijing Nova Program (20250484990), the Space Medical Experiment Project of CMSP (HYZHXMX01001), the National Natural Science Foundation of China (NSFC) Grants (No.82172110), the Beijing Natural Science Foundation-Haidian Original Innovation Joint Fund Project (No. L222143), and the Fundamental Research Funds for the Central Universities (No. JKF-20240772). X.R. Li acknowledges support from the NSFC Grants (No. 32301211). D.T. Xie and Y.X. Zhao acknowledge support from the National College Students' Innovative Entrepreneurial Training Plan (NO. 202410006165, S202410006169).

Conflict of interest

The authors declare that they have no known competing financial interests or personal relationships that could have appeared to influence the work reported in this paper.

Author contributions

Conceptualization: Fuyin Zheng, Xiaorui Li, Yu Wang, Zhongze Gu

Visualization: Diantong Xie, Yixu Zhao, Yubing Leng

Writing–original draft: Diantong Xie, Yixu Zhao, Yubing Leng, Xiaorui Li

Writing–review & editing: All authors

Ethics approval and consent to participate

Not applicable. This narrative review did not involve human participants, identifiable human data, or animal experiments conducted by the authors.

Consent for publication

Not applicable.

Availability of data

Not applicable.

References

1. Bhatia SN, Ingber DE. Microfluidic organs-on-chips. *Nat Biotechnol*. 2014;32(8):760-772.

   doi: 10.1038/nbt.2989

2. Clevers H. Modeling Development and Disease with Organoids. *Cell*. 2016;165(7):1586-1597.

   doi: 10.1016/j.cell.2016.05.082

3. Fang Y, Eglen RM. Three-Dimensional Cell Cultures in Drug Discovery and Development. *SLAS Discov*. 2017;22(5):456-472.

   doi: 10.1177/1087057117696795

4. Lancaster MA, Knoblich JA. Organogenesis in a dish: Modeling development and disease using organoid technologies. *Science*. 2014;345(6194):1247125.

   doi: 10.1126/science.1247125

5. Sato T, Vries RG, Snippert HJ, *et al*. Single Lgr5 stem cells build crypt-villus structures in vitro without a mesenchymal niche. *Nature*. 2009;459(7244):262-265.

   doi: 10.1038/nature07935

6. Quadrato G, Nguyen T, Macosko EZ, *et al*. Cell diversity and network dynamics in photosensitive human brain organoids. *Nature*. 2017;545(7652):48-53.

   doi: 10.1038/nature22047

7. Kimura M, Iguchi T, Iwasawa K, *et al*. En masse organoid phenotyping informs metabolic-associated genetic susceptibility to NASH. *Cell*. 2022;185(22):4216-4232.e16.

   doi: 10.1016/j.cell.2022.09.031

8. Gjorevski N, Nikolaev M, Brown TE, *et al*. Tissue geometry drives deterministic organoid patterning. *Science*. 2022;375(6576):eaaw9021.

   doi: 10.1126/science.aaw9021

9. Prahl LS, Liu J, Viola JM, *et al*. Jamming of nephron-forming niches in the developing mouse kidney creates cyclical mechanical stresses. *Nat Mater*. 2024;23(11):1582-1591.

   doi: 10.1038/s41563-024-02019-3

10. Mills RJ, Parker BL, Quaife-Ryan GA, *et al*. Drug Screening in Human PSC-Cardiac Organoids Identifies Pro-proliferative

Compounds Acting via the Mevalonate Pathway. *Cell Stem Cell*. 2019;24(6):895-907.e6.

doi: 10.1016/j.stem.2019.03.009

11. Huh D, Matthews BD, Mammoto A, Montoya-Zavala M, Hsin HY, Ingber DE. Reconstituting Organ-Level Lung Functions on a Chip. *Science*. 2010;328(5986):1662-1668.

doi: 10.1126/science.1188302

12. McAleer CW, Long CJ, Elbrecht D, *et al*. Multi-organ system for the evaluation of efficacy and off-target toxicity of anticancer therapeutics. *Sci Transl Med*. 2019;11(497):eaav1386.

doi: 10.1126/scitranslmed.aav1386

13. Ingber DE. Human organs-on-chips for disease modelling, drug development and personalized medicine. *Nat Rev Genet*. 2022;23(8):467-491.

doi: 10.1038/s41576-022-00466-9

14. Hofer M, Lutolf MP. Engineering organoids. *Nat Rev Mater*. 2021;6(5):402-420.

doi: 10.1038/s41578-021-00279-y

15. Vunjak-Novakovic G, Ronaldson-Bouchard K, Radisic M. Organs-on-a-chip models for biological research. *Cell*. 2021;184(18):4597-4611.

doi: 10.1016/j.cell.2021.08.005

16. Zhao Y, Landau S, Okhovatian S, *et al*. Integrating organoids and organ-on-a-chip devices. *Nat Rev Bioeng*. 2024;2(7):588-608.

doi: 10.1038/s44222-024-00207-z

17. Ronaldson-Bouchard K, Teles D, Yeager K, *et al*. A multi-organ chip with matured tissue niches linked by vascular flow. *Nat Biomed Eng*. 2022;6(4):351-371.

doi: 10.1038/s41551-022-00882-6

18. Zheng F, Xiao Y, Liu H, Fan Y, Dao M. Patient-Specific Organoid and Organ-on-a-Chip: 3D Cell-Culture Meets 3D Printing and Numerical Simulation. *Adv Biol (Weinh)*. 2021;5(6):e2000024.

doi: 10.1002/adbi.202000024

19. Post Y, Clevers H. Defining Adult Stem Cell Function at Its Simplest: The Ability to Replace Lost Cells through Mitosis. *Cell Stem Cell*. 2019;25(2):174-183.

doi: 10.1016/j.stem.2019.07.002

20. Yi SA, Zhang Y, Rathnam C, Pongkulapa T, Lee KB. Bioengineering Approaches for the Advanced Organoid Research. *Adv Mater*. 2021;33(45):2007949.

doi: 10.1002/adma.202007949

21. Xu Y, Kuppe C, Perales-Patón J, *et al*. Adult human kidney organoids originate from CD24+ cells and represent an advanced model for adult polycystic kidney disease. *Nat Genet*. 2022;54(11):1690-1701.

doi: 10.1038/s41588-022-01202-z

22. Guan J, Wang G, Wang J, *et al*. Chemical reprogramming of human somatic cells to pluripotent stem cells. *Nature*. 2022;605(7909):325-331.

doi: 10.1038/s41586-022-04593-5

23. Hou P, Li Y, Zhang X, *et al*. Pluripotent Stem Cells Induced from Mouse Somatic Cells by Small-Molecule Compounds. *Science*. 2013;341(6146):651-654.

doi: 10.1126/science.1239278

24. Hendriks D, Artegiani B, Hu H, Chuva de Sousa Lopes S, Clevers H. Establishment of human fetal hepatocyte organoids and CRISPR–Cas9-based gene knockin and knockout in organoid cultures from human liver. *Nat Protoc*. 2021;16(1):182-217.

doi: 10.1038/s41596-020-00411-2

25. Taguchi A, Kaku Y, Ohmori T, *et al*. Redefining the In Vivo Origin of Metanephric Nephron Progenitors Enables Generation of Complex Kidney Structures from Pluripotent Stem Cells. *Cell Stem Cell*. 2014;14(1):53-67.

doi: 10.1016/j.stem.2013.11.010

26. Sachs N, de Ligt J, Kopper O, *et al*. A Living Biobank of Breast Cancer Organoids Captures Disease Heterogeneity. *Cell*. 2018;172(1):373-386.e10.

doi: 10.1016/j.cell.2017.11.010

27. Strating E, Verhagen MP, Wensink E, *et al*. Co-cultures of colon cancer cells and cancer-associated fibroblasts recapitulate the aggressive features of mesenchymal-like colon cancer. *Front Immunol*. 2023;14:1053920.

doi: 10.3389/fimmu.2023.1053920

28. Schuth S, Le Blanc S, Krieger TG, *et al*. Patient-specific modeling of stroma-mediated chemoresistance of pancreatic cancer using a three-dimensional organoid-fibroblast co-culture system. *J Exp Clin Cancer Res*. 2022;41(1):312.

doi: 10.1186/s13046-022-02519-7

29. Liu X, Wang X, Zhang L, *et al*. 3D Liver Tissue Model with Branched Vascular Networks by Multimaterial Bioprinting. *Adv Healthc Mater*. 2021;10(23):2101405.

doi: 10.1002/adhm.202101405

30. Miller AJ, Dye BR, Ferrer-Torres D, *et al*. Generation of lung organoids from human pluripotent stem cells in vitro. *Nat Protoc*. 2019;14(2):518-540.

doi: 10.1038/s41596-018-0104-8

31. Budeus B, Kroepel C, Stasch LM, Klein D. Matrix-free human lung organoids derived from induced pluripotent stem cells to model lung injury. *Stem Cell Res Ther*. 2024;15(1):468.

doi: 10.1186/s13287-024-04106-3

32. Branco MA, Dias TP, Cabral JMS, Pinto-do-Ó P, Diogo MM. Human multilineage pro-epicardium/foregut organoids support the development of an epicardium/myocardium organoid. *Nat Commun*. 2022;13(1):6981.

doi: 10.1038/s41467-022-34730-7

33. Tadokoro T, Murata S, Kato M, *et al*. Human iPSC–liver organoid transplantation reduces fibrosis through immunomodulation. *Sci Transl Med*. 2024;16(757):eadg0338.

doi: 10.1126/scitranslmed.adg0338

34. Hu Y, Sui X, Song F, *et al*. Lung cancer organoids analyzed on microwell arrays predict drug responses of patients within a week. *Nat Commun*. 2021;12(1):2581.

doi: 10.1038/s41467-021-22676-1

35. Yang L, Wang X, Zhou X, *et al*. A tunable human intestinal organoid system achieves controlled balance between self-renewal and differentiation. *Nat Commun*. 2025;16(1):315.

doi: 10.1038/s41467-024-55567-2

36. Zhang R, Chen Y, Feng Z, *et al*. Reprogramming human urine cells into intestinal organoids with long-term expansion ability and barrier function. *Heliyon*. 2024;10(13):e33736.

doi: 10.1016/j.heliyon.2024.e33736

37. Lorenzo-Martín LF, Hübscher T, Bowler AD, *et al*. Spatiotemporally resolved colorectal oncogenesis in mini-colons ex vivo. *Nature*. 2024;629(8011):450-457.

doi: 10.1038/s41586-024-07330-2

38. Baghdadi MB, Houtekamer RM, Perrin L, *et al*. PIEZO-dependent mechanosensing is essential for intestinal stem cell fate decision and maintenance. *Science*. 2024;386(6725):eadj7615.

doi: 10.1126/science.adj7615

39. Tran T, Song CJ, Nguyen T, *et al*. A scalable organoid model of human autosomal dominant polycystic kidney disease for disease mechanism and drug discovery. *Cell Stem Cell*. 2022;29(7):1083-1101.e7.

doi: 10.1016/j.stem.2022.06.005

40. Vanslambrouck JM, Wilson SB, Tan KS, *et al*. Enhanced metanephric specification to functional proximal tubule enables toxicity screening and infectious disease modelling in kidney organoids. *Nat Commun*. 2022;13(1):5943.

doi: 10.1038/s41467-022-33623-z

41. Freedman BS, Brooks CR, Lam AQ, *et al*. Modelling kidney disease with CRISPR-mutant kidney organoids derived from human pluripotent epiblast spheroids. *Nat Commun*. 2015;6(1):8715.

doi: 10.1038/ncomms9715

42. Kroll KT, Homan KA, Uzel SGM, *et al*. A perfusable, vascularized kidney organoid-on-chip model. *Biofabrication*. 2024;16(4):045003.

doi: 10.1088/1758-5090/ad5ac0

43. Pezet MG, Torres JA, Thimraj TA, *et al*. Human respiratory airway progenitors derived from pluripotent cells generate alveolar epithelial cells and model pulmonary fibrosis. *Nat Biotechnol*. 2026;44(3):394-405.

doi: 10.1038/s41587-025-02569-0

44. Salahudeen AA, Choi SS, Rustagi A, *et al*. Progenitor identification and SARS-CoV-2 infection in human distal lung organoids. *Nature*. 2020;588(7839):670-675.

doi: 10.1038/s41586-020-3014-1

45. Leibel SL, McVicar RN, Murad R, *et al*. A therapy for suppressing canonical and noncanonical SARS-CoV-2 viral entry and an intrinsic intrapulmonary inflammatory response. *Proc Natl Acad Sci USA*. 2024;121(30):e2408109121.

doi: 10.1073/pnas.2408109121

46. Basil MC, Cardenas-Diaz FL, Kathiriya JJ, *et al*. Human distal airways contain a multipotent secretory cell that can regenerate alveoli. *Nature*. 2022;604(7904):120-126.

doi: 10.1038/s41586-022-04552-0

47. Jones DL, Morley MP, Li X, *et al*. An injury-induced mesenchymal-epithelial cell niche coordinates regenerative responses in the lung. *Science*. 2024;386(6727):eado5561.

doi: 10.1126/science.ado5561

48. Yang P, Zhu L, Wang S, *et al*. Engineered model of heart tissue repair for exploring fibrotic processes and therapeutic interventions. *Nat Commun*. 2024;15(1):7996.

doi: 10.1038/s41467-024-52221-9

49. Volmert B, Kiselev A, Juhong A, *et al*. A patterned human primitive heart organoid model generated by pluripotent stem cell self-organization. *Nat Commun*. 2023;14:8245.

doi: 10.1038/s41467-023-43999-1

50. Zhang Z, Zhou X, Fang Y, Xiong Z, Zhang T. AI-driven 3D bioprinting for regenerative medicine: From bench to bedside. *Bioact Mater*. 2025;45:201-230.

doi: 10.1016/j.bioactmat.2024.11.021

51. Lewis J, Yaseen B, Wu H, Saraf A. Novel 2D/3D Hybrid Organoid System for High-Throughput Drug Screening in iPSC Cardiomyocytes. *Therapeutics*. 2025;2(3):11.

doi: 10.3390/therapeutics2030011

52. Fan F, Shang J, Li J, *et al*. High-Throughput Formation of Pre-Vascularized hiPSC-Derived Hepatobiliary Organoids on a Chip via Nonparenchymal Cell Grafting. *Adv Sci*. 2025;12(8):2407945.

doi: 10.1002/advs.202407945

53. Leite SB, Roosens T, El Taghdouini A, *et al*. Novel human hepatic organoid model enables testing of drug-induced liver fibrosis in vitro. *Biomaterials*. 2016;78:1-10.

doi: 10.1016/j.biomaterials.2015.11.026

54. Wu H, Wang J, Liu S, *et al*. Large-Scale Production of Expandable Hepatoblast Organoids and Polarised Hepatocyte Organoids From hESCs Under 3D Static and Dynamic Suspension Conditions. *Cell Prolif*. 2025;58(7):e70001.

doi: 10.1111/cpr.70001

55. Liu J, Hanson A, Yin W, *et al*. Decellularized liver scaffolds for constructing drug-metabolically functional ex vivo human liver models. *Bioact Mater*. 2025;43:162-180.

doi: 10.1016/j.bioactmat.2024.09.029

56. Wang L, Koui Y, Kanegae K, *et al*. Establishment of human induced pluripotent stem cell-derived hepatobiliary organoid with bile duct for pharmaceutical research use. *Biomaterials*. 2024;310:122621.

doi: 10.1016/j.biomaterials.2024.122621

57. Utami T, Danoy M, Khadim RR, *et al*. A highly efficient cell culture method using oxygen-permeable PDMS-based honeycomb microwells produces functional liver organoids from human induced pluripotent stem cell-derived carboxypeptidase M liver progenitor cells. *Biotechnol Bioeng*. 2024;121(4):1177-1189.

doi: 10.1002/bit.28640

58. Qian X, Nguyen HN, Song MM, *et al*. Brain-Region-Specific Organoids Using Mini-bioreactors for Modeling ZIKV Exposure. *Cell*. 2016;165(5):1238-1254.

doi: 10.1016/j.cell.2016.04.032

59. Son J, Park SJ, Ha T, Lee SN, Cho HY, Choi JW. Electrophysiological Monitoring of Neurochemical-Based Neural Signal Transmission in a Human Brain–Spinal Cord Assembliod. *ACS Sens*. 2022;7(2):409-414.

doi: 10.1021/acssensors.1c02279

60. Xiang Y, Tanaka Y, Cakir B, *et al*. hESC-Derived Thalamic Organoids Form Reciprocal Projections When Fused with Cortical Organoids. *Cell Stem Cell*. 2019;24(3):487-497.e7.

doi: 10.1016/j.stem.2018.12.015

61. Yin Y, Zhou W, Zhu J, *et al*. Generation of self-organized neuromusculoskeletal tri-tissue organoids from human pluripotent stem cells. *Cell Stem Cell*. 2025;32(1):157-171.e8.

doi: 10.1016/j.stem.2024.11.005

62. Du Y, Wang YR, Bao QY, *et al*. Personalized Vascularized Tumor Organoid-on-a-Chip for Tumor Metastasis and Therapeutic Targeting Assessment. *Adv Mater*. 2025;37(6):e2412815.

doi: 10.1002/adma.202412815

63. Yu J, Yin Y, Leng Y, *et al*. Emerging strategies of engineering retinal organoids and organoid-on-a-chip in modeling intraocular drug delivery: Current progress and future perspectives. *Adv Drug Deliv Rev*. 2023;197:114842.

doi: 10.1016/j.addr.2023.114842

64. Gabriel E, Albanna W, Pasquini G, *et al*. Human brain organoids assemble functionally integrated bilateral optic vesicles. *Cell Stem Cell*. 2021;28(10):1740-1757.e8.

doi: 10.1016/j.stem.2021.07.010

65. Wimmer RA, Leopoldi A, Aichinger M, Kerjaschki D, Penninger JM. Generation of blood vessel organoids from human pluripotent stem cells. *Nat Protoc*. 2019;14(11):3082-3100.

doi: 10.1038/s41596-019-0213-z

66. Sun XY, Ju XC, Li Y, *et al*. Generation of vascularized brain organoids to study neurovascular interactions. *eLife*. 2022;11:e76707.

doi: 10.7554/eLife.76707

67. Liu H, Zhang X, Liu J, Qin J. Vascularization of engineered organoids. *BMEMat*. 2023;1(3):e12031.

doi: 10.1002/bmm2.12031

68. Skylar-Scott MA, Huang JY, Lu A, *et al*. Orthogonally induced differentiation of stem cells for the programmatic patterning of vascularized organoids and bioprinted tissues. *Nat Biomed Eng*. 2022;6(4):449-462.

doi: 10.1038/s41551-022-00856-8

69. Holloway EM, Wu JH, Czerwinski M, *et al*. Differentiation of Human Intestinal Organoids with Endogenous Vascular Endothelial Cells. *Dev Cell*. 2020;54(4):516-528.e7.

doi: 10.1016/j.devcel.2020.07.023

70. Zhao Y, Sun M, Pan Z, *et al*. A novel quantitative angiogenesis assay based on visualized vascular organoid. *Angiogenesis*. 2025;28(1):10.

doi: 10.1007/s10456-024-09967-z

71. Papargyriou A, Najajreh M, Cook DP, *et al*. Heterogeneity-driven phenotypic plasticity and treatment response in branched-organoid models of pancreatic ductal adenocarcinoma. *Nat Biomed Eng*. 2024;9(6):836-864.

doi: 10.1038/s41551-024-01273-9

72. Peng T, Ma X, Hua W, *et al*. Individualized patient tumor organoids faithfully preserve human brain tumor ecosystems and predict patient response to therapy. *Cell Stem Cell*. 2025;32(4):652-669.e11.

doi: 10.1016/j.stem.2025.01.002

73. Rao J, Song C, Hao Y, *et al*. Leveraging Patient-Derived Organoids for Personalized Liver Cancer Treatment. *Int J Biol Sci*. 2024;20(13):5363-5374.

doi: 10.7150/ijbs.96317

74. Jia Z, Xu H, Zhang Y, *et al*. Distinct discrepancy in breast cancer organoids recapitulation among molecular subtypes revealed by single-cell transcriptomes analysis. *Clin Transl Med*. 2024;14(9):e70023.

doi: 10.1002/ctm2.70023

75. Xu Z, Yang H, Zhou Y, Dzakah EE, Zhao B. Whole-process 3D ECM-encapsulated organoid-based automated high-throughput screening platform accelerates drug discovery for rare diseases. *Life Med*. 2025;4(5):lnaf021.

doi: 10.1093/lifemedi/lnaf021

76. Mo S, Tang P, Luo W, *et al*. Patient-Derived Organoids from Colorectal Cancer with Paired Liver Metastasis Reveal Tumor Heterogeneity and Predict Response to Chemotherapy. *Adv*

Sci. 2022;9(31):2204097.

doi: 10.1002/advs.202204097

77. Liu C, Li K, Sui X, *et al*. Patient-Derived Tumor Organoids Combined with Function-Associated ScRNA-Seq for Dissecting the Local Immune Response of Lung Cancer. *Adv Sci*. 2024;11(31):2400185.

doi: 10.1002/advs.202400185

78. Huang Y, Liu T, Huang Q, Wang Y. From Organ-on-a-Chip to Human-on-a-Chip: A Review of Research Progress and Latest Applications. *ACS Sens*. 2024;9(7):3466-3488.

doi: 10.1021/acssensors.4c00004

79. Dhiman N, Kingshott P, Sumer H, Sharma CS, Rath SN. On-chip anticancer drug screening – Recent progress in microfluidic platforms to address challenges in chemotherapy. *Biosens Bioelectron*. 2019;137:236-254.

doi: 10.1016/j.bios.2019.02.070

80. Shinohara M, Arakawa H, Oda Y, *et al*. Coculture with hiPS-derived intestinal cells enhanced human hepatocyte functions in a pneumatic-pressure-driven two-organ microphysiological system. *Sci Rep*. 2021;11(1):5437.

doi: 10.1038/s41598-021-84861-y

81. Shinha K, Nihei W, Ono T, Nakazato R, Kimura H. A pharmacokinetic–pharmacodynamic model based on multi-organ-on-a-chip for drug–drug interaction studies. *Biomicrofluidics*. 2020;14(4):044108.

doi: 10.1063/5.0011545

82. Monteduro AG, Rizzato S, Caragnano G, Trapani A, Giannelli G, Maruccio G. Organs-on-chips technologies – A guide from disease models to opportunities for drug development. *Biosens Bioelectron*. 2023;231:115271.

doi: 10.1016/j.bios.2023.115271

83. van Berlo D, van de Steeg E, Amirabadi HE, Masereeuw R. The potential of multi-organ-on-chip models for assessment of drug disposition as alternative to animal testing. *Curr Opin Toxicol*. 2021;27:8-17.

doi: 10.1016/j.cotox.2021.05.001

84. Pramotton FM, Spitz S, Kamm RD. Challenges and Future Perspectives in Modeling Neurodegenerative Diseases Using Organ-on-a-Chip Technology. *Adv Sci*. 2024;11(32):2403892.

doi: 10.1002/advs.202403892

85. Rezaei NT, Kumar H, Liu H, Lee SS, Park SS, Kim K. Recent Advances in Organ-on-Chips Integrated with Bioprinting Technologies for Drug Screening. *Adv Healthc Mater*. 2023;12(20):2203172.

doi: 10.1002/adhm.202203172

86. Ballerini M, Galiè S, Tyagi P, *et al*. A gut-on-a-chip incorporating human faecal samples and peristalsis predicts responses to immune checkpoint inhibitors for melanoma. *Nat Biomed Eng*. 2025;9(6):967-984.

doi: 10.1038/s41551-024-01318-z

87. Kim HJ, Li H, Collins JJ, Ingber DE. Contributions of microbiome and mechanical deformation to intestinal bacterial overgrowth and inflammation in a human gut-on-a-chip. *Proc Natl Acad Sci USA*. 2016;113(1):E7-E15.

doi: 10.1073/pnas.1522193112

88. Li S, Li C, Khan MI, *et al*. Microneedle array facilitates hepatic sinusoid construction in a large-scale liver-acinus-chip microsystem. *Microsyst Nanoeng*. 2023;9(1):75.

doi: 10.1038/s41378-023-00544-w

89. Agarwal A, Adrian Goss J, Cho A, Laura McCain M, Kit Parker K. Microfluidic heart on a chip for higher throughput pharmacological studies. *Lab Chip*. 2013;13(18):3599-3608.

doi: 10.1039/C3LC50350J

90. Musah S, Mammoto A, Ferrante TC, *et al*. Mature induced-pluripotent-stem-cell-derived human podocytes reconstitute kidney glomerular-capillary-wall function on a chip. *Nat Biomed Eng*. 2017;1(5):0069.

doi: 10.1038/s41551-017-0069

91. Li Y, Xie M, Lv S, *et al*. A bionic controllable strain membrane for cell stretching at air–liquid interface inspired by papercutting. *Int J Extrem Manuf*. 2023;5(4):045502.

doi: 10.1088/2631-7990/acef77

92. Baptista D, Moreira Teixeira L, Barata D, *et al*. 3D Lung-on-Chip Model Based on Biomimetically Microcurved Culture Membranes. *ACS Biomater Sci Eng*. 2022;8(6):2684-2699.

doi: 10.1021/acsbiomaterials.1c01463

93. Jung O, Tung YT, Sim E, *et al*. Development of human-derived, three-dimensional respiratory epithelial tissue constructs with perfusable microvasculature on a high-throughput microfluidics screening platform. *Biofabrication*. 2022;14(2):025012.

doi: 10.1088/1758-5090/ac32a5

94. Huang D, Liu T, Liao J, *et al*. Reversed-engineered human alveolar lung-on-a-chip model. *Proc Natl Acad Sci USA*. 2021;118(19):e2016146118.

doi: 10.1073/pnas.2016146118

95. Cao T, Shao C, Yu X, *et al*. Biomimetic Alveolus-on-a-Chip for SARS-CoV-2 Infection Recapitulation. *Research*. 2022;2022:9819154.

doi: 10.34133/2022/9819154

96. Si L, Bai H, Rodas M, *et al*. A human-airway-on-a-chip for the rapid identification of candidate antiviral therapeutics and prophylactics. *Nat Biomed Eng*. 2021;5(8):815-829.

doi: 10.1038/s41551-021-00718-9

97. Deinhardt-Emmer S, Rennert K, Schicke E, *et al*. Co-infection with Staphylococcus aureus after primary influenza virus infection leads to damage of the endothelium in a human alveolus-on-a-chip model. *Biofabrication*.

2020;12(2):025012.

doi: 10.1088/1758-5090/ab7073

98. Zhang M, Wang P, Luo R, *et al*. Biomimetic Human Disease Model of SARS-CoV-2-Induced Lung Injury and Immune Responses on Organ Chip System. *Adv Sci*. 2021;8(3):2002928.

doi: 10.1002/advs.202002928

99. Thacker VV, Sharma K, Dhar N, Mancini G, Sordet-Dessimoz J, McKinney JD. Rapid endotheliitis and vascular damage characterize SARS-CoV-2 infection in a human lung-on-chip model. *EMBO Rep*. 2021;22(6):e52744.

doi: 10.15252/embr.202152744

100. Dasgupta Q, Jiang A, Wen AM, *et al*. A human lung alveolus-on-a-chip model of acute radiation-induced lung injury. *Nat Commun*. 2023;14(1):6506.

doi: 10.1038/s41467-023-42171-z

101. Ringquist R, Bhatia E, Chatterjee P, *et al*. An immune-competent lung-on-a-chip for modelling the human severe influenza infection response. *Nat Biomed Eng*. 2026;10:897-919.

doi: 10.1038/s41551-025-01491-9

102. Grassart A, Malardé V, Gobaa S, *et al*. Bioengineered Human Organ-on-Chip Reveals Intestinal Microenvironment and Mechanical Forces Impacting Shigella Infection. *Cell Host Microbe*. 2019;26(3):435-444.e4.

doi: 10.1016/j.chom.2019.08.007

103. Guo Y, Li Z, Su W, Wang L, Zhu Y, Qin J. A Biomimetic Human Gut-on-a-Chip for Modeling Drug Metabolism in Intestine. *Artif Organs*. 2018;42(12):1196-1205.

doi: 10.1111/aor.13163

104. Shim KY, Lee D, Han J, Nguyen NT, Park S, Sung JH. Microfluidic gut-on-a-chip with three-dimensional villi structure. *Biomed Microdevices*. 2017;19(2):37.

doi: 10.1007/s10544-017-0179-y

105. Jing B, Wang ZA, Zhang C, *et al*. Establishment and Application of Peristaltic Human Gut-Vessel Microsystem for Studying Host–Microbial Interaction. *Front Bioeng Biotechnol*. 2020;8:272.

doi: 10.3389/fbioe.2020.00272

106. Valiei A, Aminian-Dehkordi J, Mofrad MRK. Gut-on-a-chip models for dissecting the gut microbiology and physiology. *APL Bioeng*. 2023;7(1):011502.

doi: 10.1063/5.0126541

107. Kim HJ, Huh D, Hamilton G, Ingber DE. Human gut-on-a-chip inhabited by microbial flora that experiences intestinal peristalsis-like motions and flow. *Lab Chip*. 2012;12(12):2165-2174.

doi: 10.1039/C2LC40074J

108. Wu J, Zhang B, Liu X, *et al*. An Intelligent Intestine-on-a-Chip for Rapid Screening of Probiotics with Relief-Enteritis Function. *Adv Mater*. 2024;36(47):2408485.

doi: 10.1002/adma.202408485

109. Shin YC, Shin W, Koh D, *et al*. Three-Dimensional Regeneration of Patient-Derived Intestinal Organoid Epithelium in a Physiodynamic Mucosal Interface-on-a-Chip. *Micromachines*. 2020;11(7):663.

doi: 10.3390/mi11070663

110. Donkers JM, van der Vaart JI, van de Steeg E. Gut-on-a-Chip Research for Drug Development: Implications of Chip Design on Preclinical Oral Bioavailability or Intestinal Disease Studies. *Biomimetics*. 2023;8(2):226.

doi: 10.3390/biomimetics8020226

111. Özkan A, LoGrande NT, Feitor JF, Goyal G, Ingber DE. Intestinal organ chips for disease modelling and personalized medicine. *Nat Rev Gastroenterol Hepatol*. 2024;21(11):751-773.

doi: 10.1038/s41575-024-00968-3

112. Shao C, Liu Y, Chi J, Wang J, Zhao Z, Zhao Y. Responsive Inverse Opal Scaffolds with Biomimetic Enrichment Capability for Cell Culture. *Research*. 2019;2019:9783793.

doi: 10.34133/2019/9783793

113. Bircsak KM, DeBiasio R, Miedel M, *et al*. A 3D microfluidic liver model for high throughput compound toxicity screening in the OrganoPlate®. *Toxicology*. 2021;450:152667.

doi: 10.1016/j.tox.2020.152667

114. Ya S, Ding W, Li S, *et al*. On-Chip Construction of Liver Lobules with Self-Assembled Perfusable Hepatic Sinusoid Networks. *ACS Appl Mater Interfaces*. 2021;13(28):32640-32652.

doi: 10.1021/acsami.1c00794

115. Lee JB, Park JS, Shin YM, *et al*. Implantable Vascularized Liver Chip for Cross-Validation of Disease Treatment with Animal Model. *Adv Funct Mater*. 2019;29(23):1900075.

doi: 10.1002/adfm.201900075

116. Özkan A, Stolley DL, Cressman ENK, *et al*. Vascularized hepatocellular carcinoma on a chip to control chemoresistance through cirrhosis, inflammation and metabolic activity. *Small Struct*. 2023;4(9):2200403.

doi: 10.1002/sstr.202200403

117. Matsumoto S, Safitri AR, Danoy M, *et al*. Investigation of the hepatic respiration and liver zonation on rat hepatocytes using an integrated oxygen biosensor in a microscale device. *Biotechnol Prog*. 2019;35(5):e2854.

doi: 10.1002/btpr.2854

118. Chhabra A, Song HHG, Grzelak KA, *et al*. A vascularized model of the human liver mimics regenerative responses. *Proc Natl Acad Sci USA*. 2022;119(28):e2115867119.

doi: 10.1073/pnas.2115867119

119. Nawroth JC, Petropolis DB, Manatakis DV, *et al*. Modeling alcohol-associated liver disease in a human Liver-Chip. *Cell Rep*. 2021;36(3):109393.

doi: 10.1016/j.celrep.2021.109393

120. Hou Y, Gao Z, Tu P, Ai X, Jiang Y. Establishment of an idiosyncratic drug-induced liver injury model on a stacked array chip for identification of CCL5-mediated paracrine dynamics. *Anal Chem*. 2024;96(49):19370-19377.

doi: 10.1021/acs.analchem.4c03552

121. Zhao Y, Rafatian N, Feric NT, *et al*. A Platform for Generation of Chamber-Specific Cardiac Tissues and Disease Modeling. *Cell*. 2019;176(4):913-927.e18.

doi: 10.1016/j.cell.2018.11.042

122. Veldhuizen J, Cutts J, Brafman DA, Migrino RQ, Nikkhah M. Engineering anisotropic human stem cell-derived three-dimensional cardiac tissue on-a-chip. *Biomaterials*. 2020;256:120195.

doi: 10.1016/j.biomaterials.2020.120195

123. Park SJ, Zhang D, Qi Y, *et al*. Insights Into the Pathogenesis of Catecholaminergic Polymorphic Ventricular Tachycardia From Engineered Human Heart Tissue. *Circulation*. 2019;140(5):390-404.

doi: 10.1161/CIRCULATIONAHA.119.039711

124. Gaballah M, Penttinen K, Kreutzer J, Mäki AJ, Kallio P, Aalto-Setälä K. Cardiac Ischemia On-a-Chip: Antiarrhythmic Effect of Levosimendan on Ischemic Human-Induced Pluripotent Stem Cell-Derived Cardiomyocytes. *Cells*. 2022;11(6):1045.

doi: 10.3390/cells11061045

125. Liu H, Bolonduro OA, Hu N, *et al*. Heart-on-a-Chip Model with Integrated Extra- and Intracellular Bioelectronics for Monitoring Cardiac Electrophysiology under Acute Hypoxia. *Nano Lett*. 2020;20(4):2585-2593.

doi: 10.1021/acs.nanolett.0c00076

126. Chen X, Liu S, Han M, *et al*. Engineering Cardiac Tissue for Advanced Heart-On-A-Chip Platforms. *Adv Healthc Mater*. 2024;13(1):2301338.

doi: 10.1002/adhm.202301338

127. Wu H, Shi S, Liu Y, *et al*. Recent progress of organ-on-a-chip towards cardiovascular diseases: advanced design, fabrication, and applications. *Biofabrication*. 2023;15(4):042001.

doi: 10.1088/1758-5090/acdaf9

128. Qiang Y, Sissoko A, Liu ZL, *et al*. Microfluidic study of retention and elimination of abnormal red blood cells by human spleen with implications for sickle cell disease. *Proc Natl Acad Sci USA*. 2023;120(6):e2217607120.

doi: 10.1073/pnas.2217607120

129. Petrosyan A, Cravedi P, Villani V, *et al*. A glomerulus-on-a-chip to recapitulate the human glomerular filtration barrier. *Nat Commun*. 2019;10:3656.

doi: 10.1038/s41467-019-11577-z

130. Mou X, Shah J, Roye Y, Du C, Musah S. An ultrathin membrane mediates tissue-specific morphogenesis and barrier function in a human kidney chip. *Sci Adv*. 2024;10(23):eadn2689.

doi: 10.1126/sciadv.adn2689

131. Lin NYC, Homan KA, Robinson SS, *et al*. Renal reabsorption in 3D vascularized proximal tubule models. *Proc Natl Acad Sci USA*. 2019;116(12):5399-5404.

doi: 10.1073/pnas.1815208116

132. Uzel SGM, Platt RJ, Subramanian V, *et al*. Microfluidic device for the formation of optically excitable, three-dimensional, compartmentalized motor units. *Sci Adv*. 2016;2(8):e1501429.

doi: 10.1126/sciadv.1501429

133. Lyu Z, Park J, Kim KM, *et al*. A neurovascular-unit-on-a-chip for the evaluation of the restorative potential of stem cell therapies for ischaemic stroke. *Nat Biomed Eng*. 2021;5(8):847-863.

doi: 10.1038/s41551-021-00744-7

134. Kim J, Lee KT, Lee JS, *et al*. Fungal brain infection modelled in a human-neurovascular-unit-on-a-chip with a functional blood–brain barrier. *Nat Biomed Eng*. 2021;5(8):830-846.

doi: 10.1038/s41551-021-00743-8

135. Neto E, Monteiro AC, Leite Pereira C, *et al*. Micropathological Chip Modeling the Neurovascular Unit Response to Inflammatory Bone Condition. *Adv Healthc Mater*. 2022;11(11):2102305.

doi: 10.1002/adhm.202102305

136. Leng Y, Li X, Zheng F, *et al*. Advances in In Vitro Models of Neuromuscular Junction: Focusing on Organ-on-a-Chip, Organoids, and Biohybrid Robotics. *Adv Mater*. 2023;35(41):2211059.

doi: 10.1002/adma.202211059

137. Ionescu A, Zahavi EE, Gradus T, Ben-Yaakov K, Perlson E. Compartmental microfluidic system for studying muscle–neuron communication and neuromuscular junction maintenance. *Eur J Cell Biol*. 2016;95(2):69-88.

doi: 10.1016/j.ejcb.2015.11.004

138. Vila OF, Chavez M, Ma SP, *et al*. Bioengineered optogenetic model of human neuromuscular junction. *Biomaterials*. 2021;276:121033.

doi: 10.1016/j.biomaterials.2021.121033

139. Yamamoto K, Yamaoka N, Imaizumi Y, *et al*. Development of a human neuromuscular tissue-on-a-chip model on a 24-well-plate-format compartmentalized microfluidic device. *Lab Chip*. 2021;21(10):1897-1907.

doi: 10.1039/D1LC00048A

140. Chen WLK, Edington C, Suter E, *et al*. Integrated gut/liver microphysiological systems elucidates inflammatory inter-

tissue crosstalk. *Biotechnol Bioeng*. 2017;114(11):2648-2659.

doi: 10.1002/bit.26370

141. Schimek K, Busek M, Brincker S, *et al*. Integrating biological vasculature into a multi-organ-chip microsystem. *Lab Chip*. 2013;13(18):3588-3598.

doi: 10.1039/C3LC50217A

142. Jiang N, Ying G, Yin Y, *et al*. A closed-loop modular multiorgan-on-chips platform for self-sustaining and tightly controlled oxygenation. *Proc Natl Acad Sci USA*. 2024;121(47):e2413684121.

doi: 10.1073/pnas.2413684121

143. Herland A, Maoz BM, Das D, *et al*. Quantitative prediction of human pharmacokinetic responses to drugs via fluidically coupled vascularized organ chips. *Nat Biomed Eng*. 2020;4(4):421-436.

doi: 10.1038/s41551-019-0498-9

144. Saiding Q, Ma J, Ke C, Cui W. From "organs on a chip" to "patient on a chip." *Innovation*. 2022;3(5):100282.

doi: 10.1016/j.xinn.2022.100282

145. Kim JJ, Park JY, Nguyen VVT, *et al*. Pathophysiological Reconstruction of a Tissue-Specific Multiple-Organ On-A-Chip for Type 2 Diabetes Emulation using 3D Cell Printing. *Adv Funct Mater*. 2023;33(22):2213649.

doi: 10.1002/adfm.202213649

146. Wagner I, Materne EM, Brincker S, *et al*. A dynamic multi-organ-chip for long-term cultivation and substance testing proven by 3D human liver and skin tissue co-culture. *Lab Chip*. 2013;13(18):3538-3547.

doi: 10.1039/C3LC50234A

147. Milani N, Parrott N, Franyuti DO, *et al*. Application of a gut–liver-on-a-chip device and mechanistic modelling to the quantitative in vitro pharmacokinetic study of mycophenolate mofetil. *Lab Chip*. 2022;22(15):2853-2868.

doi: 10.1039/D2LC00276K

148. Sakai Y, Matsumura M, Yamada H, *et al*. Development of a Perfusing Small Intestine–Liver Microphysiological System Device. *Appl Sci*. 2023;13(18):10510.

doi: 10.3390/app131810510

149. Nguyen VVT, Ye S, Gkouzioti V, *et al*. A human kidney and liver organoid-based multi-organ-on-a-chip model to study the therapeutic effects and biodistribution of mesenchymal stromal cell-derived extracellular vesicles. *J Extracell Vesicles*. 2022;11(11):12280.

doi: 10.1002/jev2.12280

150. Li Z, Su W, Zhu Y, *et al*. Drug absorption related nephrotoxicity assessment on an intestine-kidney chip. *Biomicrofluidics*. 2017;11(3):034114.

doi: 10.1063/1.4984768

151. Kurniawan DA, Leo S, Inamatsu M, *et al*. Gut–liver microphysiological systems revealed potential crosstalk mechanism modulating drug metabolism. *PNAS Nexus*. 2024;3(2):pgae070.

doi: 10.1093/pnasnexus/pgae070

152. Shah P, Fritz JV, Glaab E, *et al*. A microfluidics-based in vitro model of the gastrointestinal human–microbe interface. *Nat Commun*. 2016;7(1):11535.

doi: 10.1038/ncomms11535

153. Wang P, Jin L, Zhang M, *et al*. Blood–brain barrier injury and neuroinflammation induced by SARS-CoV-2 in a lung–brain microphysiological system. *Nat Biomed Eng*. 2024;8(8):1053-1068.

doi: 10.1038/s41551-023-01054-w

154. Gao Z, Du Z, Hou Y, *et al*. A microfluidic coculture model for mapping signaling perturbations and precise drug screening against macrophage-mediated dynamic myocardial injury. *Acta Pharm Sin B*. 2024;14(12):5393-5406.

doi: 10.1016/j.apsb.2024.11.004

155. Zhang SY, Mahler GJ. A glomerulus and proximal tubule microphysiological system simulating renal filtration, reabsorption, secretion, and toxicity. *Lab Chip*. 2023;23(2):272-284.

doi: 10.1039/D2LC00887D

156. Doi K, Kimura H, Hyeon Kim S, *et al*. Enhanced podocyte differentiation and changing drug toxicity sensitivity through pressure-controlled mechanical filtration stress on a glomerulus-on-a-chip. *Lab Chip*. 2023;23(3):437-450.

doi: 10.1039/D2LC00941B

157. Mitrofanova O, Nikolaev M, Xu Q, *et al*. Bioengineered human colon organoids with in vivo-like cellular complexity and function. *Cell Stem Cell*. 2024;31(8):1175-1186.e7.

doi: 10.1016/j.stem.2024.05.007

158. Zhang T, Yang S, Ge Y, *et al*. Unveiling the Heart's Hidden Enemy: Dynamic Insights into Polystyrene Nanoplastic-Induced Cardiotoxicity Based on Cardiac Organoid-on-a-Chip. *ACS Nano*. 2024;18(45):31569-31585.

doi: 10.1021/acsnano.4c13262

159. Wang Y, Wang L, Guo Y, Zhu Y, Qin J. Engineering stem cell-derived 3D brain organoids in a perfusable organ-on-a-chip system. *RSC Adv*. 2018;8(3):1677-1685.

doi: 10.1039/C7RA11714K

160. Wang Y, Wang H, Deng P, *et al*. In situ differentiation and generation of functional liver organoids from human iPSCs in a 3D perfusable chip system. *Lab Chip*. 2018;18(23):3606-3616.

doi: 10.1039/C8LC00869H

161. Kasendra M, Tovaglieri A, Sontheimer-Phelps A, *et al*. Development of a primary human Small Intestine-on-a-Chip using biopsy-derived organoids. *Sci Rep*. 2018;8:2871.

doi: 10.1038/s41598-018-21201-7

162. Workman MJ, Gleeson JP, Troisi EJ, *et al*. Enhanced Utilization of Induced Pluripotent Stem Cell–Derived Human Intestinal Organoids Using Microengineered Chips. *Cell Mol Gastroenterol Hepatol*. 2018;5(4):669-677.e2.

doi: 10.1016/j.jcmgh.2017.12.008

163. Nikolaev M, Mitrofanova O, Broguiere N, *et al*. Homeostatic mini-intestines through scaffold-guided organoid morphogenesis. *Nature*. 2020;585(7826):574-578.

doi: 10.1038/s41586-020-2724-8

164. Rajasekar S, Lin DSY, Abdul L, *et al*. IFlowPlate—A Customized 384-Well Plate for the Culture of Perfusable Vascularized Colon Organoids. *Adv Mater*. 2020;32(46):2002974.

doi: 10.1002/adma.202002974

165. Sontheimer-Phelps A, Chou DB, Tovaglieri A, *et al*. Human Colon-on-a-Chip Enables Continuous In Vitro Analysis of Colon Mucus Layer Accumulation and Physiology. *Cell Mol Gastroenterol Hepatol*. 2020;9(3):507-526.

doi: 10.1016/j.jcmgh.2019.11.008

166. Trujillo-de Santiago G, Lobo-Zegers MJ, Montes-Fonseca SL, Zhang YS, Alvarez MM. Gut-microbiota-on-a-chip: an enabling field for physiological research. *Microphysiol Syst*. 2018;2:7.

doi: 10.21037/mps.2018.09.01

167. Mills RJ, Humphrey SJ, Fortuna PRJ, *et al*. BET inhibition blocks inflammation-induced cardiac dysfunction and SARS-CoV-2 infection. *Cell*. 2021;184(8):2167-2182.e22.

doi: 10.1016/j.cell.2021.03.026

168. Hoang P, Kowalczewski A, Sun S, *et al*. Engineering spatial-organized cardiac organoids for developmental toxicity testing. *Stem Cell Reports*. 2021;16(5):1228-1244.

doi: 10.1016/j.stemcr.2021.03.013

169. Shirure VS, Hughes CCW, George SC. Engineering Vascularized Organoid-on-a-Chip Models. *Annu Rev Biomed Eng*. 2021;23(1):141-167.

doi: 10.1146/annurev-bioeng-090120-094330

170. Min S, Kim S, Sim WS, *et al*. Versatile human cardiac tissues engineered with perfusable heart extracellular microenvironment for biomedical applications. *Nat Commun*. 2024;15(1):2564.

doi: 10.1038/s41467-024-46928-y

171. Kupfer ME, Lin WH, Ravikumar V, *et al*. In Situ Expansion, Differentiation, and Electromechanical Coupling of Human Cardiac Muscle in a 3D Bioprinted, Chambered Organoid. *Circ Res*. 2020;127(2):207-224.

doi: 10.1161/CIRCRESAHA.119.316155

172. Mathur A, Loskill P, Shao K, *et al*. Human iPSC-based Cardiac Microphysiological System For Drug Screening Applications. *Sci Rep*. 2015;5(1):8883.

doi: 10.1038/srep08883

173. Cui K, Chen W, Cao R, *et al*. Brain organoid-on-chip system to study the effects of breast cancer derived exosomes on the neurodevelopment of brain. *Cell Regen*. 2022;11(1):7.

doi: 10.1186/s13619-021-00102-7

174. Tsai YC, Ozaki H, Morikawa A, *et al*. Proof of concept for brain organoid-on-a-chip to create multiple domains in forebrain organoids. *RSC Adv*. 2025;15(5):3749-3755.

doi: 10.1039/D4RA04194A

175. Wang Y, Wang L, Zhu Y, Qin J. Human brain organoid-on-a-chip to model prenatal nicotine exposure. *Lab Chip*. 2018;18(6):851-860.

doi: 10.1039/C7LC01084B

176. Cui K, Wang Y, Zhu Y, *et al*. Neurodevelopmental impairment induced by prenatal valproic acid exposure shown with the human cortical organoid-on-a-chip model. *Microsyst Nanoeng*. 2020;6(1):49.

doi: 10.1038/s41378-020-0165-z

177. Karzbrun E, Kshirsagar A, Cohen SR, Hanna JH, Reiner O. Human brain organoids on a chip reveal the physics of folding. *Nat Phys*. 2018;14(5):515-522.

doi: 10.1038/s41567-018-0046-7

178. Ao Z, Song S, Tian C, *et al*. Understanding Immune-Driven Brain Aging by Human Brain Organoid Microphysiological Analysis Platform. *Adv Sci*. 2022;9(27):2200475.

doi: 10.1002/advs.202200475

179. Ma LD, Wang YT, Wang JR, *et al*. Design and fabrication of a liver-on-a-chip platform for convenient, highly efficient, and safe in situ perfusion culture of 3D hepatic spheroids. *Lab Chip*. 2018;18(17):2547-2562.

doi: 10.1039/C8LC00333E

180. Wang Y, Wang H, Deng P, *et al*. Modeling Human Nonalcoholic Fatty Liver Disease (NAFLD) with an Organoids-on-a-Chip System. *ACS Biomater Sci Eng*. 2020;6(10):5734-5743.

doi: 10.1021/acsbiomaterials.0c00682

181. Zhang Y, Huang C, Sun L, *et al*. hESCs-derived organoids achieve liver zonation by LSEC modulation. Preprint. Posted online May 5, 2024. bioRxiv. 592562.

doi: 10.1101/2024.05.05.592562

182. Messelmani T. Development and Characterisation of a Biomimetic Liver on Chip Featuring 3D Hepatic Coculture with an Endothelial Barrier [PhD thesis]. Compiègne, France: Université de Technologie de Compiègne; 2023. Accessed February 19, 2025. https://theses.hal.science/tel-04582454

183. Kumari K, Sanyal A, Rawat P, *et al*. Current landscape and opportunities in the development of bioengineered in-vitro vascularized liver tissue models. *Bioprinting*. 2024;41:e00350.

doi: 10.1016/j.bprint.2024.e00350

184. Tao T, Deng P, Wang Y, *et al*. Microengineered Multi-Organoid System from hiPSCs to Recapitulate Human Liver-Islet Axis in Normal and Type 2 Diabetes. *Adv Sci*. 2022;9(5):2103495.

doi: 10.1002/advs.202103495

185. Ramme AP, Koenig L, Hasenberg T, *et al*. Autologous Induced Pluripotent Stem Cell-Derived Four-Organ-Chip. *Future Sci OA*. 2019;5(8):FSO413.

doi: 10.2144/fsoa-2019-0065

186. Jin Y, Kim J, Lee JS, *et al*. Vascularized Liver Organoids Generated Using Induced Hepatic Tissue and Dynamic Liver-Specific Microenvironment as a Drug Testing Platform. *Adv Funct Mater*. 2018;28(37):1801954.

doi: 10.1002/adfm.201801954

187. Edington CD, Chen WLK, Geishecker E, *et al*. Interconnected Microphysiological Systems for Quantitative Biology and Pharmacology Studies. *Sci Rep*. 2018;8(1):4530.

doi: 10.1038/s41598-018-22749-0

188. Wikswo JP, Curtis EL, Eagleton ZE, *et al*. Scaling and systems biology for integrating multiple organs-on-a-chip. *Lab Chip*. 2013;13(18):3496-3511.

doi: 10.1039/C3LC50243K

189. Schutgens F, Rookmaaker MB, Margaritis T, *et al*. Tubuloids derived from human adult kidney and urine for personalized disease modeling. *Nat Biotechnol*. 2019;37(3):303-313.

doi: 10.1038/s41587-019-0048-8

190. Aizenshtadt A, Wang C, Abadpour S, *et al*. Pump-Less, Recirculating Organ-on-Chip (rOoC) Platform to Model the Metabolic Crosstalk between Islets and Liver. *Adv Healthc Mater*. 2024;13(13):2303785.

doi: 10.1002/adhm.202303785

191. Trapecar M, Wogram E, Svoboda D, *et al*. Human physiomimetic model integrating microphysiological systems of the gut, liver, and brain for studies of neurodegenerative diseases. *Sci Adv*. 2021;7(5):eabd1707.

doi: 10.1126/sciadv.abd1707

192. Trapecar M, Communal C, Velazquez J, *et al*. Gut-Liver Physiomimetics Reveal Paradoxical Modulation of IBD-Related Inflammation by Short-Chain Fatty Acids. *Cell Syst*. 2020;10(3):223-239.e9.

doi: 10.1016/j.cels.2020.02.008

193. Koenig L, Ramme AP, Faust D, *et al*. A Human Stem Cell-Derived Brain-Liver Chip for Assessing Blood-Brain-Barrier Permeation of Pharmaceutical Drugs. *Cells*. 2022;11(20):3295.

doi: 10.3390/cells11203295

194. Yin F, Zhang X, Wang L, *et al*. HiPSC-derived multi-organoids-on-chip system for safety assessment of antidepressant drugs. *Lab Chip*. 2021;21(3):571-581.

doi: 10.1039/D0LC00921K

195. Brassard JA, Nikolaev M, Hübscher T, Hofer M, Lutolf MP. Recapitulating macro-scale tissue self-organization through organoid bioprinting. *Nat Mater*. 2021;20(1):22-29.

doi: 10.1038/s41563-020-00803-5

196. Grigoryan B, Paulsen SJ, Corbett DC, *et al*. Multivascular networks and functional intravascular topologies within biocompatible hydrogels. *Science*. 2019;364(6439):458-464.

doi: 10.1126/science.aav9750

197. Wang X, Liu X, Li K, *et al*. A Microgel–Hydrogel Hybrid for Functional Compensation and Mechanical Stability in 3D Printed Cell-Dense Vascularized Liver Tissue. *Adv Mater*. 2025;37(28):2413940.

doi: 10.1002/adma.202413940

198. Lind JU, Busbee TA, Valentine AD, *et al*. Instrumented cardiac microphysiological devices via multimaterial three-dimensional printing. *Nat Mater*. 2017;16(3):303-308.

doi: 10.1038/nmat4782

199. Cai S, Li H, Zheng F, *et al*. Artificial intelligence velocimetry and microaneurysm-on-a-chip for three-dimensional analysis of blood flow in physiology and disease. *Proc Natl Acad Sci USA*. 2021;118(13):e2100697118.

doi: 10.1073/pnas.2100697118

200. Bożek J, Kurchakova O, Michel J, *et al*. Pneumatic conveying inkjet bioprinting for the processing of living cells. *Biofabrication*. 2025;17(2):025003.

doi: 10.1088/1758-5090/ada8e2

201. Liu J, Xu C. Improving Uniformity of Cell Distribution in Post-Inkjet-Based Bioprinting. *J Manuf Sci Eng*. 2023;146(1):014501.

doi: 10.1115/1.4063134

202. Kang R, Wu J, Cheng R, *et al*. 3D bioprinting technology and equipment based on microvalve control. *Biotechnol Bioeng*. 2024;121(12):3768-3781.

doi: 10.1002/bit.28850

203. Guo R, Tang W. Optimizing Printhead Design for Enhanced Temperature Control in Extrusion-Based Bioprinting. *Micromachines*. 2024;15(8):943.

doi: 10.3390/mi15080943

204. Sun J, Gong Y, He Y, *et al*. Process optimization for coaxial extrusion-based bioprinting: A comprehensive analysis of material behavior, structural precision, and cell viability. *Addit Manuf*. 2025;100:104682.

doi: 10.1016/j.addma.2025.104682

205. Lombardi L, Scalzone A, Ausilio C, Gentile P, Tammaro D. Optimizing nozzle design in extrusion-based 3D bioprinting to minimize mechanical stress and enhance cell viability. *Int J Bioprint*. 2025;11(4):315-327.

doi: 10.36922/IJB025190182

206. Lee SY, Phuc HD, Um SH, Mongrain R, Yoon JK, Bhang SH. Photocuring 3D printing technology as an advanced tool for promoting angiogenesis in hypoxia-related diseases. *J Tissue Eng*. 2024;15:20417314241282476.

doi: 10.1177/20417314241282476

207. Shen J, Song W, Liu J, *et al*. 3D bioprinting by reinforced bioink based on photocurable interpenetrating networks for cartilage tissue engineering. *Int J Biol Macromol*. 2024;254:127671.

doi: 10.1016/j.ijbiomac.2023.127671

208. He CF, Qiao TH, Wang GH, Sun Y, He Y. High-resolution projection-based 3D bioprinting. *Nat Rev Bioeng*. 2025;3(2):143-158.

doi: 10.1038/s44222-024-00218-w

209. Lian L, Xie M, Luo Z, *et al*. Rapid Volumetric Bioprinting of Decellularized Extracellular Matrix Bioinks. *Adv Mater*. 2024;36(34):2304846.

doi: 10.1002/adma.202304846

210. Ribezzi D, Zegwaart JP, Van Gansbeke T, *et al*. Multi-material Volumetric Bioprinting and Plug-and-play Suspension Bath Biofabrication via Bioresin Molecular Weight Tuning and via Multiwavelength Alignment Optics. *Adv Mater*. 2025;37(13):2409355.

doi: 10.1002/adma.202409355

211. Aizarna-Lopetegui U, Größbacher G, Herrero-Ruiz A, *et al*. Hybrid Plasmonic Bioresins and dECM-Based Materials for Volumetric Bioprinting of Vascular-Inspired Architectures. *ACS Appl Mater Interfaces*. 2025;17(25):36982-36991.

doi: 10.1021/acsami.5c03880

212. Pramanick A, Hayes T, Sergis V, McEvoy E, Pandit A, Daly AC. 4D Bioprinting Shape-Morphing Tissues in Granular Support Hydrogels: Sculpting Structure and Guiding Maturation. *Adv Funct Mater*. 2025;35(5):2414559.

doi: 10.1002/adfm.202414559

213. Wu G, Wang L, Cao Y, Wang M, Yang C, Zhang J. 4D bioprinting of transformable living constructs with sustained local growth factor presentation for advanced tissue engineering applications. *Colloids Surf B Biointerfaces*. 2025;248:114484.

doi: 10.1016/j.colsurfb.2024.114484

214. Lai J, Xiong T, Chen S, *et al*. Facile Single-Nanocomposite 4D Bioprinting of Dynamic Hydrogel Constructs with Thickness-Controlled Gradient. *Adv Sci*. 2025;12(39):e09449.

doi: 10.1002/advs.202509449

215. Zhang C, Hua W, Mitchell K, *et al*. Multiscale embedded printing of engineered human tissue and organ equivalents. *Proc Natl Acad Sci USA*. 2024;121(9):e2313464121.

doi: 10.1073/pnas.2313464121

216. Li S, Li J, Xu J, *et al*. Removal-Free and Multicellular Suspension Bath-Based 3D Bioprinting. *Adv Mater*. 2024;36(48):2406891.

doi: 10.1002/adma.202406891

217. Wang X, Luo Y, Ma Y, Wang P, Yao R. Converging bioprinting and organoids to better recapitulate the tumor microenvironment. *Trends Biotechnol*. 2024;42(5):648-663.

doi: 10.1016/j.tibtech.2023.11.006

218. Tian Y, Zhang Z, Wu B, *et al*. Integrating periosteum derived organoids and 3D printed scaffolds for enhanced craniofacial bone regeneration. *Mater Today Commun*. 2025;49:113931.

doi: 10.1016/j.mtcomm.2025.113931

219. Xu L, Ding H, Wu S, *et al*. Artificial Meshed Vessel-Induced Dimensional Breaking Growth of Human Brain Organoids and Multiregional Assembloids. *ACS Nano*. 2024;18(38):26201-26214.

doi: 10.1021/acsnano.4c07844

220. Liu Y, Liu X, Guo H, *et al*. 3D bioprinting bioglass to construct vascularized full-thickness skin substitutes for wound healing. *Mater Today Bio*. 2024;24:100899.

doi: 10.1016/j.mtbio.2023.100899

221. Lu TY, Ji Y, Lyu C, *et al*. Bioprinted high cell density liver model with improved hepatic metabolic functions. *Biomaterials*. 2025;320:123256.

doi: 10.1016/j.biomaterials.2025.123256

222. Liu Q, Dong X, Qi H, *et al*. 3D printable strong and tough composite organo-hydrogels inspired by natural hierarchical composite design principles. *Nat Commun*. 2024;15(1):3237.

doi: 10.1038/s41467-024-47597-7

223. Wang X, Liu X, Liu W, *et al*. 3D bioprinting microgels to construct implantable vascular tissue. *Cell Prolif*. 2023;56(5):e13456.

doi: 10.1111/cpr.13456

224. Xu R, Dou B, Yu S, *et al*. Enabling 3D printability and vascular morphogenesis with double network dynamic hydrogels. *Mater Today*. 2025;84:10-27.

doi: 10.1016/j.mattod.2025.01.019

225. Duan J, Fang Y, Tian Y, Wang Z, Yang B, Xiong Z. 3D Bioprinting of Prevascularized Bone Organoids for Rapid In Situ Cranial Bone Reconstruction. *Adv Healthc Mater*. 2025;14(16):2501376.

doi: 10.1002/adhm.202501376

226. Li G, He J, Shi J, *et al*. Bioprinting functional hepatocyte organoids derived from human chemically induced pluripotent stem cells to treat liver failure. *Gut*. 2025;74(7):1150-1164.

doi: 10.1136/gutjnl-2024-333885

227. Kong W, Chen H, Yuan X, *et al*. A biohydrogel battery. *Cell Biomater*. 2026;2(1):100189.

doi: 10.1016/j.celbio.2025.100189

228. Li X, Zheng F, Wang X, *et al*. Biomaterial inks for extrusion-based 3D bioprinting: Property, classification, modification, and selection. *Int J Bioprint*. 2022;9(2):649.

doi: 10.18063/ijb.v9i2.649

229. Wang J, Qiao H, Wang Z, *et al*. Rational Design and Acoustic Assembly of Human Cerebral Cortex-Like Microtissues from hiPSC-Derived Neural Progenitors and Neurons. *Adv Mater*. 2023;35(32):2210631.

doi: 10.1002/adma.202210631

230. Gu L, Jiang S, Xu X, *et al*. Size- and density-dependent acoustic differential bioassembly of spatially-defined heterocellular architecture. *Biofabrication*. 2023;15(1):015019.

doi: 10.1088/1758-5090/aca79c

231. Wang Y, Huang S, Wang S, *et al*. Acoustically tunable intra-droplet assembly of organoids towards high-throughput tumor model construction. *Chem Eng J*. 2024;500:157425.

doi: 10.1016/j.cej.2024.157425

232. Kim J, Kim J, Jin Y, Cho SW. In situ biosensing technologies for an organ-on-a-chip. *Biofabrication*. 2023;15(4):042002.

doi: 10.1088/1758-5090/aceaae

233. Yang W, Li T, Liao S, Zhou J, Huang L. Organ-on-a-chip platforms integrated with biosensors for precise monitoring of the cells and cellular microenvironment. *TrAC Trends Anal Chem*. 2024;172:117569.

doi: 10.1016/j.trac.2024.117569

234. Zhang YS, Aleman J, Shin SR, *et al*. Multisensor-integrated organs-on-chips platform for automated and continual in situ monitoring of organoid behaviors. *Proc Natl Acad Sci USA*. 2017;114(12):E2293-E2302.

doi: 10.1073/pnas.1612906114

235. Su H, Ma T, Liu X, *et al*. Microfluidic organ chip of fluid–solid dynamic curved interface. *Appl Phys Rev*. 2024;11(1):011404.

doi: 10.1063/5.0177386

236. Pavesi A, Adriani G, Rasponi M, Zervantonakis IK, Fiore GB, Kamm RD. Controlled electromechanical cell stimulation on-a-chip. *Sci Rep*. 2015;5(1):11800.

doi: 10.1038/srep11800

237. Dornhof J, Kieninger J, Muralidharan H, Maurer J, Urban GA, Weltin A. Microfluidic organ-on-chip system for multi-analyte monitoring of metabolites in 3D cell cultures. *Lab Chip*. 2022;22(2):225-239.

doi: 10.1039/D1LC00689D

238. Duc P, Vignes M, Hugon G, *et al*. Human neuromuscular junction on micro-structured microfluidic devices implemented with a custom micro electrode array (MEA). *Lab Chip*. 2021;21(21):4223-4236.

doi: 10.1039/D1LC00497B

239. Cai H, Ao Z, Tian C, *et al*. Brain organoid reservoir computing for artificial intelligence. *Nat Electron*. 2023;6(12):1032-1039.

doi: 10.1038/s41928-023-01069-w

240. Liu K, Ding H, Li S, *et al*. 3D printing colloidal crystal microstructures via sacrificial-scaffold-mediated two-photon lithography. *Nat Commun*. 2022;13(1):4563.

doi: 10.1038/s41467-022-32317-w

241. Fu F, Shang L, Chen Z, Yu Y, Zhao Y. Bioinspired living structural color hydrogels. *Sci Robot*. 2018;3(16):eaar8580.

doi: 10.1126/scirobotics.aar8580

242. Chen J. Incorporating biomechanics as a key evaluation metric for organoids. *Biofabrication*. 2025;17(2):023001.

doi: 10.1088/1758-5090/adb802

243. Shin W, Kim HJ. 3D in vitro morphogenesis of human intestinal epithelium in a gut-on-a-chip or a hybrid chip with a cell culture insert. *Nat Protoc*. 2022;17(3):910-939.

doi: 10.1038/s41596-021-00674-3

244. Tang J, Wang Z, Khutsishvili D, *et al*. Converging neural-centric and mechano-regulation in organoid modeling for system biology and medicine. *TIME*. 2024;2(3):100076.

doi: 10.59717/j.xinn-med.2024.100076

245. Aung A, Bhullar IS, Theprungsirikul J, *et al*. 3D cardiac μtissues within a microfluidic device with real-time contractile stress readout. *Lab Chip*. 2016;16(1):153-162.

doi: 10.1039/C5LC00820D

246. Lyu Q, Gong S, Lees JG, *et al*. A soft and ultrasensitive force sensing diaphragm for probing cardiac organoids instantaneously and wirelessly. *Nat Commun*. 2022;13(1):7259.

doi: 10.1038/s41467-022-34860-y

247. Morimoto Y, Mori S, Sakai F, Takeuchi S. Human induced pluripotent stem cell-derived fiber-shaped cardiac tissue on a chip. *Lab Chip*. 2016;16(12):2295-2301.

doi: 10.1039/C6LC00422A

248. Michas C, Karakan MÇ, Nautiyal P, *et al*. Engineering a living cardiac pump on a chip using high-precision fabrication. *Sci Adv*. 2022;8(16):eabm3791.

doi: 10.1126/sciadv.abm3791

249. Fang G, Chen YC, Lu H, Jin D. Advances in Spheroids and Organoids on a Chip. *Adv Funct Mater*. 2023;33(19):2215043.

doi: 10.1002/adfm.202215043

250. Shin SR, Kilic T, Zhang YS, *et al*. Label-Free and Regenerative Electrochemical Microfluidic Biosensors for Continual Monitoring of Cell Secretomes. *Adv Sci*. 2017;4(5):1600522.

doi: 10.1002/advs.201600522

251. Cho S, Lee S, Ahn SI. Design and engineering of organ-on-a-chip. *Biomed Eng Lett*. 2023;13(2):97-109.

doi: 10.1007/s13534-022-00258-4

252. Wang L, Han J, Su W, *et al*. Gut-on-a-chip for exploring

the transport mechanism of Hg(II). *Microsyst Nanoeng*. 2023;9(1):2.

doi: 10.1038/s41378-022-00447-2

253. Nicolas A, Schavemaker F, Kosim K, *et al*. High throughput transepithelial electrical resistance (TEER) measurements on perfused membrane-free epithelia. *Lab Chip*. 2021;21(9):1676-1685.

doi: 10.1039/D0LC00770F

254. Shinde A, Illath K, Kasiviswanathan U, *et al*. Recent Advances of Biosensor-Integrated Organ-on-a-Chip Technologies for Diagnostics and Therapeutics. *Anal Chem*. 2023;95(6):3121-3146.

doi: 10.1021/acs.analchem.2c05036

255. Li H, Shi W, Song J, *et al*. Chemical and Biomolecule Sensing with Organic Field-Effect Transistors. *Chem Rev*. 2019;119(1):3-35.

doi: 10.1021/acs.chemrev.8b00016

256. Huang Z, Xu K, Zhao L, *et al*. AND-Gated Nanosensor for Imaging of Glutathione and Apyrimidinic Endonuclease 1 in Cells, Animals, and Organoids. *ACS Appl Mater Interfaces*. 2023;15(22):26316-26327.

doi: 10.1021/acsami.3c02236

257. Zhu L, Shao C, Chen H, Chen Z, Zhao Y. Hierarchical Hydrogels with Ordered Micro-Nano Structures for Cancer-on-a-Chip Construction. *Research*. 2021;2021:9845679.

doi: 10.34133/2021/9845679

258. Tolabi H, Davari N, Khajehmohammadi M, *et al*. Progress of Microfluidic Hydrogel-Based Scaffolds and Organ-on-Chips for the Cartilage Tissue Engineering. *Adv Mater*. 2023;35(26):2208852.

doi: 10.1002/adma.202208852

259. Ortega MA, Rodríguez-Comas J, Yavas O, *et al*. In Situ LSPR Sensing of Secreted Insulin in Organ-on-Chip. *Biosensors*. 2021;11(5):138.

doi: 10.3390/bios11050138

260. Rothbauer M, Höll G, Eilenberger C, *et al*. Monitoring tissue-level remodelling during inflammatory arthritis using a three-dimensional synovium-on-a-chip with non-invasive light scattering biosensing. *Lab Chip*. 2020;20(8):1461-1471.

doi: 10.1039/C9LC01097A

261. Carvalho DJ, Kip AM, Romitti M, *et al*. Thyroid-on-a-Chip: An Organoid Platform for In Vitro Assessment of Endocrine Disruption. *Adv Healthc Mater*. 2023;12(8):2201555.

doi: 10.1002/adhm.202201555

262. Liu P, Mu Z, Ji M, *et al*. Robust Carbonated Structural Color Barcodes with Ultralow Ontology Fluorescence as Biomimic Culture Platform. *Research*. 2021;2021:9851609.

doi: 10.34133/2021/9851609

263. Shang Y, Chen Z, Fu F, *et al*. Cardiomyocyte-Driven Structural Color Actuation in Anisotropic Inverse Opals. *ACS Nano*. 2019;13(1):796-802.

doi: 10.1021/acsnano.8b08230

264. Li Q, Chen Z, Zhang Y, *et al*. Imaging cellular forces with photonic crystals. *Nat Commun*. 2023;14(1):7369.

doi: 10.1038/s41467-023-43090-9

265. Martinelli E, Akouissi O, Liebi L, *et al*. The e-Flower: A hydrogel-actuated 3D MEA for brain spheroid electrophysiology. *Sci Adv*. 2024;10(42):eadp8054.

doi: 10.1126/sciadv.adp8054

266. Choi SJ, Liu Z, Yang F, *et al*. 3D Spatiotemporal Electrophysiology of Cardiac Organoids Using Shell Microelectrode Arrays. *Adv Mater*. 2026;38(2):e06793.

doi: 10.1002/adma.202506793

267. Lee J, Liu J. Flexible and stretchable bioelectronics for organoids. *Med-X*. 2025;3(1):5.

doi: 10.1007/s44258-024-00046-y

268. Yang X, Forró C, Li TL, *et al*. Kirigami electronics for long-term electrophysiological recording of human neural organoids and assembloids. *Nat Biotechnol*. 2024;42(12):1836-1843.

doi: 10.1038/s41587-023-02081-3

269. Park Y, Franz CK, Ryu H, *et al*. Three-dimensional, multifunctional neural interfaces for cortical spheroids and engineered assembloids. *Sci Adv*. 2021;7(12):eabf9153.

doi: 10.1126/sciadv.abf9153

270. Kong L, Li W, Zhang T, *et al*. Wireless Technologies in Flexible and Wearable Sensing: From Materials Design, System Integration to Applications. *Adv Mater*. 2024;36(27):2400333.

doi: 10.1002/adma.202400333

271. Lu P, Liao X, Guo X, *et al*. Gel-Based Triboelectric Nanogenerators for Flexible Sensing: Principles, Properties, and Applications. *Nano-Micro Lett*. 2024;16(1):206.

doi: 10.1007/s40820-024-01432-2

272. Liu Z, Cai M, Hong S, *et al*. Data-driven inverse design of flexible pressure sensors. *Proc Natl Acad Sci USA*. 2024;121(28):e2320222121.

doi: 10.1073/pnas.2320222121

273. Cheng X, Fan Z, Yao S, *et al*. Programming 3D curved mesosurfaces using microlattice designs. *Science*. 2023;379(6638):1225-1232.

doi: 10.1126/science.adf3824

274. Huang Q, Tang B, Romero JC, *et al*. Shell microelectrode arrays (MEAs) for brain organoids. *Sci Adv*. 2022;8(33):eabq5031.

doi: 10.1126/sciadv.abq5031

275. Takebe T, Zhang B, Radisic M. Synergistic Engineering: Organoids Meet Organs-on-a-Chip. *Cell Stem Cell*. 2017;21(3):297-300.

doi: 10.1016/j.stem.2017.08.016

276. Li Z, Chen L, Wu J, *et al*. A review of 3D bioprinting for organoids. *Med Rev*. 2025;5(4):318-338.

doi: 10.1515/mr-2024-0089

277. Azizgolshani H, Coppeta JR, Vedula EM, *et al*. High-throughput organ-on-chip platform with integrated programmable fluid flow and real-time sensing for complex tissue models in drug development workflows. *Lab Chip*. 2021;21(8):1454-1474.

doi: 10.1039/D1LC00067E

278. Li X, Zhu H, Gu B, *et al*. Advancing Intelligent Organ-on-a-Chip Systems with Comprehensive In Situ Bioanalysis. *Adv Mater*. 2024;36(18):2305268.

doi: 10.1002/adma.202305268

279. Guo L, Li C, Gong W. Toward reproducible tumor organoid culture: focusing on primary liver cancer. *Front Immunol*. 2024;15:1290504.

doi: 10.3389/fimmu.2024.1290504

280. Gjorevski N, Sachs N, Manfrin A, *et al*. Designer matrices for intestinal stem cell and organoid culture. *Nature*. 2016;539(7630):560-564.

doi: 10.1038/nature20168

281. Barnhart AJ, Dierickx K. The Many Moral Matters of Organoid Models: A systematic review of reasons. *Med Health Care Philos*. 2022;25(3):545-560.

doi: 10.1007/s11019-022-10082-3

282. Boers SN, van Delden JJ, Clevers H, Bredenoord AL. Organoid biobanking: identifying the ethics. *EMBO Rep*. 2016;17(7):938-941.

doi: 10.15252/embr.201642613

283. Lensink MA, Jongsma KR, Boers SN, Noordhoek JJ, Beekman JM, Bredenoord AL. Responsible use of organoids in precision medicine: the need for active participant involvement. *Development*. 2020;147(7):dev177972.

doi: 10.1242/dev.177972

284. de Jongh D, Massey EK, Berishvili E, *et al*. Organoids: a systematic review of ethical issues. *Stem Cell Res Ther*. 2022;13(1):337.

doi: 10.1186/s13287-022-02950-9

285. U.S. Congress. Public Law 117-328: Consolidated Appropriations Act, 2023. GovInfo. December 29, 2022. Accessed August 29, 2026. https://www.govinfo.gov/app/details/PLAW-117publ328

286. U.S. Food and Drug Administration. Animal Welfare, Testing and Research of FDA-Regulated Products. U.S. Food and Drug Administration. 2025. Accessed August 29, 2026. https://www.fda.gov/consumers/consumer-updates/animal-welfare-testing-and-research-fda-regulated-products

287. U.S. Congress. S. 5046 (ES) - FDA Modernization Act 3.0, 118th Congress. GovInfo. December 12, 2024. Accessed August 29, 2026. https://www.govinfo.gov/app/details/BILLS-118s5046es

288. U.S. Food and Drug Administration. Roadmap to Reducing Animal Testing in Preclinical Safety Studies. U.S. Food and Drug Administration; 2025. Accessed August 29, 2026. https://www.fda.gov/files/newsroom/published/roadmap_to_reducing_animal_testing_in_preclinical_safety_studies.pdf

Appendix

Table A1. Reported quantitative parameters for principal chip-based and bioprinted platforms discussed in this review

Platform	Ref.	Channel dimensions	Membrane porosity	Shear stress	Residence time	Oxygen gradient	Diffusion distance	Cell density
Human breathing lung chip	11	Device 1–2 cm long; central channels millimeters wide (exact cross-section not reported)	10-μm-thick PDMS membrane; 10-μm pores	15 dyn/cm^2 (endothelial preconditioning)	Not reported	Not reported	Not reported	Not reported
Gut chip with microbiome and cyclic deformation	87	Culture channel 1 mm wide × 10 mm long × 0.15 mm high	20-μm-thick PDMS membrane; 10-μm pores at 25-μm spacing	0.02 dyn/cm^2	Not reported	Not reported	Not reported	Not reported
Microneedle-assisted hepatic acinus chip	88	Primary sinusoid channels, radius 100, 150, or 200 μm; porous inserts 10 × 5 × 0.1 mm	Pore size not reported	Not reported	Not reported	HA/PV dissolved O_2 set to 3.5/1.5 mg/L	Not reported	HepaRG 2 × 10^7 cells/mL; HHSEC 4 × 10^6 cells/mL
Higher-throughput heart-on-a-chip	89	Fluid chamber 11.5 × 11.5 mm and 2.5 mm deep; MTFs about 1.2 × 0.3 mm	Not applicable (single open chamber; no separating membrane)	Not reported	Not reported	Not reported	Not reported	1 × 10^5 cells/cm^2
Human glomerulus chip	90	Urinary channel 1 × 1 mm; microvascular channel 1 × 0.2 mm	50-μm-thick PDMS membrane; 7-μm pores at 40-μm spacing	0.0007 dyn/cm^2 (urinary) and 0.017 dyn/cm^2 (microvascular)	Not reported	Not reported	Not reported	4 × 10^4 cells per channel
Neurovascular-unit-on-a-chip	133	Channel height 400 μm; blood-side width 1 mm	Not applicable (adjacent channels separated by a hydrogel boundary)	Maximum 3.4 dyn/cm^2	Not reported	No spatial gradient reported; uniform conditions were about 20% and 2% O_2	Not reported	Neural cells 8 × 10^6 cells/mL; BMEC/pericytes 1 × 10^6 cells/mL
Integrated gut–liver MPS	140	Liver scaffold 0.25 mm thick with 301 channels of 0.3-mm diameter	Gut Transwell membrane: 0.4-μm pores	Not reported	Not reported	Not reported	Not reported	Liver: 6 × 10^5 hepatocytes + 6 × 10^4 Kupffer cells; gut: 1 × 10^5 cells/cm^2
Closed-loop oxygen-controlled multi-organ platform	142	45 GelMA microdots in the bioreactor (individual dot dimensions not reported)	O_2 scavenger PDMS membrane 20 μm; O_2 generator membrane 50 μm	Not reported	Not reported	Controlled branches 5%, 13%, and 20% O_2; bioreactor target 13% inlet/3% outlet	Not reported	1 × 10^6 cells/mL

(*Cont'd...*)

Table A1. (*Continued*)

Platform	Ref.	Channel dimensions	Membrane porosity	Shear stress	Residence time	Oxygen gradient	Diffusion distance	Cell density
First-pass gut–liver–kidney chip system	143	Not reported	Porous ECM-coated membranes; pore size not reported in the reviewed article	Not reported	Not reported	Not reported	Not reported	Not reported
Perfusable brain organoid-on-a-chip	159	Channel height ≈600 μm; culture chambers 2.5 × 14 mm; central channel 1 × 20 mm	Not reported	Not reported	Not reported	Not reported	Not reported	Not reported
Perfusable liver organoid-on-a-chip	160	Micropillar-array culture chambers (exact dimensions not reported in the article text)	Not applicable (membraneless chamber array)	Not reported	Not reported	Not reported	Not reported	Not reported
Seven- and 10-MPS interconnected platform	187	Flow-through and Transwell modules in a microtiter-plate footprint (channel cross-sections not reported)	Module-dependent Transwell membranes; pore size not reported	Not reported	Not reported	Near-physiological O_2 drop reported for liver module; magnitude not reported	Not reported	Module-specific densities reported: muscle 0.24 × 10^6 and kidney 0.075 × 10^6 cells/cm^2
Bioprinting-assisted tissue emergence	195	Syringe-extruded organoid-forming cell/ECM filaments (nozzle and filament dimensions not reported in the primary article)	Not applicable (printed ECM construct; no separating membrane)	Not reported	Not reported	Not reported	Not reported	Not reported
Stereolithographic multivascular hydrogel networks	196	1-mm cylindrical channels; 150-μm mixer fins; 300-μm inter-vessel spacing	Not applicable (open lumens printed in hydrogel)	Not reported	Not reported	RBC inlet PO_2 ≤40 mmHg; adjacent O_2 source 7 kPa	300 μm (designed inter-vessel distance)	Not reported
Multimaterial-printed cardiac MPS	198	Printed PDMS microfilaments 20 μm high × 60 μm wide	Not applicable (printed cantilever platform; no separating membrane)	Not reported	Not reported	Not reported	Not reported	1.4 × 10^5 cells/cm^2
DLP-bioprinted high-cell-density liver model	221	Printed hepatic constructs (feature dimensions not reported)	Not applicable (solid bioprinted construct; no separating membrane)	Not reported	Not reported	Not reported	Not reported	8 × 10^7 cells/mL

(*Cont'd...*)

Table A1. (*Continued*)

Platform	Ref.	Channel dimensions	Membrane porosity	Shear stress	Residence time	Oxygen gradient	Diffusion distance	Cell density
High-throughput programmable-flow organ-on-a-chip platform	277	Standard 12-well plate footprint with integrated microfluidic channels (cross-sections not reported)	Module-dependent porous barriers; pore dimensions not reported	Programmable; no single platform-wide value reported	Not reported	Real-time oxygen sensing reported; spatial gradient not reported	Not reported	Tissue-module dependent; no single platform-wide density reported

Notes: Values are transcribed only when explicitly reported in the cited primary study; no values were inferred from geometry, flow rate, or other surrogate information. Every entry was checked against the cited primary article and, where accessible, its supplementary information. "Not reported" means that an applicable parameter was not given explicitly; "Not applicable" means that the platform lacks that structural element (for example, a membraneless printed construct). Qualitative statements were not converted into numbers, and flow rates were not used to calculate residence time or shear stress. For printed systems, the channel/feature dimensions reported by the primary study are used as the geometric anchor.
Abbreviations: BMEC: Brain microvascular endothelial cells; DLP: Digital light processing; ECM: Extracellular matrix; GelMA: Gelatin methacryloyl; HA: Hepatic artery; HHSEC: Human hepatic sinusoidal endothelial cells; MPS: Microphysiological systems; MTF: Muscular thin film; PDMS: Poly(dimethylsiloxane); PV: Portal vein; RBC: Red blood cell.

Table A2. Panel-level audit of scale bars and objective magnifications for reused microscopy images

Panel	Ref.	Reused content	Scale-bar audit	Objective-magnification audit
2a	8	Microscopy montage of engineered intestinal organoids.	Retained from source: 25, 100, and 200 μm, assigned to the corresponding source subimages.	Not reported in the source article or Supporting Information (SI) for the reused images.
2b	9	Kidney-organoid fluorescence montage.	Retained from source: 100 μm.	Not reported for the reused image.
2c	30	Lung-organoid protocol with histology/immunofluorescence images.	Retained from source: 100 μm for the reused microscopy images.	Not reported for the reused images.
2d	31	Lung-organoid bright-/dark-field, immunofluorescence, and histology images.	Retained from source: 200 μm (immunofluorescence overview) and 100 μm (marker panels).	Source reports 5×/20× for bright-/dark-field imaging and 10× for histology; no additional image-specific objective was reported.
2e	32	Cardiac organoid fluorescence and day-series images.	Retained from source: 100 μm for the organoid fluorescence images. Not reported for the reused day-series block.	Not reported for the reused images.
2f	33	Liver-organoid fluorescence time series.	Retained from source: 100 μm.	Not reported for the reused image.
2g	34	Microwell-array device/workflow block.	N/A: no microscopy image is reused in this block.	N/A: no microscopy image is reused in this block.
3a	58	Brain-organoid phase-contrast and immunofluorescence images.	Retained from source: 200 μm (phase contrast) and 100 μm (immunofluorescence).	4× reported for calibrated whole-organoid bright-field size imaging; Not reported for the other reused views.
3b	59	Brain–spinal-cord assembloid workflow schematic.	N/A: no microscopy image is reused in this block.	N/A: no microscopy image is reused in this block.
3c	60	Fused thalamic/cortical organoid overview and confocal images.	Retained from source: 250 μm (whole-organoid/epifluorescence) and 50 μm (confocal details).	Not reported for the reused images.
3d	61	Neuromusculoskeletal tri-tissue organoid images.	Not assignable: calibrated bars are retained, but numerical values could not be mapped unambiguously to each reused micrograph from the source/SI.	Not reported for the reused images.

(*Cont'd...*)

Table A2. (*Continued*)

Panel	Ref.	Reused content	Scale-bar audit	Objective-magnification audit
3e	62	Confocal tumor-perivascular-niche image.	Retained from source: 400 μm.	Not reported for the reused image.
4a	11	Lung-on-a-chip device photographs and microscopy.	Retained from source: 200 μm for the reused microscopy image.	Not reported for the reused image.
4b1	86	Gut-on-a-chip architecture schematic.	N/A: no microscopy image is reused in this block.	N/A: no microscopy image is reused in this block.
4b2	87	Gut-on-a-chip device and epithelial microscopy.	Retained from source: 50 μm for the reused microscopy image.	Not reported for the reused image.
4c	88	Liver-acinus-chip SEM, CLSM, live/dead, and primary-sinusoid images.	Retained from source: 200 μm (black SEM), 50 μm (white SEM), 500 μm (CLSM overview), 100 μm (live/dead), and 150 μm (primary sinusoid).	Not reported; the source identifies the imaging platforms but not an objective for the reused images.
4d	89	Heart-on-a-chip device overview.	Retained from source: 1 mm.	Not reported for the reused image.
4e	90	Glomerular-capillary-wall confocal image.	Retained from source: 100 μm.	25×/0.95 water objective reported by the source.
5a	132	Motor-unit chip device/ microscopy block.	Not reported/Not assignable: source bar retained where present, but a reliable numerical value for the reused image was not obtained.	Not reported for the reused image.
5b	133	Neurovascular-unit immunofluorescence images.	Retained from source: 100 μm.	10× and 20× objectives reported for the reused BBB immunostaining workflow.
5c	134	Three-dimensional neurovascular-unit microscopy.	Not assignable: source bars are retained, but numerical values could not be mapped unambiguously to the reused views.	Not reported for the reused images.
5d	135	Neurovascular–bone-unit device schematic.	N/A: no microscopy image is reused in this block.	N/A: no microscopy image is reused in this block.
6a	140	Integrated gut/liver MPS schematic.	N/A: no microscopy image is reused in this block.	N/A: no microscopy image is reused in this block.
6b	141	Multi-organ-chip rendering and fluorescence image.	Not assignable: source bar retained, but its numerical value could not be assigned reliably to the reused view.	Not reported for the reused image.
6c	142	Closed-loop oxygen-control platform schematic/photo.	N/A: no microscopy image is reused in this block.	N/A: no microscopy image is reused in this block.
6d	17	Multi-organ-chip vascular-barrier fluorescence image.	Retained from source: 50 μm.	Not reported for the reused image.
6e	143	First-pass multi-organ system device photographs/schematic.	N/A: no microscopy image is reused in this block.	N/A: no microscopy image is reused in this block.
7a	157	Mini-colon immunofluorescence/ bright-field images.	Not assignable: source bars are retained, but numerical values could not be mapped unambiguously to the reused views.	Not reported for the reused images.
7b	158	Cardiac organoid-on-a-chip platform schematic.	N/A: no microscopy image is reused in this block.	N/A: no microscopy image is reused in this block.
7c	158	Cardiac-organoid bright-field/ fluorescence images.	Not assignable: source bars are retained, but numerical values could not be mapped unambiguously to the reused views.	Not reported image-specifically for the reused images.
7d	159	Brain-organoid time-series microscopy.	Retained from source: 100 μm at D3, D11, D18, D26, and D33.	Not reported for the reused images.
7e	160	Liver-organoid time-series microscopy.	Not assignable: source bars are retained, but numerical values could not be mapped unambiguously to the reused views.	Not reported for the reused images.

(*Cont'd...*)

Table A2. (*Continued*)

Panel	Ref.	Reused content	Scale-bar audit	Objective-magnification audit
8a	184	Liver–pancreatic-islet-axis device and workflow schematic.	N/A: no microscopy image is reused in this block.	N/A: no microscopy image is reused in this block.
8b	185	Autologous four-organ-chip schematic.	N/A: no microscopy image is reused in this block.	N/A: no microscopy image is reused in this block.
8c	186	Induced liver, intestinal, and stomach organoid images.	Not assignable: source bars are retained, but numerical values could not be mapped unambiguously to each reused image.	Not reported for the reused images.
8d	187	Seven-/Ten-MPS device and flow-partitioning schematic.	N/A: no microscopy image is reused in this block.	N/A: no microscopy image is reused in this block.
9a	195	Bioprinted tissue/organoid bright-field and confocal images.	Retained from source: 500 μm (printed/organoid overviews), 250 μm (viability/overview), and 75 μm (high-resolution confocal view).	Not reported for the reused images.
9b	196	Bioprinted multivascular-network photographs/images.	Retained from source: 3 mm, 1 mm, and 500 μm, as shown in the corresponding source subimages.	Not reported for the reused images.
9c	197	Microgel–hydrogel fabrication schematic.	N/A: no microscopy image is reused in this block.	N/A: no microscopy image is reused in this block.
9d	198	Instrumented cardiac-tissue confocal inset.	Retained from source: 10 μm.	Not reported for the reused image.
10a	229	Acoustically assembled cortical microtissue fluorescence images.	Retained from source: 100 μm.	Not reported for the reused images.
10b	230	Acoustic differential-bioassembly microscopy.	Not assignable: source bars are retained, but numerical values could not be mapped unambiguously to the reused views.	Not reported for the reused images.
10c	231	Intradroplet organoid-assembly microscopy.	Not assignable: source bars are retained, but numerical values could not be mapped unambiguously to the reused views.	Not reported for the reused images.
11a	235	Curved-interface organ-chip fluorescence images.	Not reported/Not assignable: source bars are retained where present, but reliable numerical values were not obtained for the reused images.	Not reported for the reused images.
11b	236	Electromechanical-stimulation chip schematic.	N/A: no microscopy image is reused in this block.	N/A: no microscopy image is reused in this block.
11c	237	Multi-analyte sensor-chip schematic/device photograph.	N/A: no microscopy image is reused in this block.	N/A: no microscopy image is reused in this block.
11d	238	Neuromuscular junction chip/MEA micrographs.	Retained from source: 1 mm for the overview. Not assignable for source-calibrated detail bars whose values could not be mapped reliably.	Not reported for the reused images.
11e	239	Brainoware system schematic.	N/A: no microscopy image is reused in this block.	N/A: no microscopy image is reused in this block.
11f	240	SEM/fluorescence views of colloidal-crystal microstructures.	Not assignable: source bars are retained, but numerical values could not be mapped unambiguously to all reused views.	Not reported for the reused images.
11g	241	Optical time series of living structural-color hydrogel.	Not assignable: calibrated source images are retained, but numerical values could not be assigned reliably.	Not reported for the reused images.
12a	265	e-Flower MEA device and brain-spheroid images.	Retained from source: 40, 200, and 500 μm, as shown in the corresponding source subimages.	Not reported; the source reports a Leica DVM6 digital microscope.

(*Cont'd...*)

Table A2. (*Continued*)

Panel	Ref.	Reused content	Scale-bar audit	Objective-magnification audit
12b	266	Shell-MEA device/SEM and cardiac-organoid interface images.	Retained from source: 200 μm for the reused microscopy image.	Not reported for the reused images.
12c	267	Stretchable organoid bioelectronic interface.	Retained from source: 500 μm (overview) and 50 μm (inset).	Not reported for the reused images.
12d	268	Kirigami interface and organoid/assembloid fluorescence images.	Not assignable: source bars are retained, but numerical values could not be mapped unambiguously to the reused views.	Not reported for the reused images.
12e	269	Three-dimensional multifunctional neural-interface images.	Retained from source: 1 mm, 500 μm, and 200 μm where shown.	Not reported for the reused images.
13a	275	Overview microscopy used in the synergistic-engineering concept panel.	Not reported in the source publication for the reused overview images.	Not reported in the source publication for the reused overview images.
13b	276	Organoid culture-method schematic.	N/A: no microscopy image is reused in this block.	N/A: no microscopy image is reused in this block.
13c	277	High-throughput organ-on-a-chip platform schematic.	N/A: no microscopy image is reused in this block.	N/A: no microscopy image is reused in this block.
13d	108	Intelligent intestine-on-a-chip workflow schematic.	N/A: no microscopy image is reused in this block.	N/A: no microscopy image is reused in this block.
13e	278	Intelligent organs-on-a-chip concept schematic.	N/A: no microscopy image is reused in this block.	N/A: no microscopy image is reused in this block.

Notes: "Objective magnification" is reported only when the source linked an objective to the reused image or imaging workflow. Microscope modality or manufacturer alone was not converted into an objective magnification. Audit scope: each review-figure block listed was checked against the cited primary article and accessible Supporting Information. "Not reported" means that no explicit value was found; "Not assignable" means that a calibrated bar was present in the source but could not be mapped reliably to a particular reused micrograph after compositing; "N/A" means that the reused block contains no microscopy image. Numerical values were not inferred from apparent bar length. Because each source bar remains embedded in and resizes together with its source image, its stated physical value is unchanged by proportional resizing in the composite.

Abbreviations: BBB: Blood–brain barrier; CLSM: Confocal laser scanning microscopy; MEA: Multielectrode array; MPS: Microphysiological systems; SEM: Scanning electron microscopy.